

**UNIVERSITY OF SZEGED
FACULTY OF SCIENCE AND INFORMATICS
DEPARTMENT OF MICROBIOLOGY**

DOCTORAL SCHOOL OF BIOLOGY

**STUDIES ON THE SEXUAL DEVELOPMENT
OF *ASPERGILLUS NIDULANS***

PHD THESIS

KEISHAM KABICHANDRA SINGH

**SUPERVISOR:
Dr. Zsuzsanna Hamari
ASSOCIATE PROFESSOR**



**SZEGED
2019**

TABLE OF CONTENTS

ABBREVIATIONS.....	5
1. INTRODUCTION	6
1.1. <i>Aspergillus nidulans</i>	6
1.2. Life cycles of <i>A. nidulans</i>	7
1.2.1. Vegetative reproduction	9
1.2.2. Sexual reproduction.....	10
1.3. Regulation of sexual development in <i>A. nidulans</i>	12
1.4. Association of sexual development with the secondary metabolite STC production	14
1.4.1. Importance of STC.....	15
1.4.2. Biosynthesis of STC	17
1.4.3. Genetic background and cluster-specific regulator of STC production.....	18
1.5. Classification of High-Mobility-Group-box (HMG-box) domain proteins	21
1.5.1. Nuclear HMGB proteins.....	23
1.5.1.1. Mammalian HMGB proteins.....	23
1.5.1.2. HMGB proteins in <i>Saccharomyces cerevisiae</i>	24
1.5.1.2.1. Hmo1p	24
1.5.1.2.2. Hmo2p	25
1.5.1.2.3. Nhp6A/Bp.....	25
1.5.1.3. HMGB proteins in <i>Podospora anserina</i>	26
1.5.1.4. HMGB proteins in <i>A. nidulans</i>	27
1.5.2. Mitochondrial HMGB proteins (mtHMGBs).....	29
1.5.2.1. Mammalian TFAMs	29
1.5.2.2. Abf2p of <i>S. cerevisiae</i>	29
1.5.2.3. Gcf1p of <i>Candida albicans</i>	30
1.5.2.4. MtHmg1 of <i>P. anserina</i>	30
2. OBJECTIVES.....	32
3. MATERIALS AND METHODS	34

3.1. Strains used in this study	34
3.2. Media and culture conditions	36
3.2.1. Media used for the cultivation of <i>A. nidulans</i>	36
3.2.1.1. Minimal medium (MM)	36
3.2.1.2. Complete medium (CM).....	36
3.2.1.3. Sucrose minimal medium.....	36
3.2.1.4. Salt solution (50x stock solution)	36
3.2.1.5. Trace elements (20x stock solution)	36
3.2.1.6. Carbon sources	36
3.2.1.7. Nitrogen sources.....	36
3.2.1.8. Vitamins.....	37
3.2.1.9. Organic bases	37
3.2.2. Culture conditions of <i>A. nidulans</i>	37
3.2.2.1. Growth conditions for transformation	37
3.2.2.2. Growth tests and growth conditions for STC production	37
3.3. Obtaining of <i>hmbA</i>Δ and <i>hmbC</i>Δ reconstitution strains.....	37
3.4. Transformation of <i>A. nidulans</i>	39
3.5. Total DNA isolation	40
3.6. RNA extraction and cDNA synthesis	40
3.7. PCR for the amplification of components of the substitution cassette	41
3.7.1. Double-joint PCR method	42
3.7.2. Quantitative PCRs (qPCR and RT-qPCR).....	43
3.7.3. List of primers	44
3.8. Southern blot analysis	46
3.9. Microscopy	47
3.10. Thin layer chromatography.....	47
3.11. Genetic crosses	48
3.12. Construction of <i>stcO</i> reporter gene substitution cassette and obtaining <i>stcO promoter-NLS-ycfp</i> carrying strain.....	48
3.13. Determination of the size of cleistothecia and germination ability of ascospores.....	49
3.14. Statistical Analysis.....	49

4. RESULTS	50
4.1. Documentation of sexual structures in the control strain during development	50
4.2. Development of <i>hmb</i> deletion strains in <i>veA</i>⁺ genetic background and analysis of their growth	52
4.3. Sexual development of <i>hmb</i> deletion strains	53
4.4. Intracolony distribution and size of cleistothecia	57
4.5. Ascospore content of cleistothecia and viability of the ascospores in control and deletion strains with <i>veA</i>⁺ genetic background	60
4.6. Transcriptional changes in the <i>veA</i>⁺ <i>hmbA</i>Δ, <i>hmbB</i>Δ and <i>hmbC</i>Δ mutant strains	62
4.7. Discussing the role of HmbA, HmbB and HmbC in the sexual development of <i>A. nidulans</i>	69
4.8. Construction of the <i>stcO</i> reporter cassette	75
4.9. Investigation of the role StcO in the STC biosynthesis	77
4.10. Investigation of the <i>stcO</i>-active vegetative hyphae that surround the center of sexual differentiation	79
4.11. Discussion of the intracolony localization of STC production	82
5. SUMMARY	84
6. ÖSSZEFOGLALÁS	88
7. ACKNOWLEDGEMENT	89
8. REFERENCES	90

ABBREVIATIONS

AF	Aflatoxin
CFU	Colony Forming Unit
CM	Complete Medium
HMG	High Mobility Group
LB	Luria-Bertani medium
MM	Minimal Medium
NLS	Nuclear Localization Signal
PBS	Phosphate Buffered Saline
PCR	Polymerase Chain Reaction
qPCR	Quantitative real time Polymerase Chain Reaction
RGA material	Reddish Granular Amorphous material
STC	Sterigmatocystin
TLC	Thin Layer Chromatography
TF	Transcription factor
UV	Ultraviolet
Wt	Wild type
yCFP	Cyan Fluorescent Protein optimized for yeasts

1. INTRODUCTION

1.1. *Aspergillus nidulans*

Aspergillus nidulans is an ascomycetous filamentous fungus (Kingdom: Fungi; Phylum: Ascomycota; Class: Plectomycetes; Order: Eurotiales; Family: Trichocomaceae) living in soil as a saprophytic organism. *A. nidulans* is also known as *Emericella nidulans* after its teleomorph. It is widely used as a model organism for studying diverse biological processes such as ontogenesis, metabolism, cellular processes and evolution. *A. nidulans* studies contributed to the better understanding of chromatin functions, DNA repair, morphogenesis, mitochondrial DNA organisation and disorders (Galagan *et al.*, 2005). *A. nidulans* has well characterized sexual cycle and well developed genetic system (vast number of auxotroph mutants, efficient genome manipulation protocols... *etc.*) that makes this organism easy to study. It is a self-fertile homothallic fungus. Its ability to undergo self-fertilization even without a mating partner makes it an excellent model organism to study the sexual development and genetic background of homothallism (Coppin *et al.*, 1997). *A. nidulans* was the first *Aspergillus* species to have its genome sequenced. Its genome is approximately 31 Mb containing about 11,000–12,000 genes on its eight chromosomes (Brody and Carbon 1989).

In addition to the industrial importance of production of certain primary metabolites, such as citric acid, *A. nidulans* can produce a wide range of secondary metabolites that are bioactive compounds of great medical importance, such as antibiotics (penicillin), anti-tumor agent (terrequinone) or antifungal compounds (echinocandin B). On the other hand *A. nidulans* can produce harmful secondary metabolites, too, such as the carcinogenic toxin, sterigmatocystin (STC). STC is the precursor compound of the more potent carcinogenic toxin, the aflatoxin (AF), which is produced by other *Aspergillus* species, such as *A. flavus*, *A. paraciticus* and *A. nomius*. *A. nidulans* has a significant value for the identification of the function of orphan filamentous fungal genes and characterization of their products as well as their biological roles (David *et al.*, 2008). Besides of the many useful and medically- or industrially important aspects of the biology of *A. nidulans*, it can be an opportunistic fungal pathogen, which can cause aspergillosis in immunocompromised patients.

In the last few decades, *A. nidulans* was the model organism of studying the genetic background and regulation of the biosynthesis of secondary metabolites, as well as the

regulation of asexual and sexual development. Remarkably, interconnection between these two latest biological processes were discovered and extensively studied in the last years (Bayram *et al.*, 2008). These studies facilitated the study of sclerotia development and aided the revealing of the regulatory pathway that control sclerotium production in other, industrially important *Aspergillus* species such as *A. flavus* or *A. parasiticus* (Dyer and O’Gorman, 2012).

1.2. Life cycles of *A. nidulans*

A. nidulans can undergo three distinct developmental cycles such as asexual, sexual and parasexual cycles (Fig. 1) (Adam *et al.*, 1998).

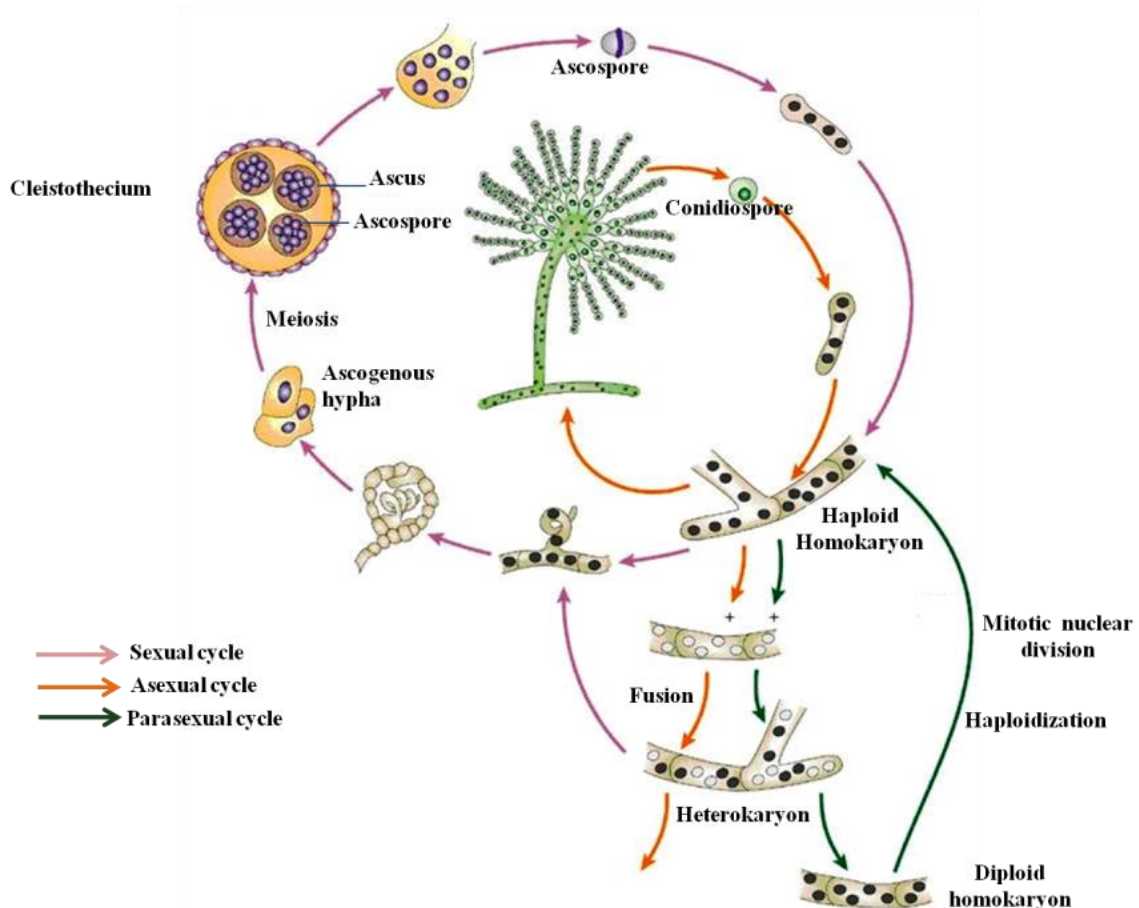


Fig. 1: Schematic representation of the sexual, asexual and parasexual life cycles of *A. nidulans* (from Casselton and Zolan, 2002).

Color of arrows marks the type of life cycle. All the reproductive cycles may occur in a single colony. Conidiospores are produced asexually, while ascospores are produced sexually.

Asexual and sexual ones are the major reproductive cycles in *A. nidulans*. The coexistence of both asexual and sexual reproduction might be complemented by the parasexual cycle (Timberlake and Clutterbuck, 1994; Yager, 1992; Aramayo *et al.*, 1989). The parasexual cycle with parameiosis plays an important role in increasing genetic diversity in filamentous fungi that do not have sexual cycle (imperfect fungi) (Bagagli *et al.*, 1991; Bonatelli *et al.*, 1983).

Choosing between the asexual- and sexual types of reproduction is largely governed by environmental factors in *A. nidulans* (Dyer *et al.*, 1992). Environmental conditions such as light and oxygen availability play pivotal role for balancing asexual and sexual development in *A. nidulans* (Mooney and Yager, 1990).

Red light and elevated oxygen level trigger conidia formation (Fig. 1 and Fig. 2) and repress the development of sexual fruiting bodies (Fig. 1). In contrast, the sexual cycle is induced when a mycelium is grown under dark condition by limiting air circulation and enhancing carbon dioxide level.

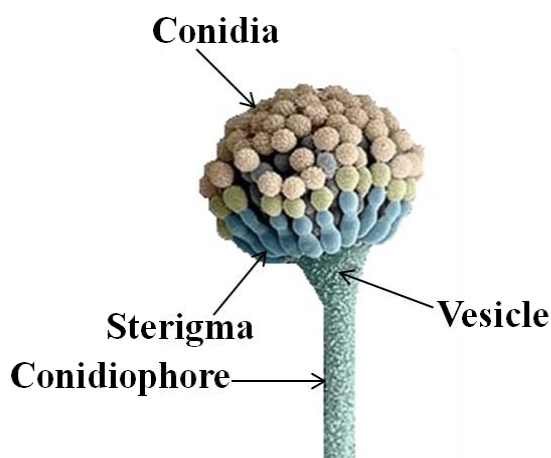


Fig. 2: Structure of conidium of *A. nidulans* (image was obtain from <http://www.dbc.uem.br>)

The developmental decisions for both asexual and sexual reproduction depend on developmental-stage-specific transcription factors (TFs). Both developmental cycles are strictly regulated by a number of specific genes, which encode proteins involved in signal sensing and signal transduction, transcription and genes directly required for the morphological and physiological changes (Adams *et al.*, 1998). Developmental competence is an important factor for development in *A. nidulans* (10-12 h after spore germination) as it enables the conidiogenesis (asexual differentiation that results in

conidiospore formation) in presence of appropriate stimuli (e.g. light illumination) other than the environmental signals that favors the sexual development (such as pheromones, stress conditions, darkness, oxygen deprivation resulting elevated carbon dioxide level) (Noble and Andrianopoulos, 2013).

1.2.1. Vegetative reproduction

The asexual reproduction of *A. nidulans* is triggered in the presence of light and results in the production of high numbers of uni- or rarely binucleate asexual spores, called conidiospores (Fig. 2), which are released to the environment.

The asexual structures are formed in a stepwise manner during conidiogenesis, such as the formation of foot cell, stalk, vesicle, metula, phialide and conidiospores (Fig. 3) (Pontecorvo, 1953). The foot cell derives from differentiated vegetative hyphal compartment that produce a growing stalk from the middle of the compartment with a swollen head at its tip, which is called vesicle. Uninucleate metula cells (finger like structures) are produced from the vesicle by budding. The metula cells cover the vesicle and form the first layer of sterigmata. Later the metula cells undergo yeast-like budding and produce the elongated, uninucleate phialide cells, which form the second sterigmata layer. By continuous budding of phialides, chains of conidiospores are produced.

Regulatory mechanisms underlying asexual reproduction and genes, which play essential roles in asexual development have been identified and extensively studied (Adams *et al.*, 1998). The AbaA TF and *brlA* gene play the key roles during conidiogenesis and initiation of asexual development (Clutterbuck 1969; Adams *et al.*, 1998). VosA (viability of spores A) had been identified as a high-copy repressor of asexual development (Ni and Yu, 2007; Sarikaya Bayram *et al.*, 2010). LaeA is light dependent regulator of asexual reproduction in *A. nidulans* (Bayram *et al.*, 2008) and the TF SteA and the MAP kinase MpkB also affects the asexual reproduction (Wei *et al.*, 2003).

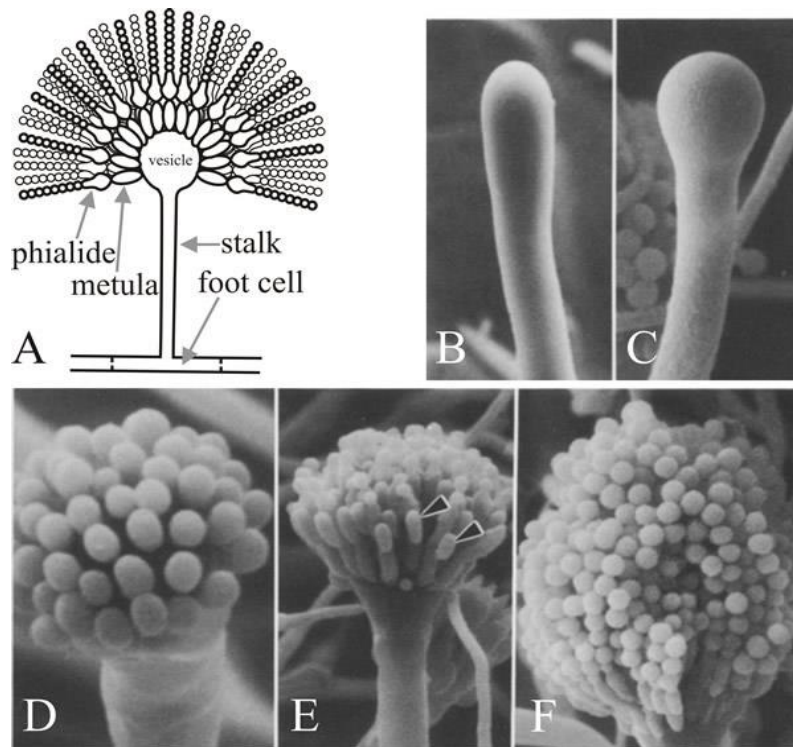


Fig. 3: Structure and development of asexual structures (from Richardson and Timberlake, 1988).

A. schematic representation of a conidium; B-F. scanning electron microscope images of the stepwise formation of the structures of conidium; B. stalk formation; C. development of vesicle; D. development of metulae; E. development of phialides and F. development of conidiospores.

1.2.2. Sexual reproduction

Sexual development in *A. nidulans* results in the formation of closed sexual fruiting bodies, called cleistothecia. Since *A. nidulans* is homothallic (self-fertile), each isolate carries and expresses the genes of both mating type factors, the α -box protein coding *matB* and the HMG-box protein coding *matA*. A mature cleistothecium may contain around 80,000 viable, binucleate ascospores (sexual spores) (Fig. 4), 8 being packed in ascus or are released and standing free (Pontecorvo, 1953; Braus *et al.*, 2002). The sexual development involves the coordinated differentiation of three important cell-types such as the Hülle cells, ascogenous hyphae and the wall of the cleistothecium (pericarp) (Bayram *et al.*, 2010).

The first sign of sexual differentiation in *A. nidulans* is the production of group of Hülle cells. The Hülle cells are large (10-15 μm) globular cells with thick cell wall. They play an important role in protection and nursing of the young cleistothecia containing

developing asci during sexual development. First, the Hülle cells surround a nest of differentiated dikaryotic hyphae, called ascogenous hyphae. At this stage the sexual structure is called primordium. Later, aerial hyphae differentiate to pericarp cells that will form the wall of the mature cleistothecium. At this stage, the developing fruiting bodies are referred to μ -cleistothecia. The μ -cleistothecia develop to unmaturing cleistothecia by the propagation of dikaryotic compartments and forming of ascus mother cells, where meiosis takes place followed by mitosis resulting in eight ascospores (Fig. 4). As a result, the ascus mother cells develop to asci, each of them containing eight ascospores (Fig. 4). The dikaryotic state of the ascogenous hyphae is maintained by the so called crozier (hook) formation (Fig. 4). Prior the fusion of two nuclei in the ascus mother cell, the two compatible nuclei undergo mitosis simultaneously and the four nuclei are separated into three compartments (Fig. 4). The apical compartment contains two nuclei, which upon karyogamy, develops an ascus mother cell with a diploid nucleus, which immediately goes through meiosis (Fig. 4). The middle (hook) and basal compartments contain a single nucleus. These two compartments must fuse together to form a dikaryotic compartment that will be the beginning of a next ascus mother cell formation (Fig. 4). These two compartments meet each other through the elongation of the middle compartment. The elongated middle compartment is called hook. When the hook reaches the level of the basal compartment, the two compartments (hook and the basal) fuse together and a dikaryotic compartment is established. Thereafter the cycle is repeated. The two nuclei of the dikaryotic compartment undergo mitosis and again, the four nuclei will be separated into three compartments. During the maturation of asci, the ascospores begin to accumulate a red pigment, and their nuclei undergo mitosis. As a result, the mature ascospores become red-colored with an oval shape, carrying two nuclei. The proliferation of dikaryotic hyphae accompanied by continuous hook and ascus formation results in cleistothecia containing up to 100,000 asci, each ascus containing eight ascospores.

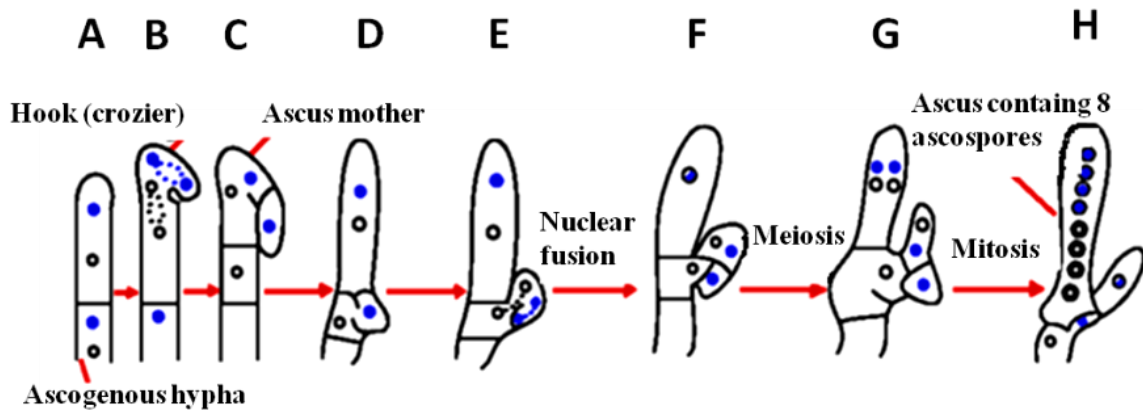


Fig. 4: Ascospore formation in *A. nidulans* (from Dyer and O’Gorman, 2012).

The digramatic presentation explains overall process of ascospores formation. Ascus mother with two haploid nuclei undergoes nuclear fusion producing a diploid cell which then undergoes meiosis resulting four haploid cells which then undergoes mitosis producing eight haploid ascospores.

1.3. Regulation of sexual development in *A. nidulans*

Sexual development of *A. nidulans* is a complex multistep process that requires special regulators and environmental conditions (Fig. 5). Well nourished environmental condition with balanced carbon and nitrogen sources (Han *et al.*, 2003), darkness (Yager, 1992), pH (neutral value) (Rai *et al.*, 1967; Thakur, 1973), elevated level of carbon dioxide (Zonneveld, 1988) favor sexual cycle. Sexual cycle can be induced under laboratory conditions by modifying certain environmental conditions, which supports sexual development. However, certain environmental conditions inhibit sexual cycle such as osmotic stress, strong light, high salt concentration (Lee *et al.*, 1994).

Several genes such as *veA*, *nsdD*, *stuA*, *steC*, *rosA*, *nosA* and *noxA* are well known as genes involved in sexual development (Kim *et al.*, 2002; Han *et al.*, 2001; Miller *et al.*, 1991; Dutton *et al.*, 1997; Wu and Miller, 1997; Vallim *et al.*, 2000; Lara-Ortiz *et al.*, 2003; Vienken *et al.*, 2005; Vienken and Fischer, 2006). Regulation of development by light requires FphA which codes for the far-red and near-red light photoreceptor (Blumenstein *et al.*, 2005). This phytochrome inhibits sexual development under red light conditions. The *fphA* deletion strains produce sexual fruiting bodies abnormally when grown under light condition. Photoreceptors CryA, LreA and LreB are mediated by blue

and UV light, which suppress fungal development (Bayram *et al.*, 2008a; Purschwitz *et al.*, 2008).

The velvet protein VeA, is a major light-dependent regulator. The *veA* gene is primarily expressed in the dark, which governs developmental processes in *A. nidulans*. VeA acts as a positive regulator of sexual development. Further members of the velvet protein family in *A. nidulans* are VelB, VelC and VosA that play a pivotal role in sexual development, spore viability and spore maturation (Bayram *et al.*, 2008; Bayram and Braus, 2012; Park *et al.*, 2012; 2014; Ahmed *et al.*, 2013).

Many experimental studies showed that VeA and VelB interact in the cytoplasm and then move to the nucleus. VeA interacts with the red light sensor FphA and the two blue light photoreceptors LreA and LreB in the nucleus (Purschwitz *et al.*, 2008). VeA forms a trimeric protein complex with the VelB protein and LaeA, a global regulator of secondary metabolism (Bayram *et al.*, 2008). VelB and VeA are essential for fruiting body formation, whereas LaeA is essential to form Hülle cells to support cleistothecia development under appropriate environmental condition. Deletion of the *veA* gene results in the complete loss of the ability to undergo sexual development, while the *veA1* mutation (start codon ATG mutated to ATT) results in an N-terminal truncated protein devoid of nuclear localization signal and evokes a light-independent functioning for the protein (Kim *et al.*, 2002). The *veA1* mutant strains produce conidia abundantly even in dark conditions, produce few aerial hyphae and form fruiting bodies independently of light conditions although at a reduced level in comparison to that of the *veA*⁺ strains (Kafer, 1965).

In *A. nidulans* amino acid limitation is also an important factor, which results in reduced cleistothecia formation. CpcA is responsible for amino acid supply during starvation and induces an arrest in fruiting body formation when amino acids are lacking (Hoffmann *et al.*, 2001). In addition to the above mentioned regulatory factors, pH regulation is also an important factor during sexual development where PacC protein acts as the regulatory protein for pH sensing (Penalva *et al.*, 2008).

It was found that osmotic and oxidative stresses also have regulatory functions during sexual developmental. Saka is activated during osmotic and oxidative stress conditions, which results in repression of sexual development by blocking the formation of sexual fruiting bodies (Kawasaki *et al.*, 2002).

Sexual differentiation and secondary metabolism are correlated processes in *A. nidulans*, in which light is the inhibitor for both sexual reproduction as well as production

of the secondary metabolite STC (Bayram *et al.*, 2008). *VeA* was found to be essential for the expression of *aflR*, TF of STC cluster genes, which couple sexual differentiation and STC production.

Additional TFs are also involved in the production of secondary metabolism, such as *RsmA* that is important for linking both secondary metabolism and sexual development with the stress response in *A. nidulans* (Shaaban *et al.*, 2010; Yin *et al.*, 2012).

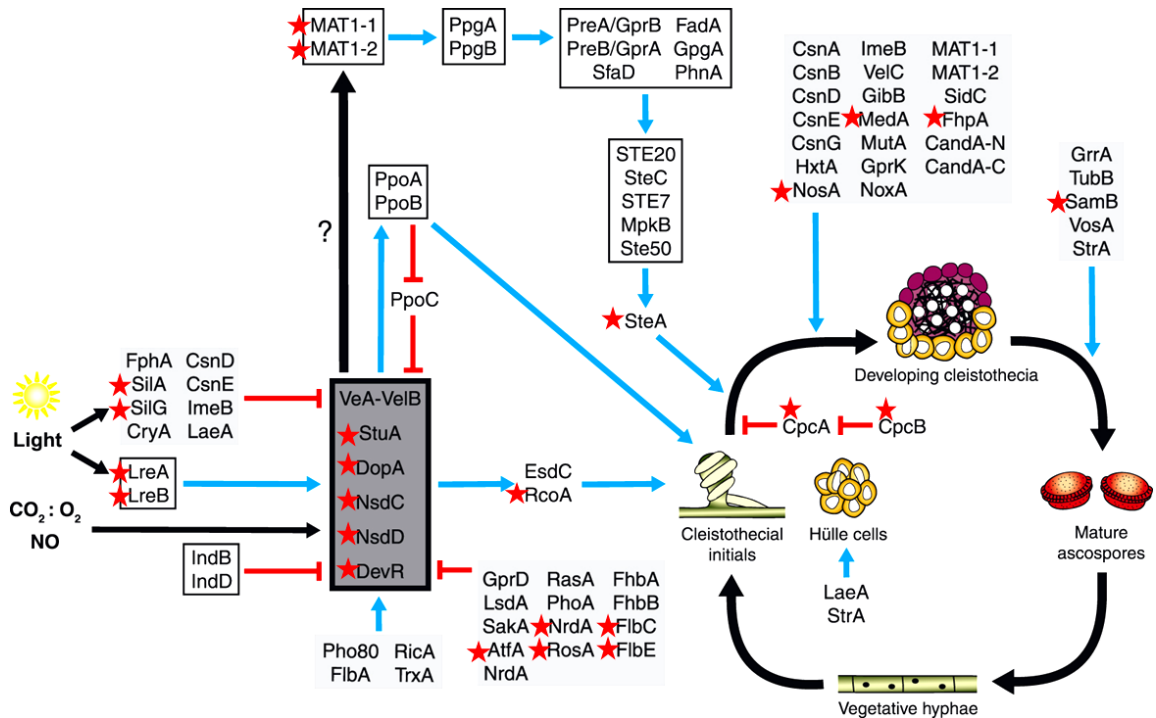


Fig. 5: Network of genes involved in the sexual reproduction of *A. nidulans* (adapted from Dyer and O’Gorman, 2012).

The regulatory genes involved in the event of sexual reproduction of *A. nidulans* form a complex networking system and in that the light is the main regulatory factor. The velvet family proteins also govern the sexual development acting as positive regulator. The red stars indicate the TFs involved in sexual reproduction in *A. nidulans*. Activation is marked with blue-colored lines, inhibition is marked with red-colored lines.

1.4. Association of sexual development with the secondary metabolite STC production

The biosynthesis of secondary metabolites is genetically co-regulated with developmental processes (Bayram and Braus, 2012). Both fungal development and secondary metabolite STC production are linked by being regulated by light (Bayram *et al.*, 2008; Bayram and Braus, 2011) (Fig. 6). On the other hand the control of secondary metabolites is often associated with fungal growth and development (Calvo *et al.*, 2002;

Yu & Keller, 2005; Braus *et al.*, 2010). Most probably, coupling of these two biological processes by co-regulation makes possible for the fungus to protect its sexual reproductive structures against fungivore insects and compete for inhabitable ecological niches (Doll *et al.*, 2013). In *A. nidulans* the STC production affects sporulation and regulated by G-protein signaling pathway (Hicks *et al.*, 1997; Shimizu and Keller, 2001).

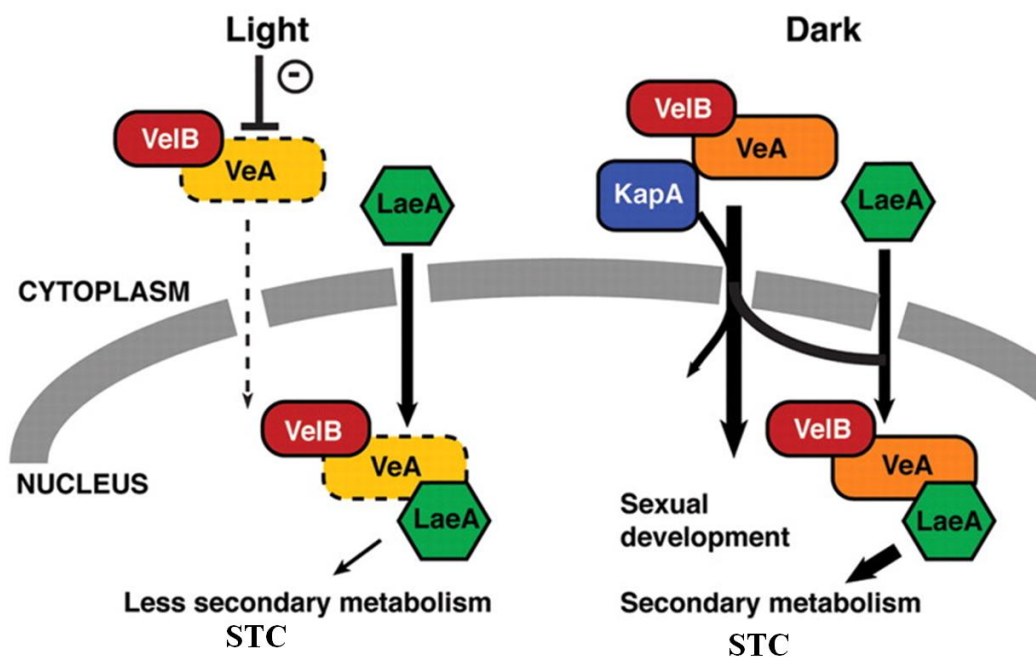


Fig. 6: Association of sexual development with STC production (Bayram *et al.*, 2008)

The velvet protein VeA controls sexual development and the secondary metabolite STC production through the regulation of velvet complex protein LaeA. In presence of light the sexual differentiation is restricted and less STC is produced. However in the absence of light, the amount of VeA is increased, sexual differentiation is induced and elevated level of STC is produced.

1.4.1. Importance of STC

STC is a carcinogenic polyketide (Fig. 7) compound produced by *A. nidulans*. STC is the precursor of the more potent carcinogene AF, the final biosynthetic product in other *Aspergillus sp.*, such as *A. parasiticus*, *A. flavus* and *A. nomius* (Fujii *et al.*, 1976; Wogan *et al.*, 1992; Cole and Cox, 1981; Branch *et al.*, 1993; Keller *et al.*, 1999). Grains, corn, bread, cheese, spices, dried fruits and animal feed are frequently contaminated by STC (Fig. 8) (Kumar *et al.*, 2017). STC and AF mycotoxins are extremely difficult to eliminate from the food because they are very stable and resistant to heat (Peraica *et al.*, 1999; Halstensen 2008; Alborch *et al.*, 2011; Viegas *et al.*, 2015).

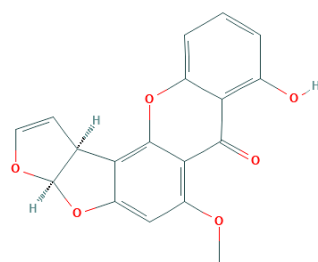


Fig. 7: Chemical structure of STC (Image source: PubChem)

Consumption of STC contaminated food products can cause food poisoning and the accumulation of the toxin can result in tumorigenesis in animals as well as in humans (McConnell and Garner 1994, Kumar *et al.*, 2017) (Fig. 8). Ingestion of this mycotoxin causes dose-dependent impairment of fitness in arthropods, too (Rohlf and Obmann, 2009). Toxic, carcinogenic effects of STC is similar to B1 type AF and it also shows immunotoxic and immunomodulatory activity (Liu *et al.*, 2014). STC is hepatotoxic in rat, mouse, monkey and guinea pig upon exposure (Purchase and Van Der Watt 1969). *In vitro* and *in vivo* studies suggest that STC induces chromosomal damage in laboratory animals (Curry *et al.*, 1984; Ueda *et al.*, 1984; Mori *et al.*, 1986; Crofton-Sleigh *et al.*, 1993; Abdel-Wahhab *et al.*, 2005).

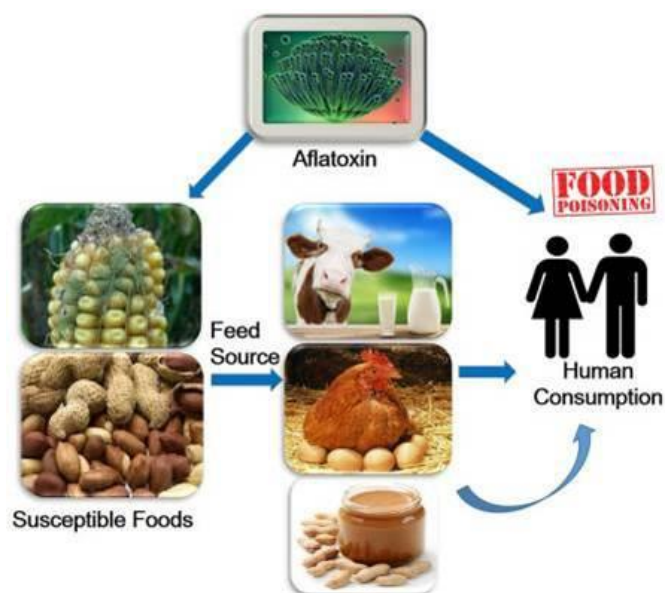


Fig. 8: Effects of STC contamination on human (Kumar *et al.*, 2017)

The image explains about the contamination of foods by aflatoxin which leads to food poisoning. The food chain system is the main mechanism for the spreading of this toxic compound.

Other *in vivo* studies also reported that STC induces cytotoxicity, inhibits cell cycle and mitosis; increase the level of reactive oxygen species and lipid peroxidation (Kawai *et al.*, 1984; Ueno *et al.*, 1995; Xie *et al.*, 2000; Sivakumar *et al.*, 2001; Bunger *et al.*, 2004). Besides the health risk caused by the consumption of mycotoxin-contaminated foods, STC and AF also pose an economical risk by reducing fitness of livestock and quality and value of crops (Miller and Marasas, 2002). Hence, a better control measure of fungal mycotoxins production is required.

1.4.2. Biosynthesis of STC

Mycotoxins are secondary metabolites produced by filamentous fungi. *Aspergillus* mycotoxins are synthesized by a set of enzymes and their coding genes are arranged in clusters on subtelomeric regions of chromosomes. STC is an intermediate metabolite of AF biosynthesis. While STC is the final biosynthetic product in *A. nidulans*, two additional enzyme reactions are performed on STC intermediate in *A. parasiticus* and *A. flavus* resulting in the production of B1 type AF (Fig. 9).

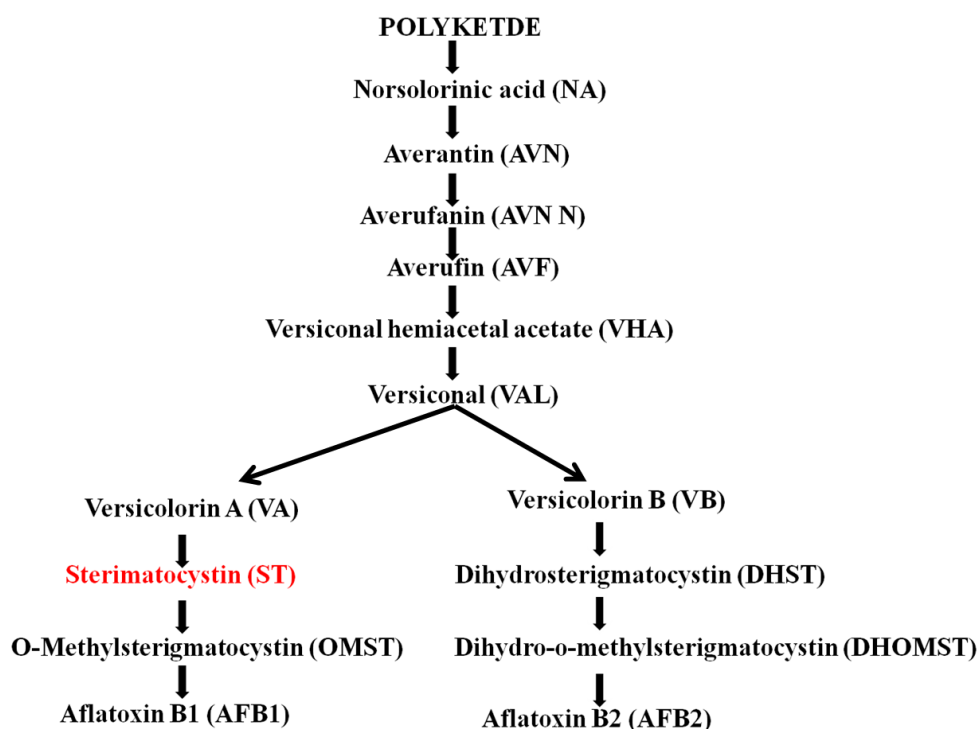


Fig. 9: Schematic presentation of STC and AF biosynthetic pathways in *Aspergillus* species (from Trail *et al.*, 1995)

The arrow indicates the steps involved in the pathway but the enzymatic reactions are not mentioned in this presentation. This pathway is the common pathway for the biosynthesis of STC and AF in *Aspergillus* species.

The STC biosynthetic pathway in *A. nidulans* is estimated to involve at least 15 enzymatic activities. Biochemical studies revealed that five oxygenase steps are required for the formation of STC. Norsolorinic acid (NA), the first stable intermediate of the pathway, undergoes several post-PKS (Polyketide Synthase) enzyme mediated transformations leading to STC and AF biosynthesis (Fig. 9). The conversion of averantin to averufin requires at least two enzymatic steps, in which one is needed for incorporation of an oxygen molecule to form putative intermediates (either 5'-hydroxyaverantin or averufanin), which later are converted to averufin by a dehydrogenase enzyme. In the next step, oxidation of averufin to 1'-hydroxyversicolorone occurs followed by incorporation of an oxygen molecule into 1'-hydroxyversicolorone to form versiconal hemiacetal acetate. The following fourth oxidation step is critical point for the biosynthesis of carcinogenic metabolites such as versicolorin A and versicolorin B from Versiconal (VAL). The last oxidation step is the conversion of versicolorin A to STC (Kelkar *et al.*, 1996; Yu *et al.*, 2004).

1.4.3. Genetic background and cluster-specific regulator of STC production

Study of the STC biosynthesis pathway has led to the identification of a 60 kb gene cluster (*stc* cluster) on chromosome IV that includes 25 co-regulated genes (Fig. 10) and a few of them have been experimentally shown to function in STC biosynthesis (Brown *et al.*, 1996). The *aflR* gene is a pathway-specific regulatory gene that encodes a zinc binuclear cluster type DNA binding domain TF, which acts as the cluster-specific regulator for the activation of the other genes in the *stc* cluster (Woloshuk *et al.*, 1994; Yu *et al.*, 1996; Keller and Hohn, 1997; Fernandes *et al.*, 1998).

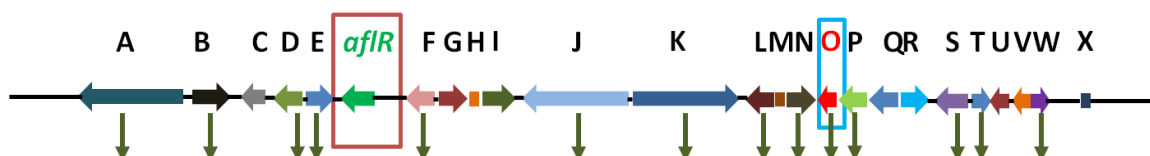


Fig. 10: Schematic representation of the *stc* cluster (developed according to Brown *et al.*, 1996; Keller and Hohn 1997).

Arrows with different colors indicate different *stc* genes (from *stcA* to *stcX*). Arrowheads indicate the orientation of the genes. Green downward arrows mark those genes which are experimentally proved as being regulated by the TF AflR. The *aflR* gene (encoding for the cluster specific TF) is indicated in red box. The *stcO* gene is indicated in blue box. *stcO* is the chosen gene for the development of an STC biosynthesis reporter system in this study (see Results section).

The expression of *aflR* is regulated during the early stationary phase of the life cycle and depends on LaeA and VeA functions (Yu *et al.*, 1996). *AflR* expression and thus the STC biosynthesis is regulated at chromatin level by the methyltransferase LaeA (Bok and Keller, 2004; Keller *et al.*, 2005). LaeA, is a global regulator of secondary metabolism, which contains a classical NLS region located at the N-terminus of the protein that results in its nuclear localization (Bok and Keller, 2004; Keller *et al.*, 2005). On the other hand, LaeA is part of the velvet complex that control development and thereby LaeA plays role in coupling developmental processes and secondary metabolite production (Bayram *et al.*, 2008; Bayram and Braus, 2012). Interconnection of STC biosynthesis with sexual development were also reported and demonstrated by many functional studies of the genes related to sexual development such as VeA, ImeB, RcoA, MpkB or FlbA (Bayram and Braus, 2011). The velvet protein VeA (described in 1.3 sections) is a global fungal regulator controlling both morphological development and secondary metabolites production in *A. nidulans* (Kato *et al.*, 2003; Sprote and Brakhage, 2007). Tandem affinity purification and yeast two hybrid experiments in *A. nidulans* led to the discovery that VeA interacts with LaeA, as well as velvet like protein B (VelB) (Bayram *et al.*, 2008). The trimeric VelB--VeA--LaeA (velvet) complex, where VeA plays a central role as an activator of secondary metabolite production (e.g. STC) and LaeA also plays an important regulatory role in *A. nidulans* morphology, is required for the light-dependent support of asexual development (Fig. 11). Deletion of either VelB or VeA results in defects in both sexual fruiting-body formation and STC biosynthesis. VeA is necessary for normal expression of the TF *aflR*, which activates the *stc* cluster gene that leads to the production of STC (Bayram *et al.*, 2008). The *A. nidulans* putative mitogen-activated protein kinase, encoded by *mpkB*, is necessary for normal expression of *laeA* to regulate cluster genes for STC production (Atoui *et al.*, 2008). ImeB is a mitogen-activated protein kinase, involved in light mediated regulation of development and in mycotoxin production of *A. nidulans* (Bayram *et al.*, 2009). Studies of the effect of light on production of STC in a *veA* wild-type and the *veA1* mutant strains found that the highest amount of STC was produced by the *veA*⁺ strain, which grew in dark (a condition that favours the accumulation of VeA in the nucleus).

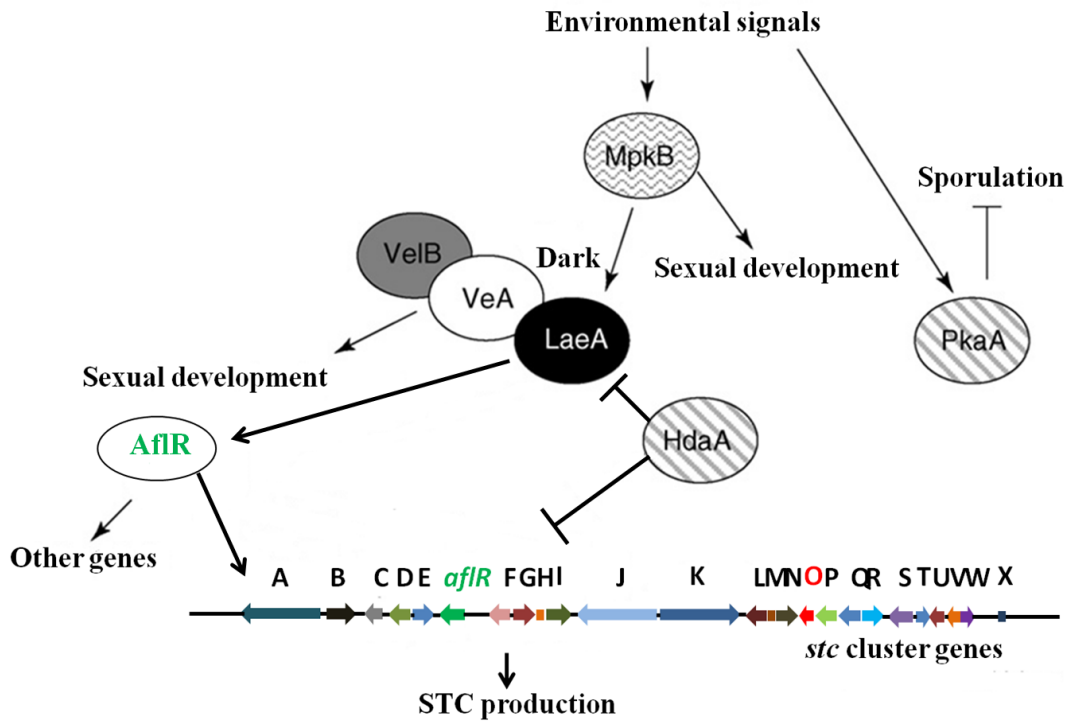


Fig. 11: Regulation of STC production in *A. nidulans* (adopted from Fox and Howlett, 2008)

This schematic figure explains the regulation process of STC production through activation of many regulators such as MpkB, velvet family proteins (VelB, VeA, LaeA) and master regulator (AflR). Histone deacetylase HdaA represses LaeA functions and inhibits STC production. PkaA: Protein kinase A, a member of the PkaA signal transduction pathway that upon activation inhibits asexual sporulation. Arrows represent gene activation, while blocked arrows represent repression. At the bottom the schematic representation of the *stc* gene cluster is shown as it is presented in Fig. 10.

Related to the pH regulation of STC cluster genes, *PacC* has also been proposed as a regulator (acts directly as a repressor under alkaline pH condition) (Keller *et al.*, 1997; Ehrlich *et al.*, 1999). The nitrogen source also plays an important role in STC production. Growth on nitrate nitrogen-source supports STC production along with sexual development; however, growth on ammonium nitrogen-source represses STC production and at the same time increases the asexual development (Bayram and Braus, 2011).

1.5. Classification of High-Mobility-Group-box (HMG-box) domain proteins

The high mobility group proteins (HMG) are structural components of chromatin with a high electrophoretic mobility in polyacrylamide gel (Johns, 1982). HMG proteins are highly abundant and the best characterized group of non-histone chromatin associated proteins. HMG proteins play important role in the architectural organization and functioning of chromatin by bending and plasticizing DNA. Chromatin architectural HMG proteins bind to the chromatin with little or no sequence specificity for the target DNA. The HMG proteins are grouped into three superfamilies such as HMGB, HMGN and HMGA. Each member of the HMG superfamilies has a unique functional motif in common according to their group. The functional motif of the HMGB family is “HMG-box” domain. The HMGN family has “nucleosomal binding” domain and the HMGA family has “AT-hook” domain.

In this work we aimed to study the functions of HMGB proteins, henceforth we focus on the introduction of HMGB proteins only. The structure of HMGB proteins is highly conserved in eukaryotic organisms. An HMGB protein comprises of HMG-box domains (one or more copies), each of them composed of about 75 amino acid residues (HMG-box PF00505). The three-dimensional structure of an HMG-box is rather conserved. An HMG-box is composed of three α -helices separated by loops that are folded into an L-shape form (Fig. 12) (Stott *et al.*, 2006; Ngo *et al.*, 2011; Rubio-Cosials *et al.*, 2011).

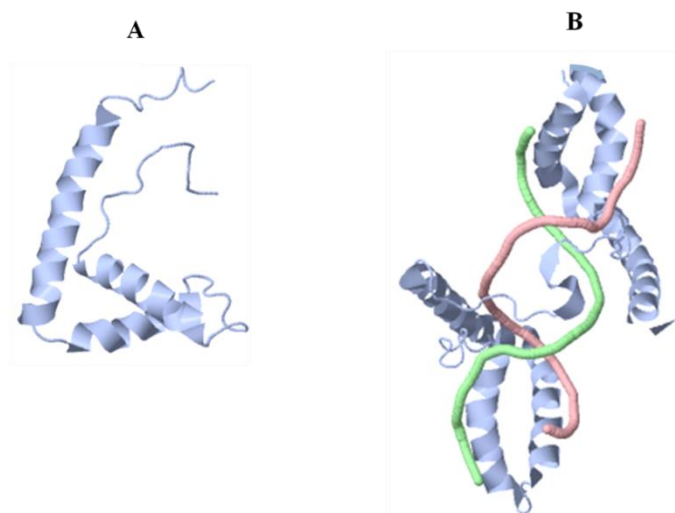


Fig. 12: Structure of HMG-box domain (Stott *et al.*, 2006).

Panel A represents single HMG-box domain where as **Panel B** represents two copies of HMG-boxes domain with the interacting DNA molecule (red and green strings) (Stott *et al.*, 2006; Ngo *et al.*, 2011; Rubio-Cosials *et al.*, 2011).

The HMG-box domain typically binds in the minor groove of DNA. It binds with high affinity to non-canonical DNA structures, such as bent DNA, single-stranded DNA, four-way DNA junctions, supercoiled and damaged DNA (Bustin, 2010; Stros, 2010). In addition to their ability to bind the DNA, they can also interact with various proteins and as a result, they influence gene expression or repression throughout the entire chromatin. They bind to the linker DNA between adjacent nucleosomes at the entry site of a nucleosome, and unfold chromatin higher-order structure. The binding of HMGB proteins is in competition with H1 histones. The interaction of HMGB proteins with DNA is transient (described by the hit-and-run model) and during the short period of DNA-binding time, DNA interaction of chromatin-associated elements involved in nuclear processes (such as transcriptional regulation, DNA repair and recombination) are established through the protein-protein interactions of these elements with HMGB proteins.

As mentioned above, HMGB proteins have no- or little sequence specificity. It is rather intriguing, because certain type of TFs possesses one HMG-box domain with which they bind to their cognate DNA motif, sequence specifically. One might ask whether what is the critical factor of a HMG-box domain that determines the sequence-specific or sequence non-specific binding nature of the domain. Malarkey and Churchill revealed that a single amino acid residue might be the responsible for the sequence specific or non-sequence-specific nature of a HMG-box domain (Malarkey and Churchill, 2012). Their work shed light to the decisive role of the amino acid residue that precedes the second α -helix of the HMG-box domain. When this particular amino acid is non-polar, the HMG-box domain binds the DNA by a non-sequence-specific manner and the protein harboring such an HMG-box domain fulfils general chromatin structuring functions. When this amino acid is a polar one, the HMG-box can bind the DNA by a sequence-specific manner, and the protein that harbors such an HMG-box domain might serve as TF of a small group of genes. An additional difference between chromatin architectural HMGB proteins and HMG-box domain carrying TFs is that TFs contain a single HMG-box domain, while the architectural HMGB proteins are composed of more than one copy of HMG-box domains. A few exceptions are found in nature, when the HMGB protein harbors only one copy of HMG-boxes (e.g. Nhp6p of yeasts and its orthologues PaHMGB6 from *Podospira anserina* and HmbA from *A. nidulans*). However, these single box harboring proteins function as homodimers, thereby at the site of action on the chromatin, two HMG-boxes establish the interaction with the DNA (Fig. 12). In order to bend DNA, at least two HMG-boxes must be present on the site of action (homodimer of a single HMG-box domain protein or a

protein with multicopy HMG-box domains). Bending of DNA thereafter makes possible for remodelling complexes, activators or repressors to establish a stable DNA interaction. Generally, HMGB proteins are involved in the regulation of DNA-dependent processes such as transcription, replication and DNA repair (such as Double Strand Break Repair - DSBR) and act at genome scale level.

1.5.1. Nuclear HMGB proteins

Nuclear HMGB proteins act as structural components of chromatin. They can establish interactions not only with DNA, but with other proteins as well. As a result, they can stabilize the DNA interactions of chromatin remodeling complexes, TFs, transcription activators or repressors.

1.5.1.1. Mammalian HMGB proteins

Mammalian HMGB proteins play important roles in the maintenance of genome integrity, DNA repair, transcription and recombination. Members of mammalian HMGB proteins are HMGB1, HMGB2, HMGB3 and HMGB4. They contain two canonical HMG-box domains (Fig. 13). Among all the four members, HMGB1 is the most highly expressed and the most conserved (Sharman *et al.*, 1997). HMGB1 acts as a DNA chaperone (Bonaldi *et al.*, 2002) with DNA binding and bending activities and regulates a number of key DNA-involved events such as DNA replication, repair, recombination and transcription. HMGB1 binds with high affinity to specific DNA structures like kinked or bent DNA and four-way junctions. The interaction between HMGB1 and nucleosomes is highly reversible during the dynamic process of chromatin remodelling (Falciola *et al.*, 1997). Expression studies of mammalian HMGBs revealed that HMGB1 is over expressed in tumor cells whereas HMGB2 and HMGB3 are only expressed in the testis and lymphoid organs. HMGB1-3 is expressed at high levels in embryos comparing to adults (Bianchi *et al.*, 2005). Previous studies identified the homolog of mammalian HMGB1 in different eukaryotic organisms such as yeast (Nhp6A/B, Hmo1 and Hmo2), drosophila (HMG-D/DSP1), chironomidae, echinoderms, plants, fish, and *Coenorhabditis elegans* (Bustin, 2001; Giavara *et al.*, 2005; Wu *et al.*, 2003).

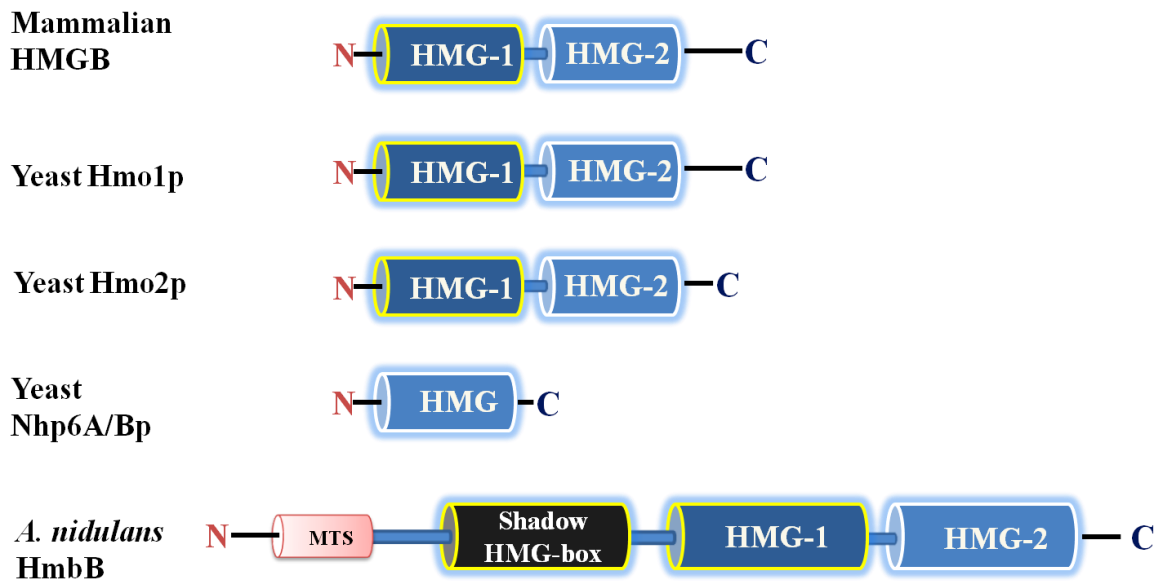


Fig. 13: Schematics presentations of nuclear HMGB proteins

The nuclear HMGB proteins are generally interacts with other proteins and establish protein-protein interaction as a result they stabilize the DNA interactions of remodeling complexes, TFs, activators or repressors. The nuclear HMGB proteins possess single or multiple HMG-boxes. These proteins can act as the architectural components of the chromatin.

1.5.1.2. HMGB proteins in *Saccharomyces cerevisiae*

1.5.1.2.1. Hmo1p

Hmo1p is a member of HMGB proteins of *S. cerevisiae* and it is composed of two HMG-boxes (Fig. 13). Hmo1p is responsible for normal size of the colonies, doubling time of the cells and plays an important role in genome maintenance (Lu *et al.*, 1996, Merz *et al.*, 2008). Deletion of the Hmo1p coding gene results in a severe growth defect (with extremely reduced colony size), reduced plasmid stability, hypersensitivity to micrococcal nuclease, and a decrease in transcription executed by RNA Pol I and II (Lu *et al.*, 1996). At the molecular level, Hmo1p promotes the transcription of rRNA genes (Albert *et al.*, 2013), as well as interacts with Fhl1p (regulator of ribosomal protein genes) (Xiao *et al.*, 2011), TBP and TFIID (Kasahara *et al.*, 2008).

1.5.1.2.2. Hmo2p

Hmo2p of *S. cerevisiae* is homologous to the Hmo1p, however the former has a shorter C-terminal tail (Fig. 13). Hmo2p is a component of the chromatin-remodeling complex INO80, which is involved in double strand break repair (DSBR). Hmo2p binds the supercoiled DNA with higher affinity than linear DNA and shows more preferences towards DNA with lesions. Hmo2p has the remarkable ability to protect DNA from exonucleolytic cleavage by recognizing and binding to DNA ends (Shen *et al.*, 2003) and recruits the INO80 complex to the damage-induced phosphorylated γ -H2A.X, therefore Hmo2p plays significant role in DSB repair (Ray and Grove, 2009).

1.5.1.2.3 Nhp6A/Bp

Nhp6A/Bp (Nhp6Ap and Nhp6Bp) of yeast are paralogs and functionally redundant proteins originated by the duplication of an ancient Nhp6p coding gene. These proteins comprise of a single HMG-box domain and act in the form of homodimers (Fig. 13) (Kolodrubetz and Burgum 1990). They are highly similar to the A- domain of HMGB1. Nhp6A and B are non-essential genes when being deleted for only one paralog. However, double deletion of *nhp6A* and *nhp6B* exerts a pleiotropic physiological effect. The mutant shows morphological and cytoskeletal defects, such as sensitivity to starvation and growth defect at high temperature settings, which can be suppressed by adding an osmotic stabilizer in the medium (Costigan *et al.*, 1994). At the molecular level, the functions of Nhp6A/Bp proteins are similar to that of mammalian HMGB1. Specifically, they regulate the transcription of Pol II-dependent genes at the genome-scale level through different mechanisms. They modulate the interaction of TATA-binding protein (TBP) to the promoter sites and the subsequent formation of the TBP/TFIIA/DNA complexes (Biswas *et al.*, 2004; Yu *et al.*, 2003; Moreira *et al.*, 2000). They also interact with the yeast FACT complex, which ensures transcription elongation by RNA Pol II through nucleosomal templates by removing histone H2A-H2B dimers (Rhoades *et al.*, 2004). In addition, they also interact with transcription activators or repressors (Laser *et al.*, 2000). The Nhp6A/Bp proteins are also important mediators of the expression of RNA Pol III-transcribed genes (Lopez *et al.*, 2001).

1.5.1.3. HMGB proteins in *Podospira anserina*

The *P. anserina* genome encodes a total of 12 HMG-boxes genes (Ait Benkhali *et al.*, 2013). The schematic diagram in Fig. 14 shows the classification of these proteins (Ait Benkhali *et al.*, 2013). They are classified into 3 groups. 5 proteins belong to the group of sequence-specific HMG-box proteins (they are TFs), 5 proteins belong to the group of non-sequence-specific HMG-box proteins (they are HMGBs) and 2 proteins could not be classified into one of these two groups.

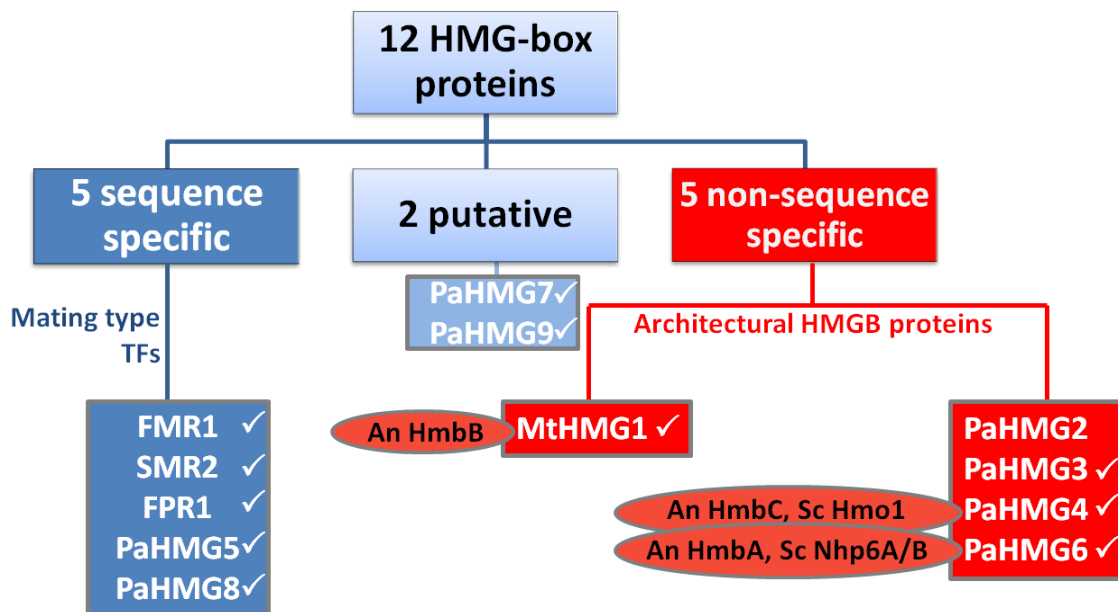


Fig. 14: Classification of HMG-box proteins in *P. anserina* (Ait Benkhali *et al.*, 2013).

Red colour highlights the chromatin architectural HMGB proteins, the blue colour highlights the mating type TFs and the light blue colour highlights the non-classified proteins. The tick mark (✓) indicates those proteins that are involved in the sexual development of *P. anserina*.

A detailed analysis on their function revealed that 11 out of the 12 HMG-box proteins were involved in sexual development. Some of them work in a functional network and they genetically interact for the regulation of mating type TFs (Fig. 15) (Ait Benkhali *et al.*, 2013). Regarding the functions of the HMGB proteins, they revealed that PaHMG6 and mtHMG1 (orthologues of yeast Nhp6A/Bp and Abf2p, respectively), govern the expression of mating-type transcription factors (such as the α -box mating-type *fmr1* and HMG-box mating-type transcription factors *fpr1*, *Pahmg5*, *Pahmg8* and *Pahmg9*) required for the sexual development (Ait Benkhali *et al.*, 2013) (Fig. 15). PaHMG6 acts as the main regulator. It directly activates MtHMG1, PaHMG5 and PaHMG8. PaHMG9 inhibits both

MtHMG1 and PaHMG5. FMR1, PaHMG8 and FPR1 are activated through PaHMG5 (Fig. 15).

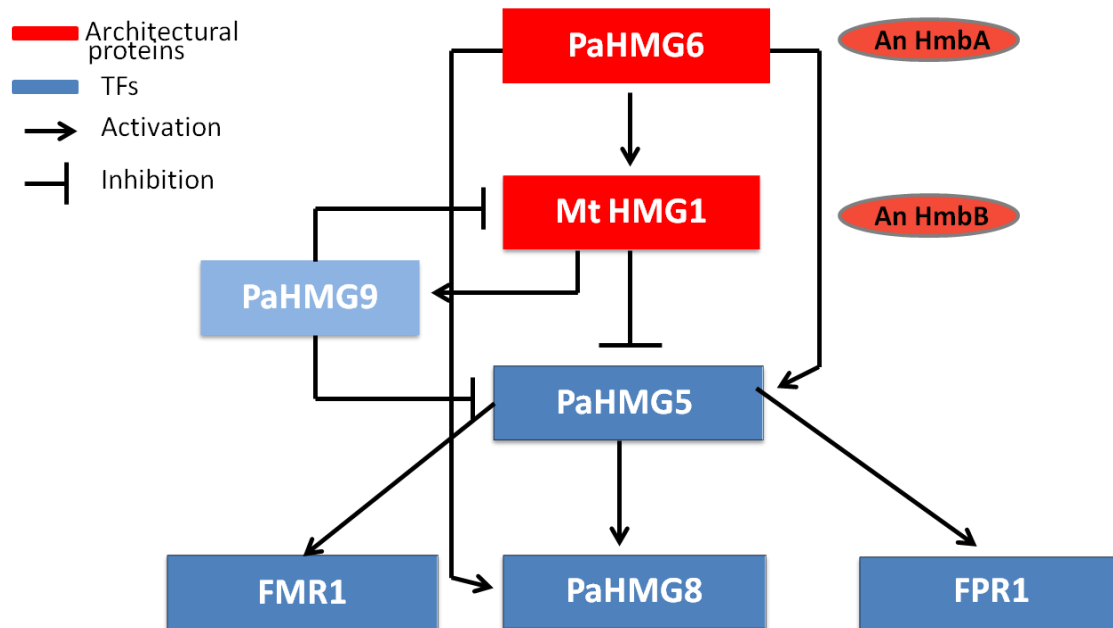


Fig. 15: Genetic networking of HMG-Box domain proteins in *P. anserina* (Ait Benkhali *et al.*, 2013)

The arrow heads and the blunt ends indicate activation and repression, respectively. HmbA and HmbB of *A. nidulans* are also shown as they are orthologues of the PaHMG6 and MtHMG1 respectively. TFs: transcription factors.

1.5.1.4. HMGB proteins in *A. nidulans*

Previous studies reported that there are seven genes in *A. nidulans* genome that encodes HMG-box containing proteins, such as AN2885, AN1267, AN10103, AN3667, AN4734, AN3549 and AN1962. Among them, AN4734 is the MatA also called MAT2 mating type TF (Paoletti *et al.*, 2007; Pyrzak *et al.*, 2008; Czaja *et al.*, 2011).

Further studies revealed that AN1962, AN3549 and AN3667 encode TFs whereas AN2885, AN1267 and AN10103 encode proteins with a more general DNA binding activity (Karácsony *et al.*, 2014). Later these three latter were named as HmbA, HmbB and HmbC with their respective cognate genes being as *hmbA*, *hmbB* and *hmbC* (Karácsony *et al.*, 2014). HmbA encodes a short protein that comprises only one HMG-box. It is an orthologue of the redundant pair NHP6A/B of *S. cerevisiae*. HmbC comprises an atypical

N-terminal HMG-box, a canonical C-terminal HMG-box, followed by a very polar sequence together with its nearest homologues Hmo1 of *S. cerevisiae* and Sp-Hmo1 from *Schizosaccharomyces pombe* (Lu *et al.*, 1996; Albert *et al.*, 2013). Neither HmbA nor HmbC was studied functionally. In *A. nidulans* the HMGB protein HmbB has structurally three successive HMG box domains. Out of which the most N-terminal domain is called as Shadow-HMG-box (ShHMG-B) (Fig. 13 and Fig. 16) that does not show homology to any known HMG-boxes, however its three-dimensional structure is a perfect HMG-box structure (Karácsony *et al.*, 2014). Karácsony *et al.* revealed that all Pezizomycotina orthologue proteins, including that of *P. anserina* (Fig. 16) carry this newly discovered Shadow HMG-box domain. The HmbB protein shows constant mitochondrial localization and additionally, rarely it can also be detected in the nucleus. The dual intracellular localization of this protein makes it unique amongst the known eukaryotic HMGB proteins, which carries the mitochondrial targeting signal (MTS) (Fig. 13 and Fig. 16) and are pivotal for the maintenance of the mitochondrial genome. HmbB plays a significant role in diverse biological processes such as germination of conidia and ascospores, oxidative stress tolerance, maintenance of mitochondrial copy number and production of STC (Karácsony *et al.*, 2014).

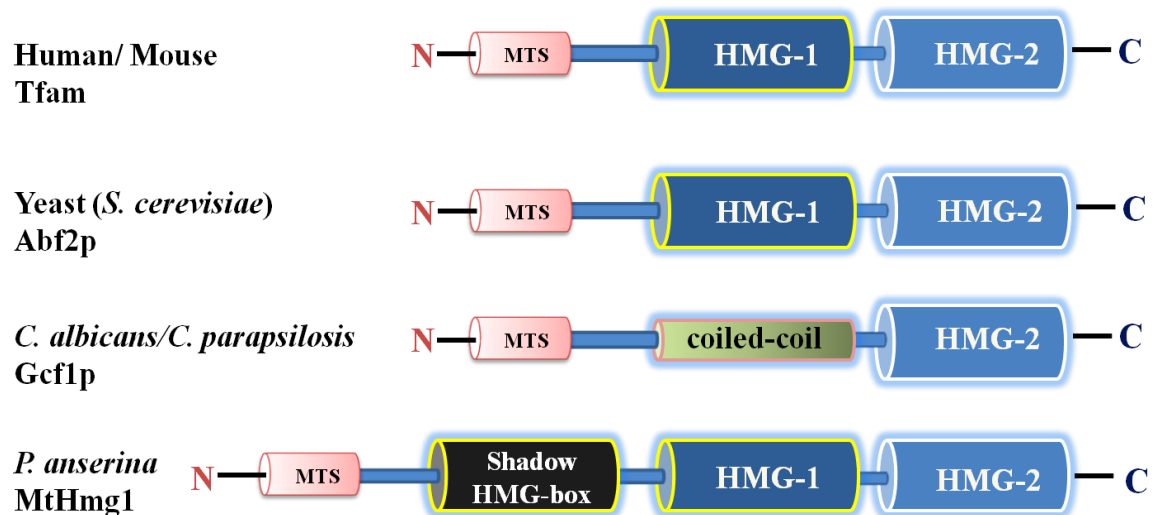


Fig. 16: Schematic presentation of mitochondrial HMGB proteins

HMGB proteins target the mitochondrial DNA due to their mitochondrial targeting signal (MTS) motif located on the N-terminus of the protein. Blue boxes mark HMG-box domains, black box marks the Shadow HMG-box domain first discovered in HmbB of *A. nidulans* and also identified in MtHMG1 of *P. anserina*. Green box indicates a coiled-coil structure.

1.5.2. Mitochondrial HMGB proteins (mtHMGBs)

The mitochondrial DNAs (mtDNAs) are bound by mitochondrial HMGB proteins (mtHMGBs) that result in the mtDNA nucleoid formation (Kuroiwa, 1982). Investigations of their structure and dynamics aided the understanding of the principles that govern mitochondrial inheritance (Chen and Butow, 2005; Kucej and Butow, 2007).

The mtHMGB proteins usually carry two canonical HMG-boxes in their structures, which are separated by an α -helical intermediate domain. The major roles of mtHMGB proteins are mtDNA packaging (condensation), mitochondrial recombination and replication processes (Brewer *et al.*, 2003; Diffley and Stillman, 1991; MacAlpine *et al.*, 1998; Miyakawa *et al.*, 2010). Members of this mtHMG-box mitochondrial proteins are the mouse and human Tfam (also called TFAM), Abf2p of *S. cerevisiae*, Gcf1p of *Candida albicans*, Mthmg1 of *P. anserina* and HmbB of *A. nidulans* (Kaufman *et al.*, 2007; Ngo *et al.*, 2011; Rubio-Cosials *et al.*, 2011; Karácsony *et al.*, 2014).

1.5.2.1. Mammalian TFAMs

TFAM (Fig. 16) plays role in packaging the mtDNA, maintaining the mitochondrial copy number and in recombination processes (Kanki *et al.*, 2004). Furthermore, TFAM also plays role in mitochondrial transcription, which function is not characteristics to the fungal mtHMGBs. TFAM shows a little sequence specificity. TFAM can recognize three promoter sequences in the mitochondrial genome such as the light strand promoter, the heavy strand promoter 1, and the heavy strand promoter 2, which bear little sequence similarity. The sequence-specific binding of TFAM to DNA upstream of the light-strand promoter leads to DNA bending.

1.5.2.2. Abf2p of *S. cerevisiae*

Abf2p contains an N-terminal MTS motif and two copies of HMG-boxes (Fig. 16). It binds to the minor groove of the DNA non-sequence-specifically, with affinity for distorted DNA such as Holliday junctions, DNA cruciforms, DNA bulges and crossovers in supercoiled DNA and induces looping of linear DNA molecules (Diffley and Stillman, 1991, 1992; Brewer *et al.*, 2003; Friddle *et al.*, 2004). Abf2p influences the level of yeast mtDNA recombination intermediates (MacAlpine *et al.*, 1998) and Abf2p was also reported to involve in mitochondrial nucleoid formation (Kucej *et al.*, 2008). Abf2p plays a

vital role in stabilization and metabolism of mtDNA by compacting the mitochondrial genom into nucleoid and controlling mitochondrial recombination frequency (Brewer *et al.*, 2003; Miyakawa *et al.*, 2010; Zelenaya-Troitskaya *et al.*, 1998). Deletion of the Abf2p coding gene has pleiotropic effects including the loss of compaction of the mitochondrial nucleoid, the decrease of mitochondrial recombination frequency and the decrease of mitochondrial genome stability on fermentable carbon sources (Diffley and Stillman, 1991; MacAlpine *et al.*, 1998). These effects are the consequences of DNA bending and wrapping, as well as the promotion and stabilization of Holliday-junction recombination intermediates (Zelenaya-Troitskaya *et al.*, 1998).

1.5.2.3. Gcf1p of *Candida albicans*

In *C. albicans*, the mtHMGB protein Gcf1p carries an N-terminal MTS motif and only one HMG-box in its C-terminal region (Fig. 16). In addition to its single HMG-box, it contains one putative coiled-coil domain with a potential role in protein dimerization (Fig. 16). Gcf1p is involved in mtDNA packaging, mtDNA replication, maintenance of mitochondrial copy number and recombination (Miyakawa *et al.*, 2009; Visacka *et al.*, 2009).

1.5.2.4. MtHmg1 of *P. anserina*

In *P. anserina* the mtHMGB protein mtHMG1 was reported to carry one canonical HMG-box in its C-terminus (residues 244–310), a putative second HMG-box (residues 147–211), a putative AT-hook sequence (residues 111– 123) and a putative mitochondrial targeting sequence in its N-terminus (Dequard-Chablat and Allandt, 2002). Recent studies in our laboratory revealed that *P. anserina* Mthmg1 is orthologous to HmbB and has structurally three successive HMG-box domains, which of them the most N-terminal domain is the Shadow-HMG-box (ShHMG-B) similarly to HmbB (Fig. 13 and Fig. 16) (Karácsony *et al.*, 2014).

MtHMG1 plays a pivotal role in preventing premature dead syndrome arising due to the rearrangement of mitochondrial DNA in *P. anserina* (Dequard-Chablat and Allandt, 2002). MtHmg1 also plays significant role in maintaining lifespan, mitochondrial genome stability, ascospore germination and ensuring of female fertility (Dequard-Chablat and

Alland, 2002). The *mthmg1* deletion strain displays altered germination, -growth, -fertility and a shortened life span in *ASI*⁺ context (Dequard-Chablat and Alland, 2002).

2. OBJECTIVES

Inspired by the regulatory functions of HMGB proteins in sexual development of *P. anserina* (Ait Benkhali *et al.*, 2013) we aimed to study the role of *A. nidulans* HMGB proteins HmbA, HmbB and HmbC in the sexual development by the analysis of *hmbAΔ*, *hmbBΔ* and *hmbCΔ* mutants (obtained earlier) and monitor the changes in transcript levels of sexual development related transcription factors in the mutants. Furthermore, we aimed to assess possible functional interaction between the key regulator of sexual development and secondary metabolism, VeA, and the HmbA, HmbB and HmbC proteins.

To pursue these goals we planned the following strategies:

- ❖ Obtaining of *hmbA*, *hmbB* and *hmbC* deletions in *veA*⁺ genetic background by genetic crosses. (The deletions of *hmbA*, *hmbB* and *hmbC* were developed earlier in recipient strains with *veA1* genetic background as reported in Karácsony *et al.*, 2014 and Bokor *et al.*, 2019)
- ❖ Characterization of sexual structures of *hmbAΔ*, *hmbBΔ* and *hmbCΔ* mutants in comparison to *hmbA*⁺ *hmbB*⁺ *hmbC*⁺ control both in *veA*⁺ and in *veA1* genetic background.
- ❖ Transcript analysis of TFs involved in sexual development in *hmbAΔ*, *hmbBΔ* and *hmbCΔ* mutants in comparison to *hmbA*⁺ *hmbB*⁺ *hmbC*⁺ control with *veA*⁺ genetic background.

Since the mycotoxin contamination of food raises a serious health and economical concerns, studying the biology of STC production assists the deeper understanding of their role in fungal life and aids us to fight against mycotoxin contaminations. STC production and sexual development are coupled biological processes *in vivo*, that is supported by the discovery of key regulators of these two processes being shared. However, the intracolony location of the STC production has never been studied, despite experiments on the grazing habits of fungivore insects indicated that STC production is heterogeneously distributed in the mycelia (Doll *et al.*, 2013). Thereby we aimed to visualize those compartments of the colony, where STC is produced.

To pursue this goal we planned the following strategies:

- ❖ The visualization of the intra-colonial localization of STC producing compartments by developing a reporter system using the promoter of one of the putative biosynthetic gene *stcO*, fused with the gene of the cyan fluorescent protein.
- ❖ Revealing the role of *stcO* gene in STC biosynthesis by detection of STC in control and *stcO*Δ strains by TLC.

3. MATERIALS AND METHODS

3.1. Strains used in this study

The *A. nidulans* strains used in the experiments are summarized in Table 1.

Table 1. List of *A. nidulans* strains used in this study.

Strain	Genotype	Purpose	Reference
<i>veA1</i> strains			
CS2902	<i>pyrG89 riboB2pyroA4 biA1 veA1</i>	parental strain in genetic crosses	Yu <i>et al.</i> , 2004
LO1516	<i>hhoA-mRFP-AfriboB⁺ riboB2 pyroA4 pyrG89 nkuAA::argB⁺ veA1</i>	recipient strain for transformation	(Nayak <i>et al.</i> , 2010)
HZS.98	<i>pantoB100 pabaA1 veA1</i>	parental strain in genetic crosses	this work
HZS.119	<i>anA1 riboB2 yA2 veA1</i>	parental strain in genetic crosses	this work
HZS.120	<i>riboB2 pabaA1 veA1</i>	recipient strain in transformation experiment	Balázs <i>et al.</i> , 2010
HZS.145	<i>veA1</i>	studies of sexual structure, RT-qPCR	this work
HZS.205	<i>hmbAΔ::riboB⁺ riboB2 pabaA1 veA1</i>	parental strain in genetic crosses	this work
HZS.212	<i>hmbBΔ::riboB⁺ riboB2 pabaA1 veA1</i>	parental strain in genetic crosses	Karácsony <i>et al.</i> , 2014
HZS.227	<i>riboB2 pantoB100 yA2 veA1</i>	parental strain in genetic crosses	this work
HZS.239	<i>hmbAΔ::riboB⁺ riboB2 veA1</i>	studies of sexual structure, RT-qPCR	this work (obtained by cross of HZS.205 with CS2902)
HZS.260	<i>pyrG89 pyroA4 yA2 veA1</i>	parental strain in genetic crosses	this work
HZS.280	<i>hmbBΔ::riboB⁺, yA2, veA1</i>	studies of sexual structure	this work (obtained by cross of HZS.212 with HZS.119)
HZS.314	<i>riboB2 pantoB100 pabaA1 biA1 veA1</i>	recipient strain in transformation experiment	this work
HZS.318	<i>hmbBΔ::riboB⁺ riboB2 pabaA1 pantoB100 veA1</i>	recipient strain in transformation experiment	this work (obtained by cross of HZS.212 with HZS.227)
HZS.320	<i>hmbAΔ::riboB⁺ riboB2 pabaA1 pantoB100 veA1</i>	recipient strain in transformation experiment	this work (obtained by cross of HZS.205 with HZS.227)
HZS.324	<i>pantoB100 riboB2 biA1 veA1</i>	parental strain in genetic crosses	this work
HZS.334	<i>hmbAΔ::riboB⁺ hmbBΔ::riboB⁺ riboB2 pabaA1 veA1</i>	parental strain in genetic crosses	this work
HZS.338	<i>hmbCΔ::pabaA⁺ pabaA1 riboB2 pantoB100 biA1 veA1</i>	parental strain in genetic crosses, recipient strain in transformation experiment	this work

HZS.621	<i>hmbAΔ::riboB⁺ riboB2 pantoB100 pabaA1 veA1</i> and 1 copy integration of pAN-HZS-9 containing <i>hmbA⁺</i>	reconstituted <i>hmbAΔ</i> strain for studies of sexual structure	this work (obtained by transformation of pAN-HZS-9 into recipient strain HZS.320)
HZS.676	<i>hmbCΔ::pabaA⁺ pabaA1 riboB2 pantoB100 biA1 veA1</i> and 1 copy integration of pAN-HZS-10 containing <i>hmbC⁺</i>	reconstituted <i>hmbCΔ</i> strain for studies of sexual structure	this work (obtained by transformation of pAN-HZS-10 into recipient strain HZS.338)
HZS.677	<i>hmbBΔ::riboB⁺ riboB2 pabaA1 pantoB100 veA1</i> and 1 copy integration of pAN-HZS-11 containing <i>hmbB⁺</i>	reconstituted <i>hmbBΔ</i> strain for studies of sexual structure	this work (obtained by transformation of pAN-HZS-11 into recipient strain HZS.318)
veA⁺ strains			
HZS.1	<i>riboB2 pabaA1</i>	parental strain in genetic crosses	Ámon <i>et al.</i> , 2018
HZS.450	<i>riboB2</i>	parental strain in genetic crosses, studies of sexual structure, RT-qPCR	this work
HZS.451	<i>pabaA1 anA1 yA2</i>	parental strain in genetic crosses	this work
HZS.489	<i>hmbAΔ::riboB⁺ riboB2 pabaA1</i>	studies of sexual structure, RT-qPCR	this work
HZS.495	<i>hmbBΔ::riboB⁺ riboB2</i>	studies of sexual structure, RT-qPCR	this work
HZS.499	<i>hmbBΔ::riboB⁺ riboB2 pabaA1</i>	parental strain in genetic crosses	this work (obtained by cross of HZS.212 with HZS.450)
HZS.531	<i>hmbCΔ::pabaA⁺ pabaA1 riboB2</i>	parental strain in genetic crosses, studies of sexual structure, RT-qPCR	this work (obtained by cross of HZS.338 with HZS.451)
HZS.521	<i>hmbAΔ::riboB⁺ riboB2 pabaA1</i>	studies of sexual structure, RT-qPCR	this work (obtained by cross of HZS.205 with HZS.450)
HZS.576	<i>hhoA-mRFP-AfriboB pyroA pabaA1 (nkuAΔ::argB⁺)</i>	recipient strain for transformation	this work (obtained by the genetic cross between the strains of LO1516 and HZS.1)
HZS.606	<i>hhoA-mRFP-AfriboB stcOpromoter-NLS-yCFP-AfpyroA⁺ pyroA4 pabaA1 veA⁺ (nkuAΔ::argB)</i>	study of the localization of STC production by using microscope	this work (obtained by the transformation of HZS.576 with a five-partite gene substitution cassette)
HZS.653	<i>hmbBΔ::riboB⁺ riboB2 pantoB100, yA2</i>	recipient strain in transformation experiment	this work (obtained by cross of HZS.499 with HZS.324)
HZS.658	<i>hmbCΔ::pabaA⁺ pabaA1 pantoB100</i>	recipient strain in transformation experiment	this work (obtained by cross of HZS.531 with HZS.98)
HZS.678	<i>hmbAΔ::riboB⁺ riboB2, pantoB100</i> and 1 copy integration of pAN-HZS-9 containing <i>hmbA⁺</i>	reconstituted <i>hmbAΔ</i> strain for studies of sexual structure	this work (obtained by transformation of pAN-HZS-9 into recipient strain HZS.655)
HZS.679	<i>hmbCΔ::pabaA⁺ pabaA1 pantoB100</i> and 1 copy integration of pAN-HZS-10 containing <i>hmbC⁺</i>	reconstituted <i>hmbCΔ</i> strain for studies of sexual structure	this work (obtained by transformation of pAN-HZS-10 into recipient strain HZS.658)
HZS.680	<i>hmbBΔ::riboB, riboB2, pantoB100, yA2</i> and 1 copy integration of pAN-HZS-11	reconstituted <i>hmbBΔ</i> strain for studies of sexual structure	this work (obtained by transformation of pAN-HZS-11 into recipient strain

	containing <i>hmbB</i> ⁺		HZS.653)
--	-------------------------------------	--	----------

Standard genetic markers are described at the following URL: http://www.fgsc.net/Aspergillus/gene_list/. The *hhoA-mRFP-AfriboB* is a H1 histone-mRFP gene-fusion coupled with the wild type *riboB* gene of *A. flavus*. *nkuAA* is the deletion of *nkuA* that is essential for non-homologous end joining of DNA in double-strand break repair (Nayak *et al.*, 2006). The *stcO::NLS-γCFP-AfpyroA*⁺ construct is described in 3.12. Alleles in parenthesis are not checked.

3.2. Media and culture conditions

3.2.1. Media used for the cultivation of *A. nidulans*

3.2.1.1. Minimal medium (MM):

2% (v/v) salt solution, 1% glucose, 10 mM nicotinic acid (1:100 dilution from 1 M nicotinic acid dissolved in 1 M sodium hydroxide), Agar (25 g/l) (pH 6.8)

3.2.1.2. Complete medium (CM):

2% (v/v) salt solution, 1% (w/v) glucose, 2 g/l pepton, 1.5 g/l Casamino acid, 1 g/l yeast extract, Agar (25 g/l) (pH 6.8)

3.2.1.3. Sucrose minimal medium:

2% (v/v) salt solution, 1% (w/v) glucose, 342.3 g/l saccharose, 0.85 g/l NaNO₃ Agar (25 g/l) (pH 6.8)

3.2.1.4. Salt solution (50x stock solution):

26 g/l KCl, 26 g/l MgSO₄×7H₂O, 76 g/l KH₂PO₄, 5% (v/v) trace elements.

3.2.1.5. Trace elements (20x stock solution):

40 mg/l Na-borate (Na₂B₄O₇×10H₂O), 400 mg/l CuSO₄×5H₂O, 714 mg/l FePO₄, 728 mg/l MnSO₄×H₂O, 800 mg/l Na₂MoO₄×2H₂O, 8 mg/l ZnSO₄×7H₂O

3.2.1.6. Carbon sources:

1% (v/w) glucose and 1% (v/w) lactose

3.2.1.7. Nitrogen sources:

Sodium nitrate (10 mM) and nicotinic acid (10 mM)

3.2.1.8. Vitamins:

Para aminobenzoic acid: 40 µg/l, riboflavin: 50 µg/l, pyridoxine: 25 µg/l

3.2.1.9. Organic bases:

Uracil: 1 g/l, uridine: 1 g/l

3.2.2. Culture conditions of *A. nidulans*

For culturing of *A. nidulans* strains, the conidiospores were collected into 0.01 m/v % Tween80 solution by using sterile toothpicks. For liquid culture medium, the conidiospores were inoculated into 300 ml of liquid MM and incubated at 37 °C in an orbital shaker at 180 rpm for 14-16 hours.

3.2.2.1. Growth conditions for transformation

The *A. nidulans* strains used for transformation were inoculated into CM by using toothpicks and incubated at 37 °C, for 3-4 days to obtain fresh conidiospores. For protoplast formation the fresh conidiospores were spreaded through the surface of cellophane on top of MM with glucose and nitrate supplemented with the required vitamins.

3.2.2.2. Growth tests and growth conditions for STC production

The *A. nidulans* control strain and the *stcO* reporter strain were grown in the presence of different nitrogen and carbon sources and on nitrogen free MM for the growth test. We used MM with nicotinic acid as the sole nitrogen-source and glucose for the source of carbon and MM with nitrate as sole nitrogen-source and lactose for carbon-source. All the strains were grown in dark at 37 °C with at least 1 second light exposure/day. For STC production we used MM nitrate-lactose medium and incubated the strains in complete darkness at 37 °C for various days.

3.3. Obtaining of *hmbAΔ* and *hmbCΔ* reconstitution strains

Deletion of *hmbB* had been reported previously (Karácsony *et al.*, 2014). Deletions of *hmbA* and *hmbC* were obtained (Bokor *et al.*, 2019) by the transformation of a *riboB*⁺ and *pabaA*⁺ containing (selection marker gene) gene substitution cassette constructed by the double-joint PCR method (Yu *et al.*, 2004). Briefly, the "A", "B" and "C" components

of the *hmbA* substitution cassette were amplified with the "hmbA up frw" – "hmbA up rev", " hmbA ribo chim frw" – hmbA ribo chim rev" and "hmbA down frw" – "hmbA down rev" primer pairs, respectively. The 3,428 bp, 2,208 bp and 3,058 bp long "A", "B" and "C" components were assembled to a 7,827 bp long substitution cassette using "hmbA up nest frw" and "hmbA down nest rev" primers. The substitution cassette was transformed into recipient strain and riboflavin prototrophic strains were selected and pre-screened for the deletion by PCR using HmbA frw-HmbA rev primers. Single copy integration mutants were selected after Southern blot analysis using the DIG-labeled "C" component as DNA probe on XbaI digested total DNA. One single copy integration mutant strain was used in this work to conduct genetic crosses to obtain prototrophic *veA*⁺ and *veA1 hmbAΔ* strains for these studies. Deletion of *hmbC* was done by construction and transformation of a *hmbC* substitution cassette. The cassette componets "A", "B" and "C" were amplified with the "hmbC up frw" – "hmbC up rev", " hmbC paba chim frw" – hmbC paba chim rev" and "hmbC down frw" – "hmbC down rev" primer pairs, respectively. The 2,634 bp, 3,846 bp and 2,320 bp long "A", "B" and "C" components were assembled to a 8,069 bp long substitution cassette using "hmbC up nest frw" and "hmbC down nest rev" primers. The substitution cassette was transformed into recipient strains and the obtained para-aminobenzoic acid prototroph transformants were pre-screened for the deletion by PCR using HmbC frw and HmbC rev primers. Single copy integration mutants were selected after Southern blot analysis using the DIG-labeled "C" component as DNA probe on EcoRV digested total DNA. One single copy integration mutant was used in this work to conduct genetic crosses to obtain prototrophic *veA*⁺ and *veA1 hmbCΔ* strains for these studies.

Reconstitution of *hmbA* and *hmbC* deletion was obtained by this work. Reconstitution of *hmbA* was carried out by cloning the *hmbA* product (amplified by "hmbA prom NotI frw" and "hmbA term NheI rev" primers) into NheI/NotI sites of pAN-HZS-1 vector (Karácsony *et al.*, 2014) and transforming the developed pAN-HZS-9 vector into suitable recipient strain. Out of 50 transformants, 4 carried single copy integration (checked by qPCR with "hmbA ReTi frw" and "hmbA ReTi rev" primers) and one of the single copy integration strains was used in further studies.

Reconstitution of *hmbC* deletion was also carried out in this work. Reconstitution was achieved by cloning the *hmbC* PCR product (obtained by using "hmbC NcoI frw" and "hmbC BamHI rev" primers) into NcoI/BamHI sites of pAN-HZS-1 vector (Karácsony *et al.*, 2014) and transforming the obtained pAN-HZS-10 into recipient strain. Out of 16

transformants, 2 carried single copy integration (checked by qPCR with "hmbC ReTi frw" and "hmbC ReTi rev" primers) and one of the single copy integration strains was used in our study.

3.4. Transformation of *A. nidulans*

Transformation of *A. nidulans* was performed by using the protoplasts from mycelia grown on the surface of cellophane membranes as described by Karácsony *et al.*, 2014. The solution of 4% Glucanex (Novozymes, Switzerland) in 0.7 M KCl was used for the protoplast formation. Preparation of protoplasts was as follows. The conidiospores of *A. nidulans* strains were inoculated on the surface of cellophane membranes and incubated for overnight at 37 °C. The protoplast formation was carried out by peeling off the cellophane membranes from the plates followed by soaking them in freshly prepared glucanex solution (30 ml-glucanex, 400 mg/10 ml of 0.7 M KCl) and then incubated for 45 minutes in room temperature. Then the cellophane membranes were washed with 100 ml 0.7 M KCl and the solution was filtered through a cheese filter having 100 µm large pores. The filter retains the mycelial debris, while it lets the protoplasts flow through the pores. The filtered protoplast suspension was centrifuged at 4000g for 25 minutes at 14 °C in order to collect the protoplasts. The supernatant was discarded and the pellet with the protoplasts was suspended by hand shaking (vortexing was strictly avoided). The protoplasts were washed with 10 ml of 0.7 M KCl and centrifuged with the same conditions as before. The number of protoplasts was counted in a Burker chamber under light microscope. 5×10^5 and 5×10^6 protoplasts were taken out and centrifuged at 2500 rpm for 6 minutes. The supernatant was discarded. A 200 µl of TN1 (0.7 M KCl, 50m M CaCl₂) and 1 µg DNA was added to the sample (in no more than 15 µl volume). Then 55 µl TN2 (60% PEG-4000, 50 mM CaCl₂, 100 mM Tris/HCl (pH 8)) was also added to the sample and incubated on ice for 30 minutes. In order to wash the PEG-4000 out of the sample, the sample was transferred into a 15 ml falcon tube and 10 ml of KCl was added to it and centrifuged at 4000g for 20 minutes at 14 °C. The protoplasts were suspended into 1 ml 0.7 M KCl by hand shaking and after adding freshly prepared top agar (40-42 °C) (about 5 ml/petri dish), the protoplasts were spreaded on the surface of selective medium (MM with nitrate and glucose that contains all the required vitamins except that one, which was used for selection of the transformants). The plates were incubated for 4-5 days at 37 °C.

3.5. Total DNA isolation

Conidiospores (10^8) were inoculated into 100 ml liquid, required vitamins supplemented glucose and nitrate MM and incubated overnight in a shaker with 120 rpm at 37 °C. The mycelial mat was collected by filtration and washed with distilled water and squeezed to dry by using paper towel. The dried mycelia were frozen in liquid nitrogen until the extraction. The total DNA was isolated by applying the method described by Specht *et al.*, (1982). The frozen mycelia was crashed and powdered by using mortar and pestle. 200-300 µg of powdered mycelia and 0.6 ml LETS buffer (0.1 M LiCl, 10 mM Na₂EDTA, 10 mM Tris/Cl (pH 8.0), 0.5% sodium dodecyl sulphate (w/v)) was added for each gram of mycelium powder and vortexed vigorously. After that an equal volume of PCI (phenol:chloroform:isoamyl alcohol mixed in 25:24:1 ratio (v/v) pH 7.4) was added to the sample and vortexed vigorously. The organic phase was separated from the DNA containing inorganic phase by centrifugation ($13,000 \times g$, 10 min). The collected inorganic phase was extracted with CI (chloroform:isoamyl alcohol mixed in 24:1 ratio (v/v)) in order to eliminate traces of phenol. After vortexing and centrifugation ($8,000 \times g$, 10 min) the aqueous phase was collected in a fresh tube and 1/10 volume of 3 M Na-acetate was added to the sample prior the precipitation of the DNA. DNA precipitation was done by adding equivalent volume of isopropanol to the sample and incubating it on -20 °C for at least 2 hours, preferably overnight. The DNA was collected by centrifugation ($13,000 \times g$, 10 min) and the pellet was washed twice with 70% (v/v) ethanol. The pellet was dried by keeping the sample on the bench with opened cap for 6-10 minutes (room temperature). The dried DNA pellet was dissolved in 100 µl distilled water containing RNase (250 µg/ml).

3.6. RNA extraction and cDNA synthesis

For RNA extraction NucleoSpin RNAPlant Kit (Macherey-Nagel) and TRIsure reagent (Bioline) were used following the instructions of the manufacturer. NucleoSpin RNAPlant Kit derived RNA samples were treated with RNase-Free DNase (Qiagen) while they were bound to the columns, according to the manufacturer's instructions. Here we must note that the extraction kit contained gDNA binding columns, which were extremely efficient and practically depleted the total DNA content of the RNA samples to zero. When TRIsure reagent (Bioline) was used for RNA extraction, the DNase treatment was done

with RNase-Free DNase Set (Qiagen) in liquid according to the manufacturer's instructions. Usually DNase treatments following TRIpure reagent extraction were repeated two-three times in order to reach DNA-free quality. DNA contamination of the RNA samples was checked by performing qPCR on 1 µg RNA samples with gamma-actin coding *actA* specific primers (actin ReTi frw2: 5'- accatgtaccctggtatctc -3' and actin ReTi rev2: 5'- ggaggagcaatgatcttgac -3') that do not span intron sequences. When Cq was lower than 32 cycle, the DNase treatment was repeated. Samples showing higher than 32 cycle Cq values in the DNA contamination test were used for reverse transcription. RNA quality was monitored by using agarose gel electrophoresis (Fig. 17). Reverse transcription was performed with RevertAid First Strand cDNASynthesis Kit (Fermentas). For the reaction, oligo (dT) 18 and random hexamer primers were used according to the manufacturer's instructions.

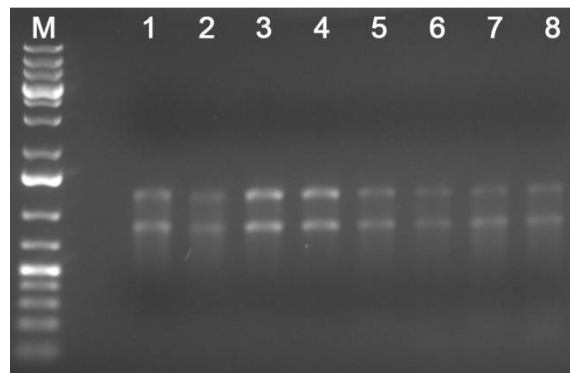


Fig. 17: Gel electrophoresis of RNA samples derived from one of the three biological replicates.

400 ng of RNAs were run on 1% TAE agarose gel with 8V/cm parameter. M: 1 kb DNA ladder Plus (Fermentas); Samples in lanes 1-4 are from the second day of sexual development (48 h after the induction of sexual development), while samples in lanes 5-8 are from the fourth day of sexual development (96 h after the induction of the sexual development). Lanes 1 and 5: *veA*⁺ control (H.ZS.450); lanes 2 and 6: *hmbAΔ veA*⁺ (H.ZS.521); Lanes 3 and 7: *hmbBΔ veA*⁺ (H.ZS.495); Lanes 4 and 8: *hmbCΔ veA*⁺ (H.ZS.531)

3.7. PCR for the amplification of components of the substitution cassette

The PCR was performed by using phusion Hot Start Polymerase (Fermentas) according to the manufacturer's instruction with the following protocol. The primers used in the PCR reactions are listed in Table 2 and Table 3.

PCR conditions:

Step 1: 94 °C 2 min (denaturation)

Step 2: 94 °C 30 s (denaturation)

Step 3: 62 °C 10 s (annealing)

Step 4: 72 °C for the required time depending on the size of the product (elongation)

Step 5: Step 2-4 was repeated 32 x

Step 6: 72 °C for 2 x elongation time (completion of elongation)

3.7.1. Double-joint PCR method

For the construction of five-partite cassette, the double-joint PCR method was performed using the strategy that was used for the assembly of a tripartite cassette composed of A, B and C components (Yu *et al.*, 2004). The method is briefly described below.

First round of PCR (amplification of basic components)

The A and C components were amplified by regular primer and the middle B component was amplified by using chimeric primers. The chimeric primers carried B component-specific sequences at their 3' half part. The 5' half of the chimeric forward primer carried A component-specific sequences, while the 5' half of the chimeric reverse primer carried C component-specific sequences.

The PCR products were checked by horizontal gel electrophoresis and the products were cleaned from reaction components by PCR cleaning kit (using Viogen kit according to the manufacturer's instruction). In case the PCR products carried aspecific products, we isolated the PCR product of A, B and C components from agarose gel (using Viogen kit according to the manufacturer's instruction).

Second round of PCR (assembly of the construct and amplification of the construction in one step)

In the second round of PCR, nested A and C component-specific primerpair was used. The assembly of the A component with B and B component with C component was ensured by the chimeric extensions on the B PCR product (A component-specific extension at the 5' end and C component-specific extension at the 3' end). The joined and

amplified PCR product can be used for transformation, or it can be used as a tripartite middle component for further assembly to construct a five-partite cassette (described in the result section).

3.7.2. Quantitative PCRs (qPCR and RT-qPCR)

For qPCR, the total DNA was extracted to assess *ycfp*, *hmbA*, *hmbB*, *hmbC* gene copy number in the transformant strains derived from various experiments by using *ycfp*, *hmbA*, *hmbB*, *hmbC* and *actA* (AN6542) reference gene specific primer pairs (Table 2 and Table 3). For RT-qPCR, total RNA was isolated from sexually developing mycelia by using RNeasy Plus Mini Kit (Qiagen) or TRIsure reagent (Bioline) with RNase-Free DNase Set (Qiagen) according to the manufacturer's instructions and cDNA synthesis was carried out on 1 µg RNAs with a mixture of oligo-dT and random primers using the RevertAid First Strand cDNASynthesis Kit (Fermentas). The qPCR reactions were executed by using Maxima SYBR Green qPCR Master Mix (2×) (Thermo Scientific) in 20 µl final volume as follows:

- 200 – 500 ng DNA or cDNA
- 0.4 µM – 0.4 µM specific primers (Table 2 and Table 3)
- 1× Maxima SYBR Green qPCR Master Mix

The reactions were performed with C1000 Thermal Cycler with CFX96 Real-Time System (Bio-Rad) along with SYBR Green/Fluorescein qPCR Master Mix (Fermentas) reaction mixture and specific primers listed in Table 2 and Table 3.

Amplification conditions were as follows:

- Step 1: 95 °C 3 min
- Step 2: 94 °C 15 sec
- Step 3: 60 °C 30 sec
- Step 4: step 2-3 were repeated 40x
- Step 5: 60 °C – 95 °C with a 0.5 °C increment (melting curve analysis)

The transcript levels were measured by standard curve method (Larionov *et al.*, 2005) using three biological and three technical replicates. Used reference genes were selected according to the MIQE guidelines (Bustin *et al.*, 2009). We monitored the expression of five housekeeping genes in three biological replicates per mutant strain. These genes included *gpdA*, *eEF-3*, *tubC*, *hhtA* and *actA*. They encode for Glyceraldehyde-3-phosphate dehydrogenase (*gpdA*/AN8041), Elongation factor 3 (*eEF-3*/AN6700), beta-

tubulin (*tubC*/AN6838), histone H3 (*hhtA*/AN0733) and gamma-actin (*actA*/AN6542). The Cq values were analysed by the geNorm software (<https://genorm.cmgg.be/>) that calculates a gene expression stability measure (M) for the candidate reference genes (Vandesompele *et al.*, 2002). According to this analysis, the five tested reference genes had similar M value and thereby all were selected for the calculation of the expression normalization factor. The expression normalization factor was calculated by taking the geometric mean of the expression levels (determined by standard curve analysis) of the *actA*, *hhtA*, *tubC*, *gpdA*, *eEF-3* reference genes. The expression normalization factor was calculated for each replicated datasets. The resulted normalization factors were then used to normalise gene expression values of genes of interest.

The heat map was developed by using the ggplot2 package in R programming environment (<https://www.R-project.org/>). Furthermore, a hierarchical clustering was too performed on the transcripts based on Euclidean distances using the complete linkage method (Quackenbush 2001). The Venn diagrams of all three samples were created by using the following website: <http://bioinfogp.cnb.csic.es/tools/venny/>.

3.7.3. List of primers

Primers used in the study of the role of HMGB proteins in sexual development are listed in Table 2. Primers used in the study of the intracolonic localization of STC production are listed in Table 3.

Table 2. List of primers used in the study of the role of HMGB proteins in sexual development

Deletion of <i>hmbA</i> and <i>hmbC</i>	
<i>hmbA</i> up frw	5'- ctctgacctgccacgaggccttgctctatg-3'
<i>hmbA</i> up rev	5'- ggtgaaggctctgaagctgttgacgaagag3'
<i>hmbA</i> up nested frw	5'- ggagacatttcgaactgtatcagggctaac-3'
<i>hmbA</i> ribo chim frw	5'-ctcttcgtccaacagcttcagacctcaccgtacgtagttagattcaggcacattgaagcg-3'
<i>hmbA</i> ribo chim rev	5'-cggagggtcaagcgactcgacactaagggtggaaaactgccatgactactaggtgggtgctatc-3'
<i>hmbA</i> down frw	5'- caccttagtgctgagtcgcttgacctccg -3'
<i>hmbA</i> down rev	5'- gcatacaatgcgagcacgggtgctgctatc -3'
<i>hmbA</i> down nested rev	5'- cgggtgctgttgctgcttgaggacgaggag -3'
<i>hmbC</i> up frw	5'- gctgtattacgtcatgtacggagtag -3'
<i>hmbC</i> up rev	5- gcgagggaatgggtatgctagttg -3'
<i>hmbC</i> up nested frw	5'- ctgacattgagattctgagccacaac -3'
<i>hmbC</i> paba chim frw	5'- caactagcataccattcctcgcgcacatagctattacagtatgtttgagac -3'
<i>hmbC</i> paba chim rev	5'- gaaaaccaatttactcgtcatcgccgtagttgcttgaatggctaacgagccattg -3'
<i>hmbC</i> down frw	5'- ggcgatgacgagtaaatggtttc -3'
<i>hmbC</i> down rev	5'- taatctgctcttcgatccaattcc -3'
<i>hmbC</i> down nested rev	5'- catccgttgacgagccgatgatc -3'
<i>hmbA</i> down nested rev	5'- cgggtgctgttgctgcttgaggacgaggag -3'
PCR products for cloning	

hmbA prom NotI frw	5'- <u>tttttttgcggccgcgatcctcaatgaaccttgccttg</u> -3'		
hmbA term NheI rev	5'- <u>tttttttctagcgtctgctgtgatattggaggacg</u> -3'		
hmbB NcoI frw	5'- <u>tttttttccatggctctcaaacctcattcgacg</u> -3'		
hmbB BamHI rev	5'- <u>tttttttggatccccttcattcatccttgctcgatttctgttc</u> -3'		
hmbC NcoI frw	5'- <u>tttttttccatggctaaaaacgattcaagaccg</u> -3'		
Other gene specific primers			
hmbA frw	5'- atgcctaaggccaatctaccgcaagacc -3'	veA DM rev	5'- tctccgcgccgtctc -3'
hmbA rev	5'- ttaggacgactcctcatcctcttcggcttc -3'	veA frw	5'- agcccatccagcccatct -3'
hmbC frw	5'- cagccagctcaaatcgcttg -3'	veA rev	5'- tctccgcgccgtctc -3'
hmbC rev	5'- cagcaacctctcgcggtagc -3'	veA seq frw	5'- gacgacaagtatcgcttgaag -3'
veA DM frw	5'- tgtgttatccatcaagagg -3'		
Real Time PCR			
hmbA ReTi frw	5'- aaagatgctcgggtgagaagtg -3'	lreA ReTi frw	5'- tgcctttgactctgtgacc -3'
hmbA ReTi rev	5'- ctctgaccgcttctgtcag -3'	lreA ReTi rev	5'- ttctcattgtaccctgttagcc -3'
hmbB ReTi frw	5'- aagactacaagaccaagaagacc -3'	lreB ReTi frw	5'- gaagaacatctgtatcccact -3'
hmbB ReTi rev	5'- ttgctcctcagtcagaacct -3'	lreB ReTi rev	5'- ctagtaccctgcttatgcc -3'
hmbC ReTi frw	5'- cattctcctgtacatgcatcac -3'	silA ReTi frw	5'- caacctaccgcaagaactc -3'
hmbC ReTi rev	5'- gtacctcgtttgagacatct -3'	silA ReTi rev	5'- tcatttccgctcgatactacag -3'
veA ReTi frw	5'- tttctcatacccgaacagac -3'	silG ReTi frw	5'- atcgtacctctcctaataacca -3'
veA ReTi rev	5'- gggctcactcctgcttatgg -3'	silG ReTi rev	5'- ttgttgggaatgaactgctg -3'
rosA ReTi frw	5'- aacaagtcataattaccacggct -3'	cpcA ReTi frw	5'- ctctgtccacaaccaaacac -3'
rosA ReTi rev	5'- tgtctctttactcgtttacctc -3'	cpcA ReTi rev	5'- gcaacagatcagattcgtc -3'
nrdA ReTi frw	5'- tccactccatctttcacct -3'	atfA ReTi frw	5'- aagacggatgatccactcag -3'
nrdA ReTi rev	5'- ggttcacaaactcatcctcgg -3'	atfA ReTi rev	5'- tcttctcttctgattcgcc -3'
nsdC ReTi frw	5'- cgtcaacctagcacttacc -3'	actin ReTi frw	5'- ggtatcatgatcggtatggg -3'
nsdC ReTi rev	5'- gccatgactgtaggaggag -3'	actin ReTi rev	5'- tatctgagtgtgaggatacca -3'
nsdD ReTi frw	5'- cagtcgctccatctatacac -3'	laeA ReTi frw	5'- ggatattcgcacatctccgt -3'
nsdD ReTi rev	5'- cactgtttggetgttgagg -3'	laeA ReTi rev	5'- aatgccgttccatctagtac -3'
dopA ReTi frw	5'- attaccgccgatatgctcc -3'	nosA ReTi frw	5'- atattgcctcccaattccc -3'
dopA ReTi rev	5'- gagatataatcccccattcct -3'	nosA ReTi rev	5'- caaatgctgtgttctggc -3'
stuA ReTi frw	5'- caacagtgtagcatcctcag -3'	velC ReTi frw	5'- tgttgatgctctctgaccc -3'
stuA ReTi rev	5'- taaggcgagtagttgagcag -3'	velC ReTi rev	5'- gtcattggagttgtgttcgt -3'
steA ReTi frw	5'- ggagatgtctactgggtctg -3'	medA ReTi frw	5'- aatgaccgacatataagccag -3'
steA ReTi rev	5'- ggaatggaaagtctcgtc -3'	medA ReTi rev	5'- cattggcgacttctcctc -3'
samB ReTi frw	5'- taatcacaatgataacgcacag -3'	mat2 ReTi frw	5'- gctatgaaatccaacacagtc -3'
samB ReTi rev	5'- atcacggaagtaagagaataggg -3'	mat2 ReTi rev	5'- ggacttcatctcgtagacc -3'
devR ReTi frw	5'- ctctcctcctcactctcgtc -3'	vosA ReTi frw	5'- gcgtaaatggaacataccc -3'
devR ReTi rev	5'- gggtagtattgtgcgactgg -3'	vosA ReTi rev	5'- gggtatccatcataggtgtc -3'
flbC ReTi frw	5'- ccgtatatccagcttccgtg -3'	velB ReTi frw	5'- ggcatcctatcagacaatcca -3'
flbC ReTi rev	5'- gaaacagagaccgagtagggc -3'	velB ReTi rev	5'- cgccatagtagttgcttactc -3'
flbE ReTi frw	5'- tctacatcgtttgcacaacc -3'	cpcB ReTi frw	5'- gtacaccatcaccgacaagg -3'
flbE ReTi rev	5'- ccgtcttctaaatgagtcag -3'	cpcB ReTi rev	5'- gagacgatgacaggggtctg -3'
fhpA ReTi frw	5'- gtctagctactcctcgtcca -3'	grrA ReTi frw	5'- gaactgccatctatcctttag -3'
fhpA ReTi rev	5'- ctacttctgatgactttgcgtg -3'	grrA ReTi rev	5'- tgtagcgttgatcaagagcc -3'
rcoA ReTi frw	5'- tcagatattcgacgtaactctgg -3'	AN1962 ReTi frw	5'- ccttaacaagatcaaaactgctgg -3'
rcoA ReTi rev	5'- gctgcgaatgtagatccc -3'	AN1962 ReTi rev	5'- catcaacggcaataacaggtc -3'
AN3549 ReTi frw	5'- aaagtcatagggaaggtcatctg -3'	AN3667 ReTi frw	5'- catacctaactcgggttaagag -3'
AN3549 ReTi rev	5'- gctccactccaacatcatctc -3'	AN3667 ReTi rev	5'- ggtgttctctgttccaactg -
AN3580 ReTi frw	5'- gccaaagcatcaaagttcca -3'	AN3580 ReTi rev	5'- cttaggagtcagaggagca -3'

Underlined letters in the primer sequences or in the primer names refer to the restriction sites designed within. Italic letters at the 5' end refer to the chimeric nature of the primer.

Table 3. List of primers used in the study of the intracolonic localization of STC production

Component A	
stcO up frw	5'- ctgtcgtagtagctgaggtcgc-3'
stcO up NLS chim rev	5'- gttgatggggcctcgtccatcctgatgtaggattaggatagaatgtatagag- 3'
Component B1	
NLS frw	5'- catctgttcagcctatctacggac-3'
NLS CFP chim rev	5'- gaataattcttcaccttagacgaaggtcctccatccgagctgaac-3'
Component B2	
CFP NLS chim frw	5'- gttcagactcggatggaggaccttcgtctaaaggatgaagaattattcactggtg- 3'
CFP AfpYROA chim rev	5'- cacagtaacatcctcttctgagatcgtgcctgttatccctagcggatctg- 3'
Component B3	
AfpYROA CFP chim frw	5'- ccgctagggataacaggcacgatctcagaagaggatgttactgtg-3'
AfpYROA down rev	5'- gaaattctgtctgccgaaggctc-3'
Component C	
stcO down AfpYROA chim frw	5'- caccctgacagcggccataaggaggacaatattactgctagtcgctc-3'
stcO down rev	5'- gcgacggatttacgatagagtcagc-3'
Components B1/B2/B3	
NLS stcO up chim frw	5'- ctctatacttctatcctaatcctacatcaggatggacgagggcccatcaac- 3'
AfpYROA stcO down chim rev	5'- gagcgactagcagtaattgtccaccttatggcgtgtcagggtg-3'
Components B1/B2/B3 and C	
stcO upst nest frw	5'- ctcacagaaccaacaatgccttc-3'
stcO down nest rev	5'- ggtcaggactactgtgtttcgaag-3'

3.8. Southern blot analysis

Southern blot analysis was carried out according to Sambrook *et al.*, (1989) using Hybond-N membrane (Amersham/GE Healthcare) and DIG DNA Labeling and Detection Kit (Roche) according to the manufacturer's instructions. For DNA blotting depurination solution (0.25 M HCl solution), denaturation buffer (0.5 M NaOH, 1.5 M NaCl), neutralisation buffer (0.5 M Tris, 1.5 M NaCl (pH 8.0) and 20x SSC (3 M NaCl, 0.3 trisodium citrate, pH 7.0) for the capillary blot were used. Hybridisation was performed with DIG-DNA labeled DNA probe containing hybridisation buffer (5x SSC, 0.1% sodium lauroyl sarcosinate, 0.02% SDS, 1% blocking reagent (Roche)). The washing and detection of the hybridization signal was done as follows. The membrane was washed twice with washing buffer I (2x SSC, 0.1% SDS) for 5 min at room temperature and twice with washing buffer II (0.1% SSC, 0.1% SDS) for 15 min at 65 °C. The detection was performed at room temperature. The filter was washed with buffer 1 (0.01 M maleic acid, 0.015 M NaCl (pH 7.5)) for 2 min, and with buffer 2 (1% blocking reagent (Roche) dissolved in detection buffer I) for 30 min. The filter was incubated in fresh buffer 2 (1% blocking reagent (Roche) dissolved in detection buffer I) supplemented with alkaline phosphatase antibody conjugate (Anti-Digoxigenin-AP Fab fragments, Roche) for 30 min. The filter was washed with buffer 3 (0.1 M Tris, 0.1 M NaCl, 50 mM MgCl₂ (pH 9.5).

Then the colour reaction was carried out in buffer 3 supplemented with NBT-BCIP (DIG DNA Labeling and Detection Kit, Roche). After the full development of the hybridization signals the reaction was terminated by washing the filter in distilled water.

3.9. Microscopy

In order to study the sexual structures of *A. nidulans*, cleistothecia were collected from the colonies by needle and the cleistothecia were cleaned individually by rolling them on the surface of the agar plate in order to eliminate mycelia, conidiospores and Hülle cells attached to the surface. Thereafter, the samples were mounted on slides by applying 1x PBS buffer (150 mM sodium phosphate, 150 mM sodium chloride and pH7.4). Then the samples were crushed between the slide and cover slip, thereby enable to see the sexual structures under the light microscope.

In order to study the intracolony localization of STC through the usage of a reporter system, we used fluorescent microscopic analysis. Samples were prepared from cellophane cultures. *A. nidulans* strains were spot inoculated on solid nicotinic acid-glucose MM covered with cellophane and incubated in dark at 37 °C for 48, 72, and 92 h. Sections of the colonies grown on the surface of cellophanes were cut longitudinally and mounted on to slides by using PBS (150 mM sodium phosphate, 150 mM sodium chloride and pH7.4) and cover slips. Olympus BX51 fluorescent microscope U-MNU2 with Olympus cube (BP 360–370 excitation filter, DM 400 dichromatic mirror, LP 420 emission filter) and U-M41035 RFP Olympus cube (U-HQ546/12, U-Q560LP, U-HQ6058/75m) was used for taking the microscopic images.

3.10. Thin layer chromatography

Thin-layer chromatography was performed for the analysis of STC contents. The sample was prepared from the 3 and 4-days old cultures grown on MM with nitrate N-source and lactose C-source. Agar blocks were excised from the centre of the colonies by a 10 mm diameter cork borer and after smashing the blocks, STC was extracted from them by incubating the smashed agar blocks in 10 ml chloroform for overnight. Then the samples were filtrated and the chloroform was concentrated into 1 ml final volume at 65 °C. 20 µl of the samples were loaded on Kieselgel 60 (Merck) plates and developed in toluol:ethyl-acetate:acetic-acid (80:10:10). The secondary metabolites were detected and recorded under UV after spraying the plate with 15% AlCl₃ (dissolved in ethanol), and

heated it to 100 °C for 10 min. For identification of STC, STC standard (Sigma) was used on the plate.

3.11. Genetic crosses

Heterozygotic crosses were carried out according to Pontecorvo (Pontecorvo *et al.*, 1953). The *veA* allele of each *veA*⁺ progeny was checked by using the "veA DM frw" – "veA DM rev" and "veA frw" – "veA rev" primer pairs (Han *et al.*, 2010) and also sequenced with the "veA seq frw" primer. Homozygotic crosses were always self-crosses made by sealing 2-day-old cultures on CM by using scotch tape. After 3 weeks of incubation at 37 °C, the fruiting bodies were collected and the progeny were analysed. Each day following the fourth day of incubation one of the replicate plates was opened and the sexual structures were studied under stereo- and light microscopes.

3.12. Construction of *stcO* reporter gene substitution cassette and obtaining *stcO* promoter-NLS-ycfp carrying strain

The *stcO* reporter cassette was constructed by the double-joint PCR method as described by Yu *et al.*, (2004). The cassette was composed of five components: the *stcO* (AN7811) promoter and its upstream region (component A, nested size 2436 bp) followed by the nuclear localization signal (NLS) of the transcription factor *prnA* (component B/1, nested size 550 bp) (Pokorska *et al.*, 2000) from wild type *A. nidulans* (HZS.145) (Amon *et al.*, 2017) ; the yCFP (Cyan Fluorescent Protein optimized for yeasts) coding gene (component B/2, 944 bp) amplified from plasmid pKT174 (Sheff *et al.*, 2004); the *pyroA* homologue (component B/3, nested size 2414 bp) of *A. fumigatus* (Afu5g08090 from *A. fumigatus*); and the downstream flanking sequence of the *stcO* gene (component C, nested size 2421 bp). The double-joint PCR was performed by using two consecutive assembly steps (assembly of B/1-B/2- B/3 and A-B1/2/3-C). The five components were amplified with primer pairs "stcO up frw" – "stcO up NLS chim rev" (component A, 3004 nt), "NLS frw" – "NLS CFP chim rev" (component B/1, 911 nt), "CFP NLS chim frw" – "CFP AfpyroA chim rev" (component B/2, 944 nt), "AfpyroA CFP chim frw" – "AfpyroA down rev" (component B/3, 2628 nt), and "stcO down AfpyroA chim frw" – "stcO down rev" (component C, 2893 nt). B/1, B/2, and B/3 components were assembled by using "NLS stcO up chim frw" and "AfpyroA stcO down chim rev primers" (B1/2/3 component, 3908 bp). The A, B1/2/3, and C components were assembled with "stcO upst nest frw" and "stcO down nest rev" primers. Components A and C served for targeting the *stcO* locus

and supporting homologous recombination, while component B1/2/3 provided the nuclear localisation yCFP and the selection marker gene. The five-partite assembled PCR product was transformed into strain HZS.576 and 9 out of hundreds of pyridoxine prototroph transformants were selected for further analysis. A Southern analysis was performed with a 2421 bp downstream flanking region of *stcO* (component C, amplified by primer pair “stcO down AfpyroA chim frw” and “stcO down nest rev”) as gene probe on BamHI digested total DNA of transformants. Based on the Southern analysis, all selected transformants carried a single copy integration of the five-partite cassette in the targeted *stcO* locus. Single copy integration in transformants was further confirmed by checking the copy number of *ycfp* using qPCR with CFP frw and CFP rev primers. The copy number was calculated as 2^Y , where $Y = Cq_{actA} - Cq_{ycfp}$. „Cq_{actA}” stands for the Cq value of the *actA* reference gene, „Cq_{ycfp}” stands for the Cq value of the *ycfp* gene; and Y stands for the difference of the two Cq values, Cq_{actA} and Cq_{ycfp}.

3.13. Determination of the size of cleistothecia and germination ability of ascospores

The size measurement of the cleistothecia was done by collection of random mass of cleistothecia from one spot of the colony and by choosing ten representative cleistothecia for purification. In order to measure their sizes, the cleaned cleistothecia were documented along with a regular ruler by capturing the images by using a live camera. To quantify the sizes, image analysis in Adobe Photoshop was carried out.

In order to determine the germination ability of the ascospores, stepwise ten times dilution series were prepared from the ascospore samples (ascospore number was counted by using Burker chamber) in 500 µl final volume, and 50 µl volumes from these dilutions were plated onto CM agar plates followed by incubation at 37 °C for 2–4 days. The colony-forming units (CFU) were counted and the germination ability of the ascospores was calculated from the number of ascospores and number of CFUs.

3.14. Statistical Analysis

All statistical analysis was performed by using GraphPad Prism version 5.02 for OSX (GraphPad Software, San Diego, CA). The significant differences between sets of data were determined by one-way ANOVA test, two-way ANOVA or Mann-Whitney *U*-test according to the data.

4. RESULTS

4.1. Documentation of sexual structures in the control strain during development

During the sexual development, the first sign of differentiation is the formation of Hülle cells (Fig. 18). They are round, multinucleate, thick walled cells, which protect and nurse the developing fruiting body. At the second developmental stage, a primordium is formed by the generation of dikaryotic ascogenous hyphae and cells of the pericarp (Fig. 18). Later, at the third stage, the primordium develops to μ -cleistothecia, where the pericarp becomes more prominent (Fig. 18). Inside the μ -cleistothecia the ascogenous hyphae proliferate, ascus mother cells and hooks are formed (Fig. 18). In a young cleistothecia immature asci can be seen with transparent ascospores. During maturation the ascospores accumulate red pigments and the pericarp cells are hardened and gain dark blackish colour by pigment accumulation (Fig. 18). When the cleistothecia are mature, the colour of the fruiting bodies is shiny black, and they are filled with red, free-standing ascospores (Fig. 18). A mature cleistothecium may contain around 80,000 viable ascospores in *A. nidulans* (Pontecorvo, 1953; Braus *et al.*, 2002).

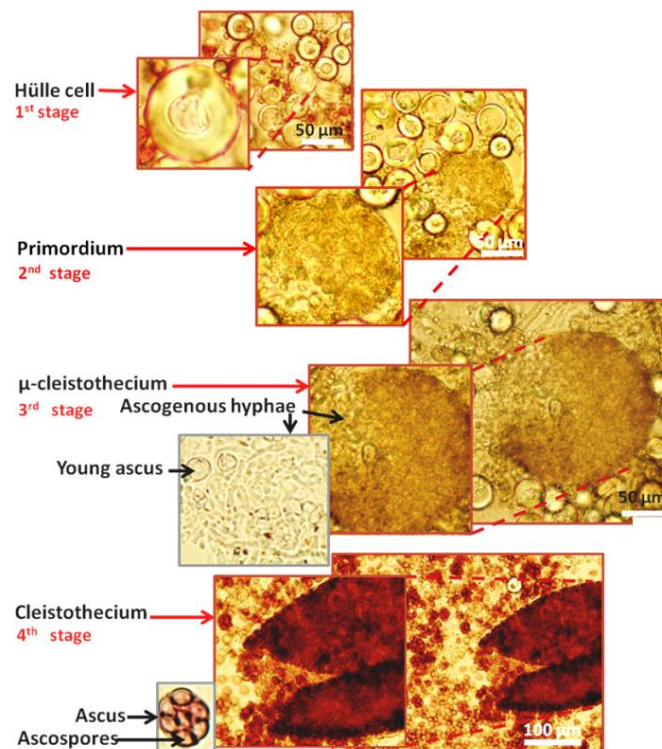


Fig. 18: Biogenesis of cleistothecia.

Images were taken from Wt strain at different time points of the sexual development. Plates were incubated in complete darkness prior documentation.

The experimental set up for the investigation of sexual structures involved the study of non-cleaned and cleaned cleistothecia (Fig. 19). In case of non-cleaned cleistothecia the microscope prepares were made by pulling a nest/ μ -cleistothecium/cleistothecium out of the colony and immediately mounting the sample onto the slide by crushing the cleistothecia between the slide and the cover slip (Fig. 19). Such samples contain Hülle cells along with vegetative and asexual reproductive structures. In case of cleaned cleistothecia the cleistothecia pulled out of the colony were subjected to purification prior mounting them on slides. The purification was executed by rolling the cleistothecia on the surface of an empty agar plate in order to eliminate attached vegetative hyphae, conidia and Hülle cells from their surface. In the cleaned-cleistothecia samples we can see only ascogenous hyphae, asci and ascospores.

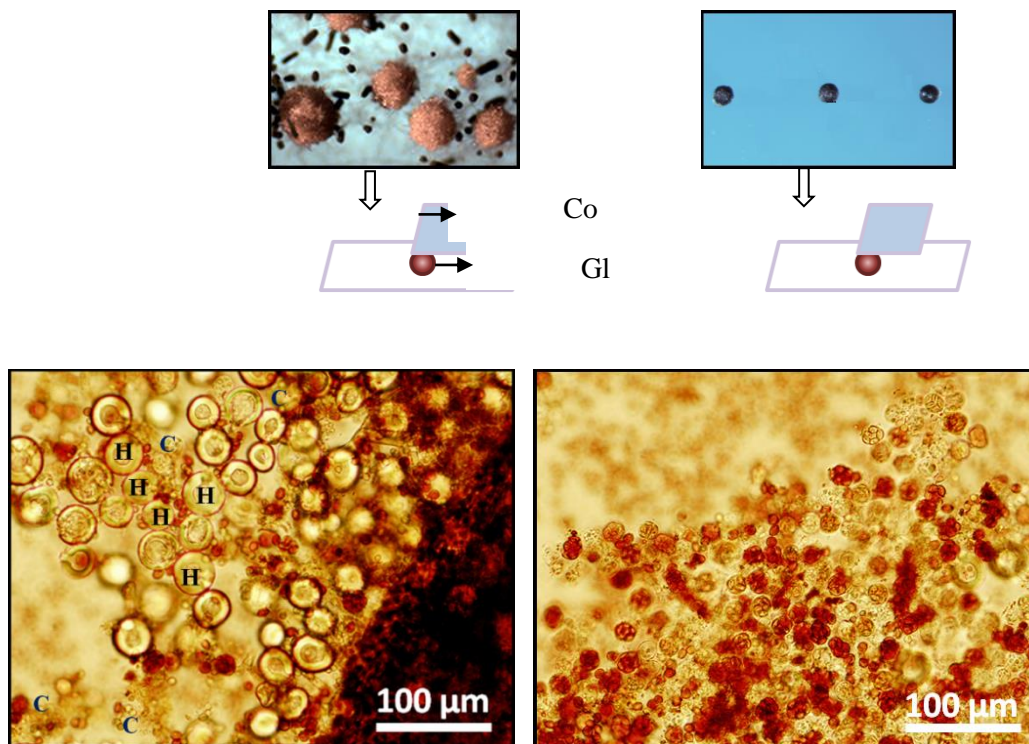


Fig. 19: Preparation of samples for the study of sexual structures from non-cleaned and cleaned cleistothecia

The schematic presentation at the top illustrates non-cleaned and cleaned cleistothecia objected to mounting. At the bottom left, image of non-cleaned cleistothecium is shown, while at the bottom right, the image of a cleaned cleistothecium is shown. H indicates Hülle cells, C indicates conidiospores. The cleaned cleistothecium at the bottom right is free from Hülle cells, conidiospores and vegetative hyphae. Scale bars are shown.

4.2. Development of *hmb* deletion strains in *veA*⁺ genetic background and analysis of their growth

We developed *hmbA* Δ , *hmbB* Δ and *hmbC* Δ deletion strains in *veA1* genetic background earlier (Karácsony *et al.*, 2014; Bokor *et al.*, 2019). The *hmbB* Δ strain has already been studied in detail and function of HmbB protein was reported (Karácsony *et al.*, 2014). The *hmbA* Δ and *hmbC* Δ strains were developed in the frame of the PhD study of Z. Karácsony, however the role of HmbA and HmbC proteins in the sexual development of *A. nidulans* was studied in this work. Since we aimed to study the potential functional interaction of VeA1 with the HMGB proteins, we carried out genetic crosses to obtain the deletions in *veA*⁺ genetic background (strains are listed in Table 1). In order to confirm that the observed phenotypes of the deletion mutants are the consequence of the deletions, we constructed complementation strains by the transformation of *hmbA*, *hmbB* and *hmbC* expressing integrative vectors to the cognate deletion strains (see 3.3. section of Materials and Methods). The *hmbB* and *hmbC* genes were expressed from the constitutive *gpdA* promoter (P_{gpdA}), while *hmbA* was expressed from its native promoter (P_{hmbA}). *In trans* expression of P_{hmbA} -*hmbA*, P_{gpdA} -*hmbB* and P_{gpdA} -*hmbC* in the corresponding *hmbA*, *hmbB* and *hmbC* deletion strains mitigated but did not completely abolish the deletion phenotype with respect to colony macromorphology and ascospore production/viability (see below). The reason for this partial complementation may be the *in trans* expression of the constructs and/or usage of the constitutive *gpdA* promoter in the case of complementation of *hmbB* and *hmbC* deletion.

Macromorphological analysis of the mutant strains was carried out by comparison of their growth ability on CM (Fig. 20). We found that the growth of the *hmbC* Δ strains were not different from the *hmbC*⁺ controls, while the *hmbA* Δ strains formed smaller colonies compared to those of the *hmbA*⁺ controls due to slower growth rate. The colonies of the *hmbB* Δ strains were also smaller than those of the controls, but as we had already revealed it in our earlier work, the reason of the reduced growth was due to delayed conidiospore germination rather than due to a slower growth rate (Karácsony *et al.*, 2014).

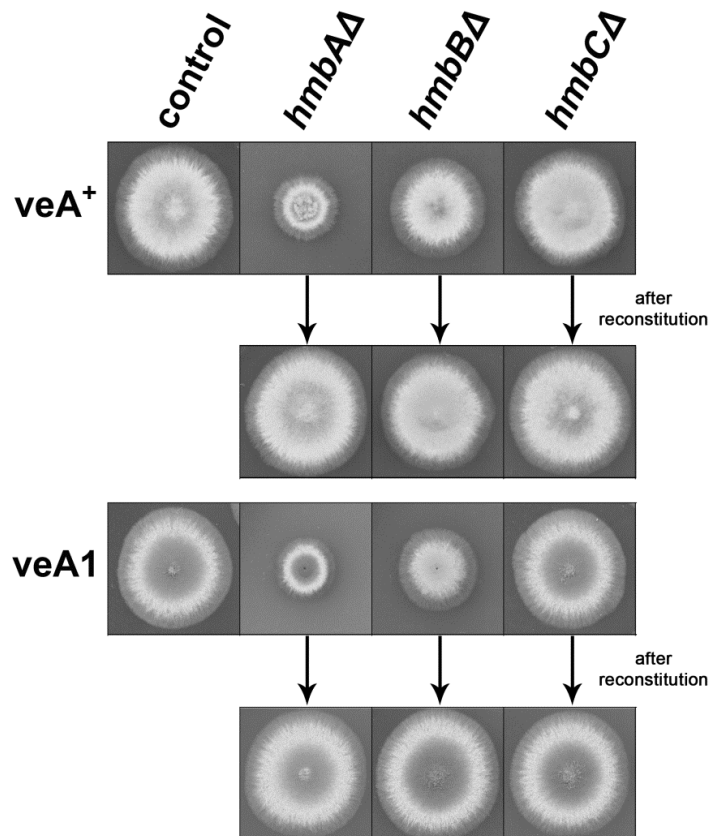


Fig. 20: Growth of veA^+ and $veA1$ controls and $hmbA\Delta$, $hmbB\Delta$ and $hmbC\Delta$ strains in both veA^+ and $veA1$ background.

The strains were inoculated on CM and incubated for 2 days at 37°C. Used strains were veA^+ control (H.ZS.450), $veA1$ control (H.ZS.145), $hmbA\Delta veA^+$ (H.ZS.521), $hmbA\Delta veA1$ (H.ZS.239), $hmbB\Delta veA^+$ (H.ZS.495), $hmbB\Delta veA1$ (H.ZS.280), $hmbC\Delta veA^+$ (H.ZS.531), $hmbC\Delta veA1$ (H.ZS.338), $hmbA\Delta veA^+ hmbA$ reconstituted (H.ZS.678), $hmbA\Delta veA1 hmbA$ reconstituted (H.ZS.621), $hmbB\Delta veA^+ hmbB$ reconstituted (H.ZS.680), $hmbB\Delta veA1 hmbB$ reconstituted (H.ZS.677), $hmbC\Delta veA^+ hmbC$ reconstituted (H.ZS.679), $hmbC\Delta veA1 hmbC$ reconstituted (H.ZS.676). The complete genotypes are listed in Table 2.

4.3. Sexual development of hmb deletion strains

The sexual development of veA^+ and $veA1$ control strains along with that of the $hmbA\Delta$, $hmbB\Delta$ and $hmbC\Delta$ strains with both veA^+ and $veA1$ background were documented from the fifth day to the eleventh day of incubation on selfing cultures on a daily basis (Fig. 21). Indeed all the deletion mutants were able to produce Hülle cells and cleistothecia with different extent of defects in ascospore formation and ascospore viability. Interestingly, the appearance of a reddish granular amorphous (RGA) material was observed in all types of deletion strains. Production of RGA material was first

described in the barren cleistothecia of MAT1-1 and MAT1-2 protein coding gene (*matB* and *matA*, respectively) deletion strains (Paoletti *et al.*, 2007).

The *veA*⁺ control strain formed primordia on day 5 (picture A on Fig. 21) and formed mature ascospores on day 10. The *veA1* control developed more rapidly than the *veA*⁺ control and μ -cleistothecia formation was observed on day 5 (picture A₁ on Fig. 22) and mature free ascospores were seen from day 6 (picture B₁ on Fig. 22). The time course of the sexual development of *hmbC* Δ *veA*⁺ strain was not different from that of *veA*⁺ control, however the primordium formation of *hmbA* Δ *veA*⁺ and *hmbB* Δ *veA*⁺ strains was delayed by one-two days in comparison to that of the *veA*⁺ control (images C, E and F on Fig. 21). The sexual development of *hmbA* Δ *veA1* and *hmbB* Δ *veA1* strains began one-two days earlier compared to their *veA*⁺ counterparts (images C₁ and F₁ on Fig. 22), a phenomenon that was also observed in the relation of the *veA*⁺ and *veA1* control strains. However, the *veA1* background did not result in the acceleration of sexual development in the *hmbC* Δ *veA1* mutant. The primordium and μ -cleistothecia formation of *hmbC* Δ *veA1* were observed one day later compared to the *hmbC* Δ *veA*⁺ strain (image H₁ on Fig. 22).

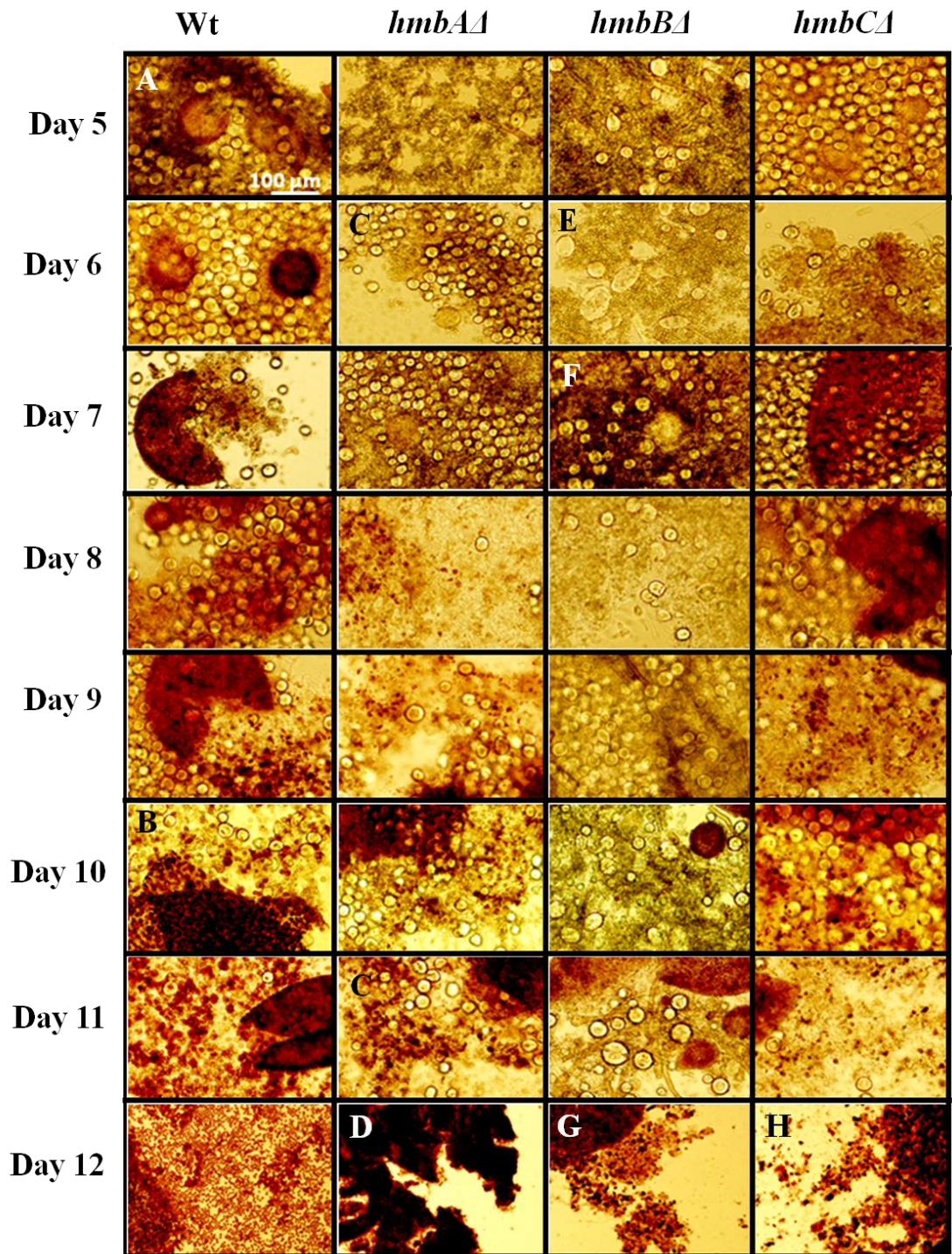


Fig. 21: Documentation of sexual structures formed in control and *hmbAΔ*, *hmbBΔ* and *hmbCΔ* strains with *veA*⁺ genetic background.

The images were taken from sexual structures from day 5 to day 11 of incubation. These images were taken from the non-cleaned cleistothecia samples except the images of the last row (day 12), which were taken from cleaned cleistothecia. Wt is HZS.450, *hmbAΔ* is HZS.489, *hmbBΔ* is HZS.499 and *hmbCΔ* is HZS.531. Selfing was done on CM at 37 °C under complete darkness and the plates were sealed by scotch tape. Images were taken by an Olympus BX51 microscope.

The 100 μm scale bar shown on image A refers to all images.

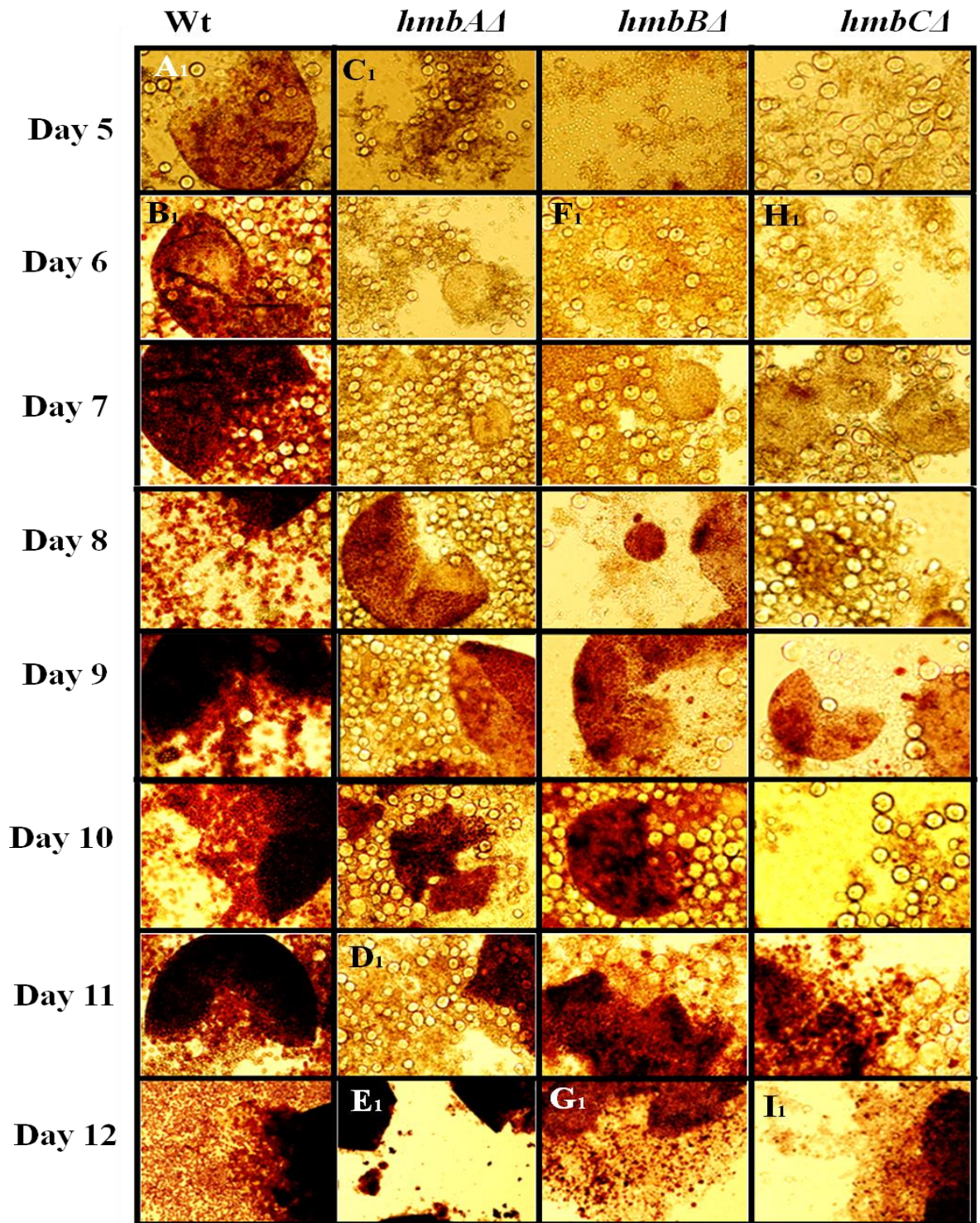


Fig. 22: Documentation of sexual structures formed in control and *hmbAΔ*, *hmbBΔ* and *hmbCΔ* strains with *veA1* genetic background.

The images were taken from sexual structures from day 5 to day 11 of incubation. These images were taken from the non-cleaned cleistothecia samples except the images of the last row (day 12), which were taken from cleaned cleistothecia. Wt is HZS.145, *hmbAΔ* is HZS.239, *hmbBΔ* is HZS. HZS.280 and *hmbCΔ* is HZS.338. Selfing was done on CM at 37 °C under complete darkness and the plates were sealed by scotch tape. Images were taken by an Olympus BX51 microscope. The 100 μm scale bar shown on image A₁ refers to all images

The mature *hmbAΔ* cleistothecia, collected on days 11 and 12 of incubation, were practically empty in both the *veA*⁺ (Fig. 21) and *veA1* background (Fig. 22). These cleistothecia contained RGA material, nearly zero amounts of ascogenous hyphae and sporadically detected ascospores. On day 12, the mature *veA*⁺ and *veA1 hmbBΔ* cleistothecia contained ascogenous hyphae, RGA material, a few asci in different maturation stages and a few matured, free ascospores (Fig. 21 and Fig. 22). Cleistothecia with somewhat improved quality and quantity of internal content could only be observed under highly specific conditions (detailed below). On day 12, the *veA*⁺ *hmbCΔ* cleistothecia still contained immature asci with transparent ascospores among the released, mature ascospores (Fig. 21). The *veA1 hmbCΔ* mutant frequently produced barren cleistothecia without any ascospores. However, when the *veA1 hmbCΔ* cleistothecia contained ascospores, these ascospores were always mature (Fig 22). RGA material was detected in both *veA*⁺ and *veA1 hmbCΔ* cleistothecia, but this was more pronounced in the *veA1* background.

4.4 Intracolony distribution and size of cleistothecia

In the case of the colonies of *veA*⁺ and *veA1* controls, cleistothecia were accumulated in the middle of the colony and were equally distributed in the rest of the area regardless whether the plates were sealed or not (Fig. 23).

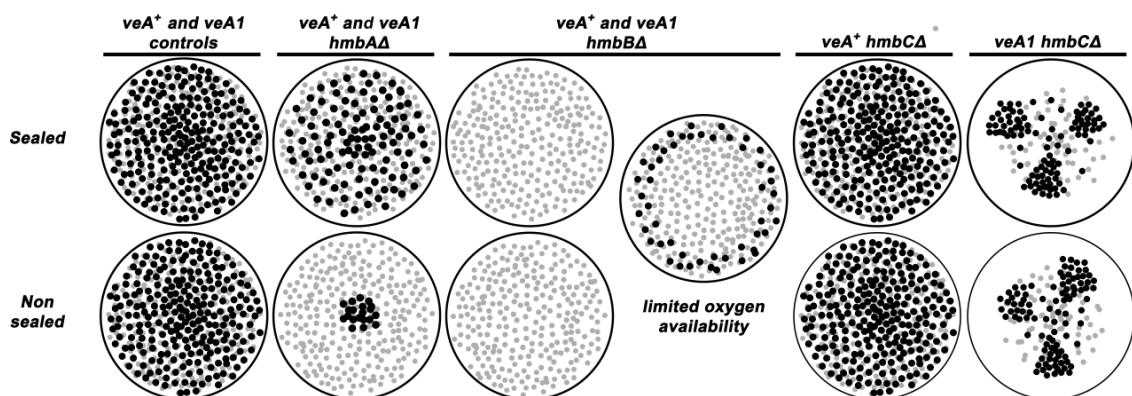


Fig. 23: Schematic representation of oxygen regulated distribution pattern of cleistothecia in control and *hmbAΔ*, *hmbBΔ* and *hmbCΔ* strains.

“Sealed” and “non-sealed” refer to conditions where plates are sealed with scotch tape or kept without sealing, respectively. “Limited oxygen availability” refers to the non-sealed condition with the applied medium almost entirely filling up the Petri dish. Small-sized grey dots mark micro-sized cleistothecia, black dots indicate normal-sized cleistothecia.

The size of the cleistothecia in *veA*⁺ and *veA1* controls was in the ranges of 183–304 μm and 216–304 μm, respectively (Fig. 24, Table 4). The distribution pattern of the *hmbAΔ* cleistothecia was detected to depend on oxygen availability. Oxygen-deprivation (via sealing the plates) resulted in a wild type-like distribution pattern both in the *veA*⁺ and the *veA1 hmbAΔ* strains (Fig. 23). However, when the plates were not sealed and thereby air exchange was not restricted, fruiting body formation was mainly exclusive to the central part of the colony in both the *veA*⁺ and the *veA1 hmbAΔ* strains (Fig. 23). The size of cleistothecia in the *veA*⁺ and *veA1 hmbAΔ* strains was in the ranges of 166–270 μm and 95–200 μm, respectively (Fig 24, Table 4).

Table 4. Summary of the phenotypic analysis of *veA*⁺ control and deletion strains

strain	time course of sexual development	median ascospore number per cleistothecium (n=10)	viability of ascospores (n=10)	RGA material	size of cleistothecia (n=10)	distribution of cleistothecia
wt (<i>veA</i> ⁺)	wild-type	3.7×10^5 $\pm 1.9 \times 10^5$	31.9% CFU	no	183–304 μm	wild-type like
<i>hmbAΔ veA</i> ⁺	delayed compared to wild-type	estimated 0–10	estimated 30% germinating	yes	166–270 μm	conditional**
<i>hmbBΔ veA</i> ⁺	delayed compared to wild-type	conditional* 4×10^4 $\pm 2.6 \times 10^4$	0.04% CFU	yes	conditional* 200–225 μm	conditional* at the perimeter of the colonies
<i>hmbCΔ veA</i> ⁺	wild-type	2×10^5 $\pm 7.3 \times 10^4$	6.9% CFU	yes	195–354 μm	wild-type like

* only upon medium level of oxygen restriction

** wild-type like distribution pattern in sealed plates; exclusive central accumulation in non-sealed plates

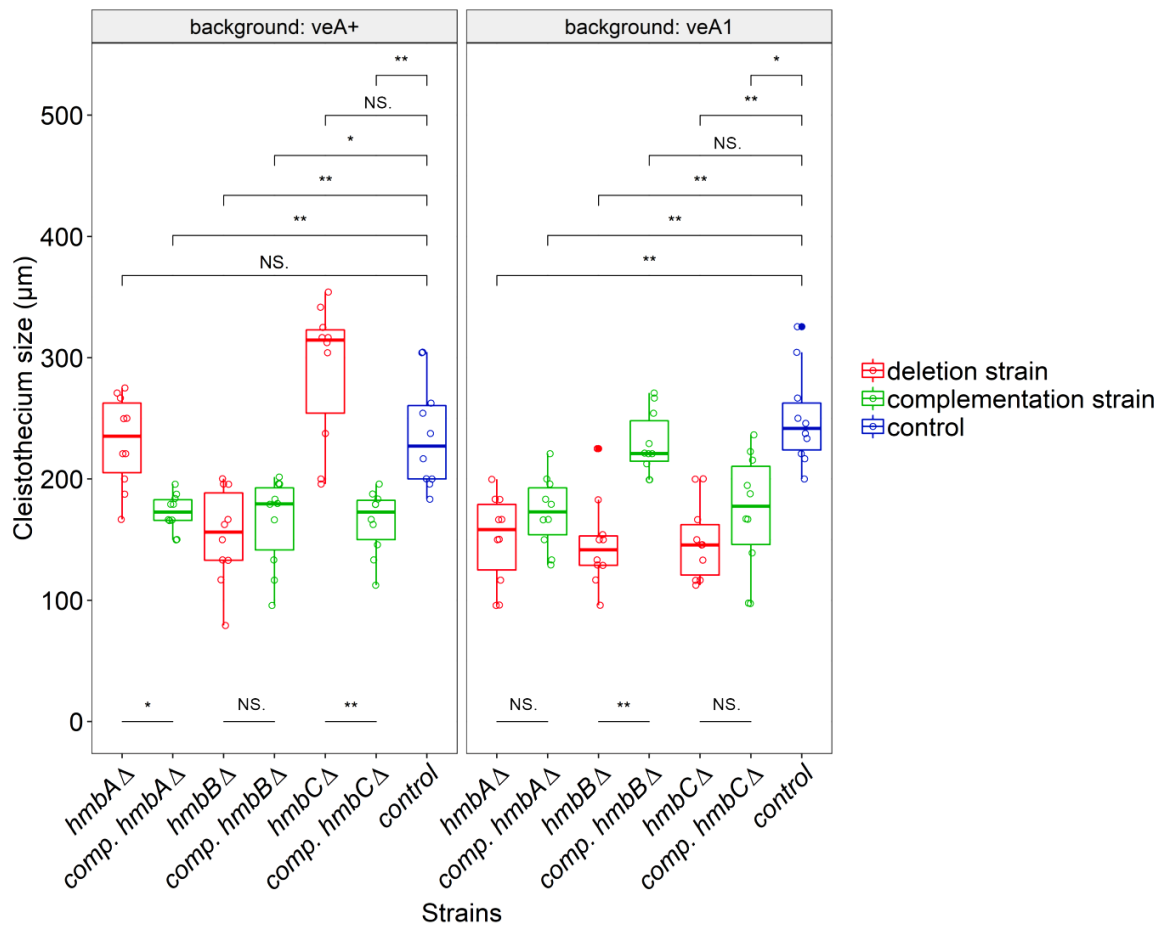


Fig. 24: Size of cleistothecia cleistothecia in *hmbA*Δ, *hmbB*Δ and *hmbC*Δ mutants in *veA*⁺ and *veA1* genetic backgrounds.

The boxplot shows the size of cleistothecia across the *hmbA*, *hmbB* and *hmbC* mutant and control strains in both the *veA*⁺ (left panel) and the *veA1* (right panel) genetic backgrounds. The strains are color-coded as follows: blue denotes control; red denotes deletion, green denotes complementation (comp.) strains originating from the corresponding deletion strains. Centre lines indicate the median of 10 independent cleistothecia measurements per strain. Mann-Whitney *U*-test was used to assess size differences between the mutant and control strains in the corresponding genetic background. */** indicates $p < 0.01/0.001$, NS indicates $p =$ not significant. Cleistothecia sizes were estimated by measuring the diameter of cleistothecia with a ruler. The strains used in the experiment are as follows: *veA*⁺ control (HZS.450), *veA1* control (HZS.145), *hmbA*Δ *veA*⁺ (HZS.521), *hmbA*Δ *veA1* (HZS.239), *hmbA*Δ *veA*⁺ with *hmbA* complementation (HZS.678), *hmbA*Δ *veA1* with *hmbA* complementation (HZS.621), *hmbB*Δ *veA*⁺ (HZS.495), *hmbB*Δ *veA1* (HZS.280), *hmbB*Δ *veA*⁺ with *hmbB* complementation (HZS.680), *hmbB*Δ *veA1* with *hmbB* complementation (HZS.677), *hmbC*Δ *veA*⁺ (HZS.531), *hmbC*Δ *veA1* (HZS.338), *hmbC*Δ *veA*⁺ with *hmbC* complementation (HZS.679), *hmbC*Δ *veA1* with *hmbC* complementation (HZS.676). The complete genotypes of the strains are listed in Table 1.

Selfing of the *hmbBΔ* strains (both *veA*⁺ and *veA1*) provided colonies with barren micro-sized cleistothecia and/or few small-sized cleistothecia (79-95 μm) with low ascospore content (~100 ascospores/cleistothecia) nearly all the time. However, selfing plates with few normal-sized cleistothecia (up to 200-225 μm), with improved ascospore content could also be obtained, sporadically (Fig. 24, Table 4). Systematic combination of environmental factors (light- and oxygen-availability) revealed that the *hmbBΔ* strain favors a medium-level of oxygen-restriction. Neither the sealed, nor the non-sealed plates provided normal-sized cleistothecia. We found that the height of the medium (40-45 ml) in the Petri dish (9 cm diameter) combined with keeping the plates unsealed was deterministic in obtaining normal-sized cleistothecia. Based on this phenomenon, we propose that the *hmbBΔ* strain needs a certain level of oxygen for the optimal sexual development in both *veA*⁺ and *veA1* backgrounds. The distribution of the sterile micro-sized cleistothecia was wild type-like, however when the environmental parameters favored the production of normal-sized cleistothecia, they were always formed at the perimeter of the colonies (Fig. 23).

The distribution and the size of the *veA*⁺ *hmbCΔ* cleistothecia were similar to that of the *veA*⁺ control (195-354 μm), whilst *veA1 hmbCΔ* produced equally-distributed, medium-sized (112-200 μm) cleistothecia in lower abundance compared to its *veA*⁺ counterpart (Fig. 24, Table 4). The *veA1 hmbCΔ* colonies tended to form conidia-depleted sectors, where the density of the cleistothecia was significantly increased (Fig. 23).

The size of cleistothecia is restored only in the *veA1 hmbB* complemented strain (Fig. 24). The other reconstitutions provided no improvement (*veA*⁺ *hmbB*, *veA1 hmbA* and *veA1 hmbC*) or even decreased (*veA*⁺ *hmbA* and *veA*⁺ *hmbC*) the size of cleistothecia (Fig. 24) most probably due to the *in trans* expression of the cognate genes and/or the usage of constitutive promoter in the case of *hmbB* and *hmbC* reconstitution.

4.5. Ascospore content of cleistothecia and viability of the ascospores in control and deletion strains with *veA*⁺ genetic background

The *veA*⁺ control strain contained 10⁵-10⁶ ascospores per cleistothecium, and 32% of them was able to form colonies (Fig. 25, Table 4). The number of ascospores in the *hmbAΔ veA*⁺ cleistothecia was less than 10 ascospores/cleistothecium (Fig. 25, Table 4).

The frequency of the viable *hmbAΔ veA⁺* ascospores could not be calculated by counting the colony forming units (CFU) due to extremely low (<10) ascospore numbers because CFUs might be also originated from mycelium-, conidiospore- or Hülle cell contamination of the cleaned cleistothecium samples. However, the germination rate of the *hmbAΔ veA⁺* ascospores does not necessarily reflect the viability (data not shown). Complementation of the *hmbAΔ* deletion (<10 ascospores per cleistothecium) by *in trans* expression of *hmbA* under the control of its native promoter resulted in $\sim 10^5$ ascospores per cleistothecium (with 38% viability rate) that was significantly lower than the wild-type control, but it nearly reached the productivity level of the control.

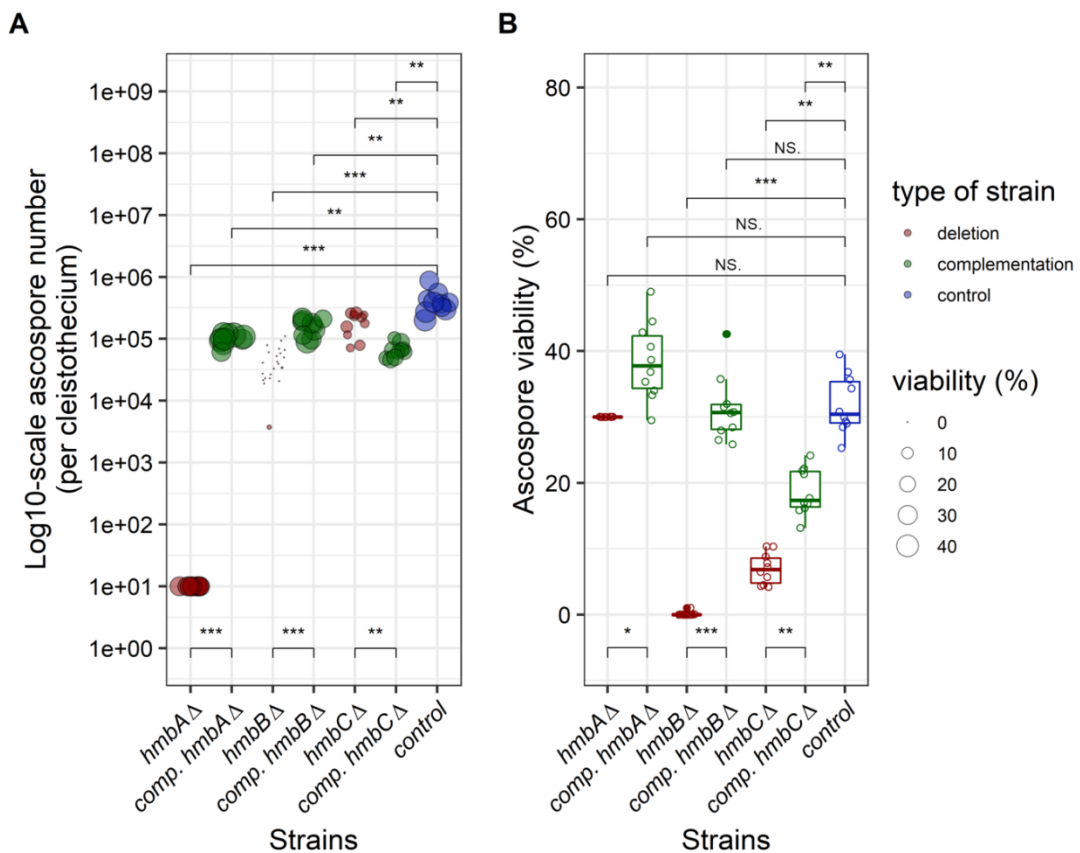


Fig. 25: Production and viability of ascospores produced by *hmbAΔ*, *hmbBΔ* and *hmbCΔ* mutants in *veA⁺* genetic background. Panel A: Graphical representation of the number of ascospores per cleistothecium. The figure shows the number of ascospores (on log₁₀-scale) per cleistothecium across the *hmbA*, *hmbB* and *hmbC* mutant and control strains in a *veA⁺* genetic background. The strains are color-coded as follows: blue denotes control; red denotes deletion, green denotes complementation (comp.) strains originating from the corresponding deletion strains. The bubbles mark the number of ascospores; the size of the bubbles is proportional to the viability of the corresponding ascospores. An estimated rate of germination was used as a proxy of viability in the case of *hmbAΔ* (explained in the main text). The number of ascospores was estimated based on 10 independent cleistothecia per strain. An estimated ascospore number was used in the case of *hmbAΔ* (explained in the main text). Mann-Whitney *U*-test was used to assess the differences between the numbers of ascospores of the mutant and the control strains. */**/** indicates $p <$

0.01/0.001/0.0001. **Panel B:** Graphical representation of the viability of ascospores. The boxplot shows the viability of the ascospores across the *hmbA*, *hmbB* and *hmbC* mutant and control strains in a *veA*⁺ genetic background. Viability was calculated by counting the number of colony-forming ascospores on solid medium. An estimated rate of germination was used as a proxy of viability in the case of *hmbAΔ* (explained in the main text). The strains are color-coded as follows: blue denotes control; red denotes deletion, green denotes complementation (comp.) strains originating from the corresponding deletion strains. Centre lines indicate the median viability of ascospores collected from 10 independent cleistothecia per strain. Mann-Whitney *U*-test was used to assess size differences between the mutant strains and the control in the corresponding genetic background. */**/** indicates *p* < 0.01/0.001/0.0001, ns indicates *p* = not significant. The strains used in the experiment are as follows: *veA*⁺ control (HZS.450), *hmbAΔ veA*⁺ (HZS.521), *hmbAΔ veA*⁺ with *hmbA* complementation (HZS.678), *hmbBΔ veA*⁺ (HZS.495), *hmbBΔ veA*⁺ with *hmbB* complementation (HZS.680), *hmbCΔ veA*⁺ (HZS.531), *hmbCΔ veA*⁺ with *hmbC* complementation (HZS.679).

The ascospore content of *hmbBΔ veA*⁺ cleistothecia increased with the age of the colony (10³ ascospores per cleistothecium at day 12, 10⁴ ascospores per cleistothecium at day 30 and 10⁵ ascospores per cleistothecium at day 45). However, the viability of these ascospores decreased with aging (1% at day 12, 0.06% at day 30 and 0% at day 45). Complementation of the *hmbBΔ* deletion (~4×10⁴ ascospores per cleistothecium) by *in trans* expression of *hmbB* under the control of the constitutive *gpdA* promoter resulted in nearly wild type-like ascospore productivity (~1.6×10⁵ ascospores per cleistothecium) with 31% viability rate. Even though the ascospore productivity was significantly lower than that of the wild-type control, the difference was marginal.

The ascospore productivity of the *hmbCΔ veA*⁺ strain was wild type-like (~2×10⁵ ascospores/cleistothecium); however, only 7% of them was found to be viable (Fig. 25, Table 4). Complementation of the *hmbCΔ* deletion (~2×10⁵ ascospores per cleistothecium) by *in trans* expression of *hmbC* under the control of the constitutive *gpdA* promoter resulted in a significantly decreased ascospore productivity (~6.3×10⁴ ascospores/cleistothecium) in comparison to that of the deleted strain, however the viability of the ascospores showed a more than two fold increase (18.6%) in comparison to that in the deletion strain.

4.6. Transcriptional changes in the *veA*⁺ *hmbAΔ*, *hmbBΔ* and *hmbCΔ* mutant strains

According to our recent knowledge, 50 genes are involved in the sexual reproduction of *A. nidulans*. In order to reveal the role of the HMGB proteins in sexual development, we determined the mRNA levels of 38 selected genes (Table 5) in the *veA*⁺

control and the *veA*⁺ *hmbAΔ*, *hmbBΔ* and *hmbCΔ* strains by RT-qPCRs followed by data analysis according to the standard curve method (Larionov *et al.*, 2005). Except two, all of the gene expressions were analyzed on the second day of sexual development (48 h after the induction of sexual development). The expression of the mating-type MAT1-1 coding *matB* and MAT1-2 coding *matA* were studied on the fourth day of sexual development (96 h after the induction of sexual development). During the selection of genes for the transcript analysis we mainly focused on DNA binding- or chromatin modulating protein coding genes with reported or potential role in sexual development (Table 5). In addition, genes encoding environmental signal sensing and regulatory proteins, and other proteins that were reported or supposed to play role in the ascospore production were also included in the analysis.

Table 5. List of genes selected for transcript analysis

Gene	Protein function or domain
HMG-box domain genes	
<i>hmbA</i>	HMGB protein, unknown (HMG-box domain)
<i>hmbB</i>	HMGB protein (HMG-box domain)
<i>hmbC</i>	HMGB protein, unknown (HMG-box domain)
AN1962	putative transcription factor, unknown (MATA-HMG-box domain)
AN3667	putative transcription factor, unknown (MATA-HMG-box domain)
AN3549	putative transcription factor, unknown (MATA-HMG-box domain)
<i>mat1</i> (<i>matB</i>)	mating-type MAT1-1 transcription factor (alpha-box domain)
<i>mat2</i> (<i>matA</i>)	mating-type MAT1-2 transcription factor (MATA-HMG-box domain)
DNA-binding protein genes involved in the activation of sexual development	
AN3580	H3-K9 specific histone demethylase (amino-oxidase domain and HMG-box domain)
<i>stuA</i>	transcription factor (bHLH APSES domain)
<i>steA</i>	transcription factor (homeodomain and zinc-finger domain)
<i>medA</i>	transcription factor (no conserved domain was identified)
<i>devR</i>	transcription factor (bHLH domain)
<i>dopA</i>	transcription factor (leucine-zipper domain)
<i>nsdC</i>	transcription factor (zinc-finger domain)
<i>nsdD</i>	transcription factor (zinc-finger domain)
<i>nosA</i>	transcription factor (zinc-finger domain)
<i>flpA</i>	transcription factor (forkhead domain)
<i>rcoA</i>	developmental regulation (WD repeat domain)
DNA-binding and chromatin modulator protein genes involved in the repression of sexual development	
<i>laeA</i>	light/dark response methyl transferase (methyl transferase domain)
<i>silG</i>	light response (zinc-finger domain)
<i>cpcA</i>	amino acid sensing (bZIP domain)
<i>atfA</i>	stress response (bZIP domain)
<i>flbC</i>	transcription factor (zinc-finger domain)
<i>flbE</i>	putative transcription factor (no conserved domain was identified)
<i>rosA</i>	transcription factor (zinc-finger domain)

<i>nrdA</i>	transcription factor (zinc-finger domain)
Genes coding for environmental signal sensing and regulatory proteins involved in activation or repression of sexual development	
<i>lreA</i>	blue light-sensing white-collar (LOV, PAS, zinc-finger domains)
<i>lreB</i>	blue light-sensing white-collar (PAS, zinc-finger domains)
<i>veA</i>	light/dark response (velvet and atrophin-1 domains)
<i>velB</i>	light/dark response (velvet and FtsK domains)
<i>velC</i>	light/dark response (velvet domain)
<i>vosA</i>	trehalose production (velvet and RRM domain)
<i>cpcB</i>	amino acid sensing (WD40 repeat domain)
<i>mpkB</i>	MAP kinase (STKc-ERK1-2-like domain)
other protein coding genes with reported or putative role in sexual development	
<i>grrA</i>	protein ubiquitinylation (F-box domain)
<i>samB</i>	cell polarity, nuclear positioning (zinc-finger domain)
<i>hhoA</i>	linker histone (linker histone H1 and H5 domain)

Expression changes with higher than 2-fold change (FC) compared to the corresponding control strain were regarded as up- or downregulation. In accordance with previously reported data (Paoletti et al., 2007), we found that the expression of the *matB* and *matA* genes can be first detected on the fourth day of the sexual development in the wild-type control. Remarkably, both mating-type genes were extremely downregulated in all the deletion mutants (with 4-9 FC value) (Fig. 26).

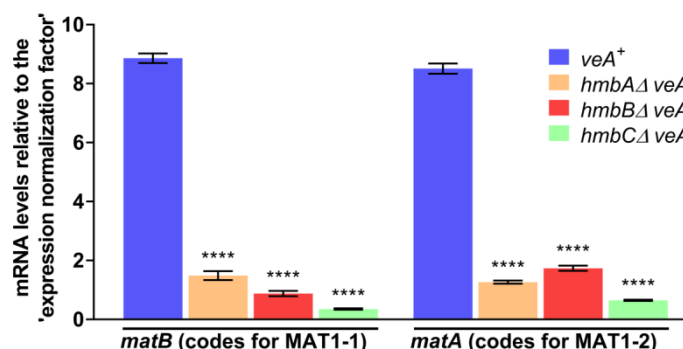


Fig. 26: mRNA levels of MAT1-1 and MAT1-2 coding *matB* and *matA* measured by qRT-PCR in *veA*⁺ control and *veA*⁺ *hmbA*Δ, *hmbB*Δ and *hmbC*Δ strains 96 h after the induction of sexual development

Results, obtained by calculations according to the standard curve method (Larionov et al., 2005), were normalized to an ‘expression normalization factor’ calculated from five tested reference genes (*actA*, *hhtA*, *tubC*, *gpdA*, *eEF-3*) (detailed in Materials and Methods). Standard deviations of three technical replicates of three biological samples are shown. The stars above the columns indicate the significance of the differences compared to the *veA*⁺ control value. Significant differences between the mutants and the control were determined by using a two-way ANOVA test. ****P < 0.00005. The following strains were used in the experiment: *veA*⁺ (H.ZS.450), *hmbA*Δ *veA*⁺ (H.ZS.521), *hmbB*Δ *veA*⁺ (H.ZS.495) and *hmbC*Δ *veA*⁺ (H.ZS.531). The cultivation settings were as follows: approximately 10⁶ conidiospores per strain were inoculated into liquid MM, and were grown for 24 hours at 37 °C with 180 rpm shaking. Then the vegetatively grown mycelia were transferred onto solid MM covered with cellophane, sealed carefully with scotch tape and incubated for 96 hours at 37 °C in complete darkness. After the incubation period, total RNA was extracted and processed.

Among the 38 investigated genes, we could not detect the expression of the AN3549 (codes for putative transcription factor with MATA-HMG-box domain) on neither the second nor the fourth day of sexual development. Out of the 35 genes investigated on the second day of sexual development, 3 were upregulated and 11 were downregulated in at least one of the mutants (Fig. 27-29).

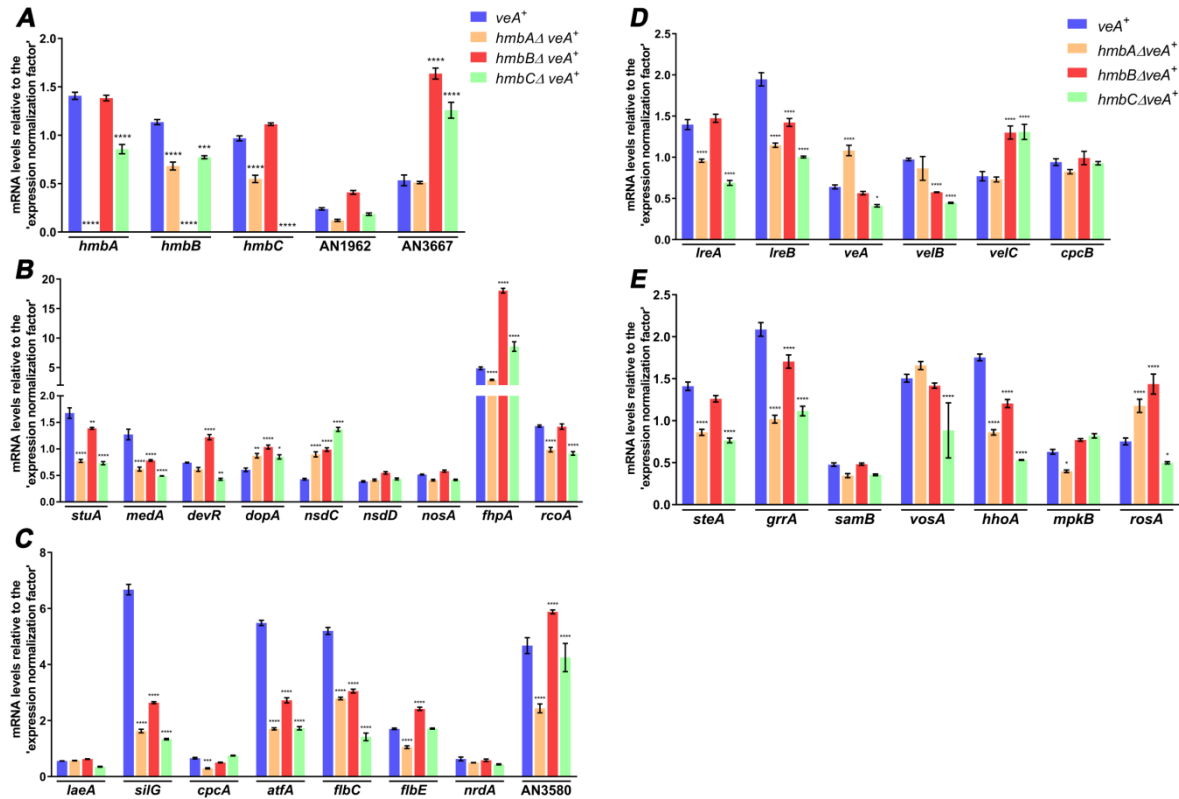


Fig. 27: mRNA levels measured by qRT-PCR for 35 genes in veA^+ , $hmbA\Delta veA^+$, $hmbB\Delta veA^+$ and $hmbC\Delta veA^+$ strains 48 h after the induction of sexual development.

The figure shows the mRNA levels of the following set of genes: HMG-box domain genes (Panel A), DNA-binding protein genes involved in the activation of sexual development (Panel B), DNA binding and chromatin modulator protein genes involved in the repression of sexual development (Panel C), genes coding for environmental signal sensing and regulatory proteins involved in activation or repression of sexual development (Panel D) and other protein coding genes with reported (*steA*, *grrA*, *samB*, *vosA*, *mpkB*, *rosA*) or putative role (*hhoA*) in sexual development. Results, obtained by calculations according to the standard curve method (Larionov *et al.*, 2005), were normalized to an expression normalization factor calculated from five tested reference genes (*actA*, *hhtA*, *tubC*, *gpdA*, *eEF-3*). Standard deviations of three technical replicates of three biological samples are shown. The stars above the columns indicate the significance of the differences compared to the veA^+ control value. Significant differences between the mutants and the control were determined by using a two-way ANOVA test. * $P < 0.05$, ** $P < 0.005$, *** $P < 0.0005$, **** $P < 0.00005$. The following strains were used in the experiment: veA^+ (HZS.450), $hmbA\Delta veA^+$ (HZS.521), $hmbB\Delta veA^+$ (HZS.495) and $hmbC\Delta veA^+$ (HZS.531). The cultivation settings were as follows: approximately 10^6 conidia per strain were inoculated into liquid MM, and were grown for 24 hours at 37 °C with 180 rpm shaking. Then the vegetatively grown mycelia were transferred onto solid MM covered with cellophane, sealed carefully with scotch tape and incubated for 48 hours at 37 °C in complete darkness. After the incubation period, total RNA was extracted and processed.

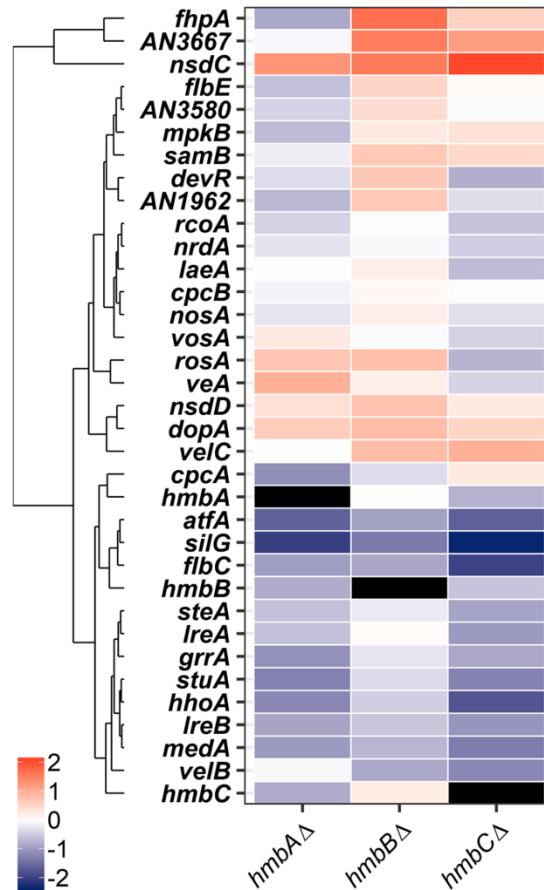


Fig. 28: Heat map of the transcript level changes of selected genes in *hmbA*Δ, *hmbB*Δ and *hmbC*Δ strains on *veA*⁺ backgrounds.

The heat map shows the log₂-scale fold change values of 35 genes across the *hmbA*, *hmbB* and *hmbC* mutant strains. The fold change values were estimated by calculating the ‘expression normalization factor’ normalized expression levels of the mutant strains relative to that of the wild-type control. The color gradient denotes the fold changes as follows: red indicates upregulation (1: 2-fold increase; 2: 4-fold increase in expression); blue indicates downregulation (-1: 2-fold decrease; -2: 4-fold decrease in expression), white indicates no change (0) of a transcript level compared to that of the control strain. Black marks no detectable transcript in the corresponding mutant strain. A hierarchical clustering (left panel) was performed on rows (transcripts), based on Euclidean distances using the *complete linkage* method [48]. The strains used in the experiment were as follows: wild-type control (*veA*⁺, HZS.450), *hmbA*Δ (*hmbA*Δ *veA*⁺, HZS. 521), *hmbB*Δ (*hmbB*Δ *veA*⁺, HZS.495) and *hmbC*Δ (*hmbC*Δ *veA*⁺, HZS.531) strains.

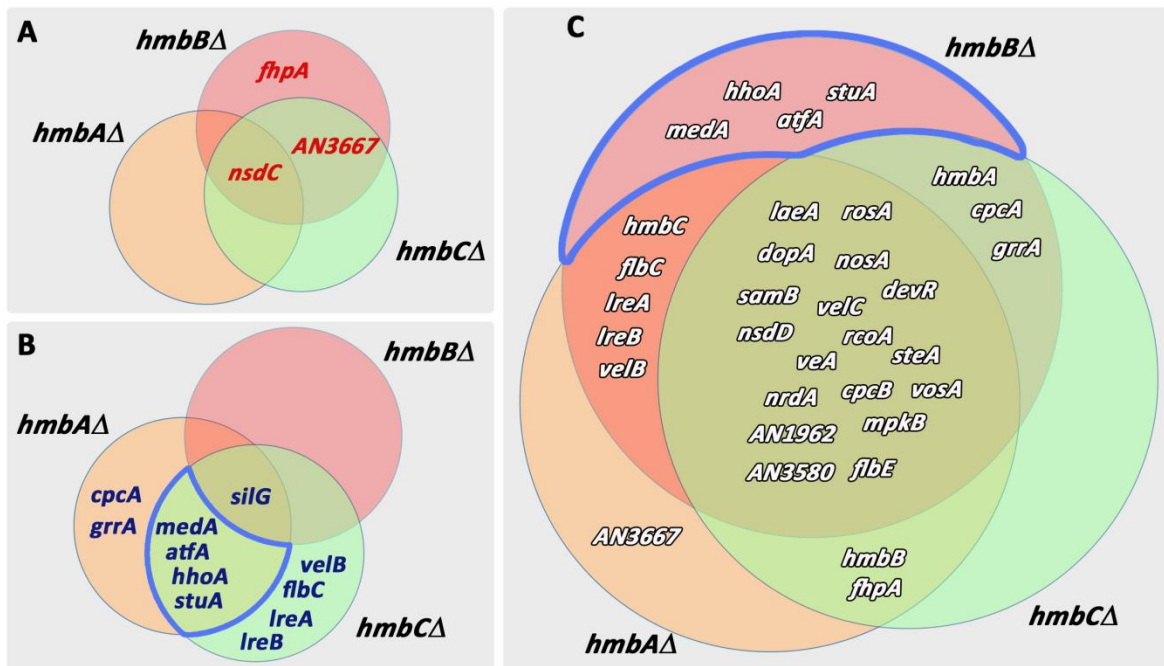


Fig. 29: The Venn diagrams show the similarly regulated genes across the *hmbAΔ*, *hmbBΔ* and *hmbCΔ* mutant strains.

Panel A, B and C show the list of up-, down- and nonregulated genes (using a 2-fold change (FC>2) cut-off), respectively. Based on the Venn diagrams, varying degree of overlap can be observed among the mutant strains, indicating that certain genes are influenced by none of, one or more HMGB proteins. Venn diagrams were prepared from the same sets of up-, down- and nonregulated genes used for creating the heat map of Fig. 28.

Remarkably, genes that were not influenced by *hmbBΔ* showed downregulation in both *hmbAΔ* and *hmbCΔ* mutants (marked intersections of the Venn diagrams in Fig. 29). The *nsdC* showed upregulation in all three deletion strains, while *fhpA* and AN3667 were upregulated only in *hmbBΔ* and in both *hmbBΔ* and *hmbCΔ*, respectively. NsdC is a positive regulator of the initial stages of sexual development and a repressor of asexual sporulation (Kim *et al.*, 2009). According to a previous study, overexpression of *nsdC* results in sexual development under repressing conditions (white light, osmotic stress) (Kim *et al.*, 2009). FhpA is a transcription factor required for the production of cleistothecia but not involved in Hülle cell formation (Lee *et al.*, 2005). AN3667 is a putative MATA-HMG-box domain transcription factor, an orthologue of the STE11 in *S. pombe* and PaHMG5 in *P. anserina* (Ait Benkhali *et al.*, 2013). Both STE11 and PaHMG5 regulate mating-type genes and are essential for the sexual development (Ait Benkhali *et al.*, 2013, Sugimoto *et al.*, 1991) of the fungus. Amongst the downregulated genes, *silG* was downregulated in all mutants; *medA*, *atfA*, *stuA* and *hhoA* were downregulated in both

hmbAΔ and *hmbCΔ* strains; *cpcA* and *grrA* were downregulated only in *hmbAΔ* strain, whilst *velB*, *flbC*, *lreA* and *lreB* were downregulated only in *hmbCΔ*. *SilG* is a repressor of the sexual development in the light. Deletion of *silG* results in the production of high numbers of cleistothecia in light (Han *et al.*, 2005). *MedA* and *StuA* transcription factors regulate both sexual and asexual development. The *medAΔ* and *stuAΔ* deletion strains do not form cleistothecia and ascospores, although *medAΔ* produces Hülle cells (Busby *et al.*, 1996; Wu *et al.*, 1997). Deletion of *AtfA*, a SakA-interacting transcription factor, results in the derepression of the sexual development (Lara-Rojas *et al.*, 2011). *HhoA* is the linker histone H1, which seems to be dispensable for *A. nidulans*, since deletion of *hhoA* has no effect on possible H1 histone functions (Ramon *et al.*, 2000). *GrrA* is an F-box protein with a role in ascospore formation. Although the *grrAΔ* mutant is able to form Hülle cells and asci-containing cleistothecia. However, the mutant asci are empty as a consequence of blocked ascospore formation at the point of meiosis (Krappmann *et al.*, 2006). *CpcA* transcription factor is involved in the sensing of amino acid levels by interacting with a *CpcC* kinase and suppresses the development of cleistothecia under limiting amino acid conditions, although it has no effect on Hülle cell production (Hoffmann *et al.*, 2000). *VelB* is a velvet domain protein that forms complexes with other velvet domain proteins. The most widely-studied velvet complex, involving *VelB*, is the *VeA-VelB-LaeA* complex that regulates the asexual and sexual development via a light dependent-manner (Kim *et al.*, 2002; Bayram *et al.*, 2008). Through interacting with the velvet protein *VosA*, *VelB* represses the asexual development and mediates the maturation of ascospores (Sarıkaya Bayram *et al.*, 2010). *FlbC* transcription factor is a positive regulator of the asexual conidiation, while it acts as a repressor of the sexual development. In the *flbCΔ* mutant, the Hülle cells and cleistothecia are formed abundantly (Kwon *et al.*, 2010). *LreA* and *LreB* are blue light-sensing white-collar proteins, which are implicated in the light-dependent balancing between the asexual and sexual development through interacting with *FphA* and *VeA* proteins as parts of the ‘light regulator complex’ in the nucleus (Purshwitz *et al.*, 2008; Bayran *et al.*, 2010).

4.7. Discussing the role of HmbA, HmbB and HmbC in the sexual development of *A. nidulans*

According to the presented results, the HmbA, HmbB and HmbC architectural chromatin components of *A. nidulans* are required for normal sexual development, especially for the formation and viability of ascospores and the spatial distribution of the cleistothecia. By studying *hmbA*, *hmbB* and *hmbC* deletions in both *veA*⁺ and *veA1* background, we investigated the possible functional interaction of these HMGB proteins with VeA, the master regulator of sexual development.

The *hmbA*Δ, *hmbB*Δ and *hmbC*Δ strains show defect in ascospore production and viability to various extent. The *hmbA* deletion resulted in nearly sterile cleistothecia with less than 10 ascospores inside, which were remarkably able to germinate with an estimated 30% rate. The *hmbB* deletion resulted in a drastic decrease both in the numbers and the viability of ascospores, whereas a drastic decrease was mainly observed in the ascospore viability but not in the number of ascospores in the case of the *hmbC* deletion. RGA material was detected in all three deleted mutants; amongst them the *hmbC*Δ strain accumulated it to a greater extent which was more pronounced in the *veA1* background. The *veA*⁺ *hmbC*Δ cleistothecia contained an equal number of immature asci and mature ascospores, however the *veA1* *hmbC*Δ cleistothecia were either barren or fertile. The fertile *veA1* *hmbC*Δ cleistothecia mostly contained free ascospores and an increased amount of RGA material. Furthermore, the abundance of the *veA1* *hmbC*Δ cleistothecia was reduced in the *veA1* background. Both the *hmbA* and *hmbB* deletions caused a delay in the time-course of the sexual development independently of VeA. However, the delay in the time-course of sexual development observed in the *veA*⁺ *hmbC*Δ strain in comparison to that of the *veA*⁺ control was more pronounced in the *veA1* background. Considering the above described *hmbC*Δ phenotypes, we propose that HmbC functionally interacts with VeA.

HmbA and HmbB might be involved in sensing and responding to the change of environmental oxygen-level. The distribution of the cleistothecia was dependent on oxygen-exposure in the *hmbA*Δ mutants, since only the strict exclusion of oxygen resulted in a wild type-like distribution of cleistothecia. The normal-sized cleistothecia formation in the *hmbB*Δ strain required a medium level of oxygen-exclusion.

The transcript analysis of regulatory genes involved in sexual development revealed that HmbA, HmbB and HmbC seem to be equally important for the normal expression of *matB* (codes for MAT1-1) and *matA* (codes for MAT1-2) genes at four days after the initiation of sexual development (Fig. 26), however neither of the *hmbB* and *hmbC* deletion phenocopied fully the *matB* Δ or *matA* Δ phenotypes. Deletion of MAT1-1 coding *matB* and MAT1-2 coding *matA* results in Hülle cell formation and cleistothecium production, however the cleistothecia are free of ascospores and contain only granular amorphous materials (Paoletti *et al.*, 2007). The MAT gene deletion phenotype was frequently, but not always observed in the *veA1 hmbC* Δ strain, which indicates that HmbC functionally interacts with VeA. On the other hand, the random occurrence of barren cleistothecia amongst fertile cleistothecia might reflect a sporadic compensation for the loss of *hmbC* in the *veA1* background. We cannot exclude the possibility that HmbA, HmbB and HmbC directly influence the gene expression of MAT-regulated genes, and that they can provide the functional backups for each other's loss. Such a compensatory effect had already been reported in the case of other types of linker proteins. Mice contain eight subtypes of the linker H1 histone that are differentially expressed during development (Lennox and Cohen, 1983; Lin *et al.*, 2000; Tanaka *et al.*, 2001). These H1 histone variants can compensate for each other's loss in homozygous knockout mouse models (e.g. H1c, H1d and H1e variants can compensate for the homozygous deletion of H1(0)) (Fan *et al.*, 2001). Only the *hmbA* Δ phenotype shares all the characteristics of the *matB* Δ and *matA* Δ phenotypes. The deletion phenotypes of *hmbB* Δ and *hmbC* Δ resemble to that of the *matB* Δ or *matA* Δ in terms of RGA material accumulation inside the cleistothecia. It is reasonable to think that besides the pronounced downregulation of MAT genes, the qualitatively different perturbation in the expression of the sexual-differentiation-involved genes further contributes to the *hmbA* Δ -, *hmbB* Δ - and *hmbC* Δ -specific phenotypes (summarized in a regulatory map, Fig. 30).

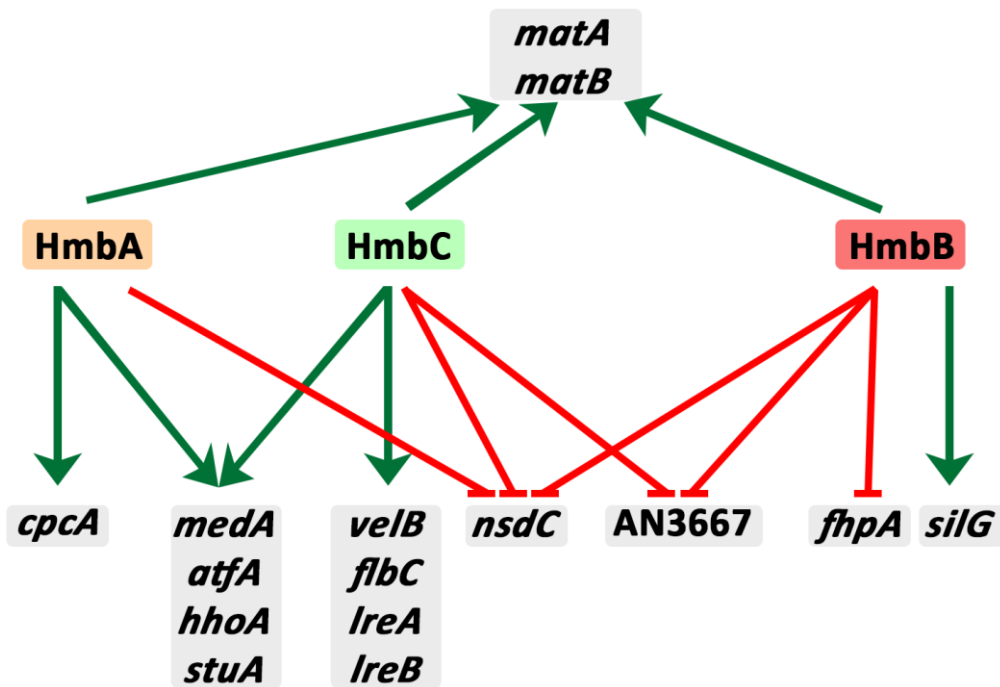


Fig. 30: Regulatory map of HmbA, HmbB and HmbC summarizing the significantly up- and downregulated genes.

The regulatory map showing the function of HmbA, HmbB and HmbC proteins was created on the bases of significant $FC > 2.0$ values detected in the *hmbAΔ*, *hmbBΔ* and *hmbCΔ* strains relative to the wild-type control. Downregulations were converted to activation (green lines), whereas upregulations were converted to repression (red lines). Gene names are explained in Table 5. Orange, green and red boxes highlight HmbA, HmbB and HmbC, while grey boxes highlight the investigated genes.

For example, downregulation of *medA*, *stuA*, *atfA* and *hhoA* might contribute to the *hmbAΔ* and *hmbCΔ* phenotypes. MedA and StuA transcription factors are important in cleistothecium formation, but we observed that the downregulation of these genes in the mutants did not inhibit the production of cleistothecia. Therefore *medA* and *stuA* downregulations should not be accounted for the mutant phenotypes. AtfA is known as a repressor of sexual development, however this transcription factor is implicated in oxidative- and osmotic stress-defence and contributes to the viability of conidiospores (Lara-Rojas *et al.*, 2011; Balázs *et al.*, 2010). The *atfA* deletion results in the drastic decrease of conidiospore viability, which worsens upon prolonged storage-time (Balázs *et al.*, 2010). Although the viability of ascospores in the *atfA* mutant was not investigated, a pivotal role of AtfA in the viability of ascospores seems to be reasonable to suppose. We included the study of H1 histone in our experiments, as we know that the *hhoA* deletion mutant behave as wild type in various aspects, such as during asexual and sexual reproduction; C- and N-source utilization; performance against various environmental

stresses; and nucleosome positioning (Ramon *et al.*, 2000). Here we uncovered that the expression of *hhoA* is governed by HmbA and HmbC, which might provide the starting point of further efforts to reveal the exact role of H1 histone.

Genes *grrA* and *cpcA* were downregulated only in *hmbAΔ*, therefore they might explain the *hmbAΔ* phenotype. The phenotype of the *grrAΔ* mutant shows resemblance with that of *hmbAΔ* in terms of the lack of ascospore production, however empty asci and ascogenous hyphae are found in *grrAΔ* (Krappmann *et al.*, 2006). Downregulation of *grrA*, together with the downregulation of mating-type coding MAT genes, might be crucial explanatory factors for the *hmbAΔ* phenotype. The transcription factor CpcA arrests cleistothecium maturation upon amino acid starvation; in the absence of CpcA mature cleistothecia are formed (Hoffmann *et al.*, 2000). Therefore downregulation of *cpcA* should not be accounted for the *hmbAΔ*-specific phenotype. The *velB*, *flbC*, *lreA* and *lreB* genes are downregulated only in the *hmbCΔ* strain. Deletion of *flbC* results in abundant cleistothecium production (Kwon *et al.*, 2010), therefore downregulation of *flbC* might contribute to the wild type-like abundance of cleistothecia in the *veA⁺ hmbCΔ* strain. The *hmbC* deletion in the *veA1* background resulted in a scarce cleistothecium production. The colonies frequently contained sectors, which were poor in conidia but rich in cleistothecia. This phenotype might be explained with a supposed intracolony fluctuation in the expression level of *flbC*, however, future studies should test this hypothesis. Downregulation of *lreA* and *lreB* in *hmbCΔ* might be the clue for the extreme delay in the time-course of sexual development in *veA1* background. LreA, LreB, FhpA and VeA form the ‘light regulator complex’ in the nucleus (Purshwitz *et al.*, 2008; Bayram *et al.*, 2010). Since the loss of the nuclear localization signal in VeA protein (creates the truncated VeA1 protein) results in a decreased presence of VeA1 in the nucleus (Stinnett *et al.*, 2007), depletion of LreA and LreB components of the ‘light regulator complex’ by the lack of HmbC might result in a delay in the progress of sexual development. Downregulation of *velB* in the *hmbCΔ* strain might contribute to the decreased viability of ascospores through compromising the functioning of the VosA-VelB complex that is important for the maturation of the ascospores (Sarıkaya Bayram *et al.*, 2010). The upregulation of *nsdC*, AN3667 and *fhpA* might contribute to the success of cleistothecium production in the mutants, by being positive regulators of sexual development (Kim *et al.*, 2009; Lee *et al.*, 2005). The positive regulatory role of AN3667 in sexual development is supported by the

reported role of its orthologues from *S. pombe* (STE11) and *P. anserina* (PaHMG5) (Ait Benkhali *et al.*, 2013; Sugimoto *et al.*, 1991).

On the basis of the orthologous relation of HmbA, HmbB and HmbC proteins with the *P. anserina* PaHMG6, mtHMG1 and PaHMG4 proteins, respectively, we compared the role of the orthologous proteins to assess functional relations. The orthologue of HmbA in *P. anserina*, PaHMG6, is required for achieving normal-sized colony (Ait Benkhali *et al.*, 2013). This is a qualitatively similar function that was seen in the case of HmbA of *A. nidulans*. In a homozygous cross, the *Pahmg6* Δ mutant produced fruiting bodies with 50 times less abundance, with smaller body and larger neck than the wild type and began to eject ascospores several days later than the wild type. Although both *A. nidulans hmbA* Δ and *P. anserina Pahmg6* Δ mutants showed a delay in the time-course of sexual development in homozygotic crosses, an analogy cannot be drawn between their functions in the aspect of sexual competency.

Absence of the orthologue of HmbB in *P. anserina* *ASI*⁺ strain (*mtHmg1* Δ , *ASI*⁺) does not result in the loss of germination ability of the ascospores (ascospores germinate slowly with a spindly phenotype (Dequard-Chablat and Allandt, 2002), thus we cannot draw an analogy between the functions of mtHMG1 and HmbB. Although the dual localization of mtHMG1 protein of *P. anserina* was not studied yet, we previously revealed a dual localization of HmbB and found that the orthologous HmbB and mtHMG1 share a third HMG-box domain, called Shadow-HMG-box, which is characteristic to the HmbB orthologues across Pezizomycotina (Karácsony *et al.*, 2014). The structural similarity between HmbB and mtHMG1 and the fact that both proteins modulate the expression of nuclear genes (Ait Benkhali *et al.*, 2013; Karácsony *et al.*, 2014) makes it reasonable to suppose that mtHMG1 fulfills nuclear-localization-linked functions as we suggested previously for HmbB (Karácsony *et al.*, 2014).

The HmbC counterpart in *P. anserina*, PaHMG4, was required for the normal distribution of the fruiting bodies (Ait Benkhali *et al.*, 2013). The PaHMG4 deletion mutant produced five times more spermatia (with wild type-like viability), whereas the deletion had no effect on female fertility (Ait Benkhali *et al.*, 2013). The PaHMG4 functions differ from that of HmbC, thereby the two proteins are functionally diverged.

Some of the physiological functions of HMGB proteins we revealed are specific for *A. nidulans* compared to yeast and *P. anserina*. This includes that HmbA and HmbB play a

role in sensing of and/or response to environmental signals. By revealing the functional connections of HmbA and HmbB with signal transduction pathways, one would gain a deeper understanding of the regulatory machinery that governs physiological responses to environmental changes. On the other hand, we found that HmbC functionally interacts with VeA, a key regulator of the coordination of asexual and sexual development, as well as of secondary metabolism. By revealing the functional interactions of HmbC, one would gain a deeper insight into the regulation of these biological processes. Finally, HmbA, HmbB and HmbC are equally important in the positive regulation of mating-type genes, and thereby have a great impact on ascospore production in *A. nidulans*. The knowledge on the regulation of fungal mating-type genes is scarce, thereby clarifying, whether these HMGB proteins influence *matA/matB* expression directly or indirectly (e.g. via the modulation of upstream regulatory factors) would be of great interest. Additionally, future works should elucidate the gene-expression modulatory role of the HMGB proteins on a genome-scale that might lead to a more detailed characterization of the physiological roles of HmbA, HmbB and HmbC.

4.8. Construction of the *stcO* reporter cassette

In order to study the intracolony site of STC production we developed a reporter system based on the promoter of one of the *stc* cluster genes, the *stcO*. Choosing the *stcO* gene for the reporter system endowed us to provide experimental evidence about the role of StcO in the STC biosynthesis. The STC biosynthesis genes form a cluster in the genome on chromosome IV (Fig. 10). It is composed of 25 genes, which of them *aflR* is the cluster specific transcription factor. Co-regulation of many of the cluster genes was shown and reported, but the functions were proved experimentally only for a very few genes (Brown *et al.*, 1996; Keller and Hohn 1997). The *stcO* reporter cassette was constructed by the double joint PCR method (Fig. 31).

Basic components of the cassettes and their primers

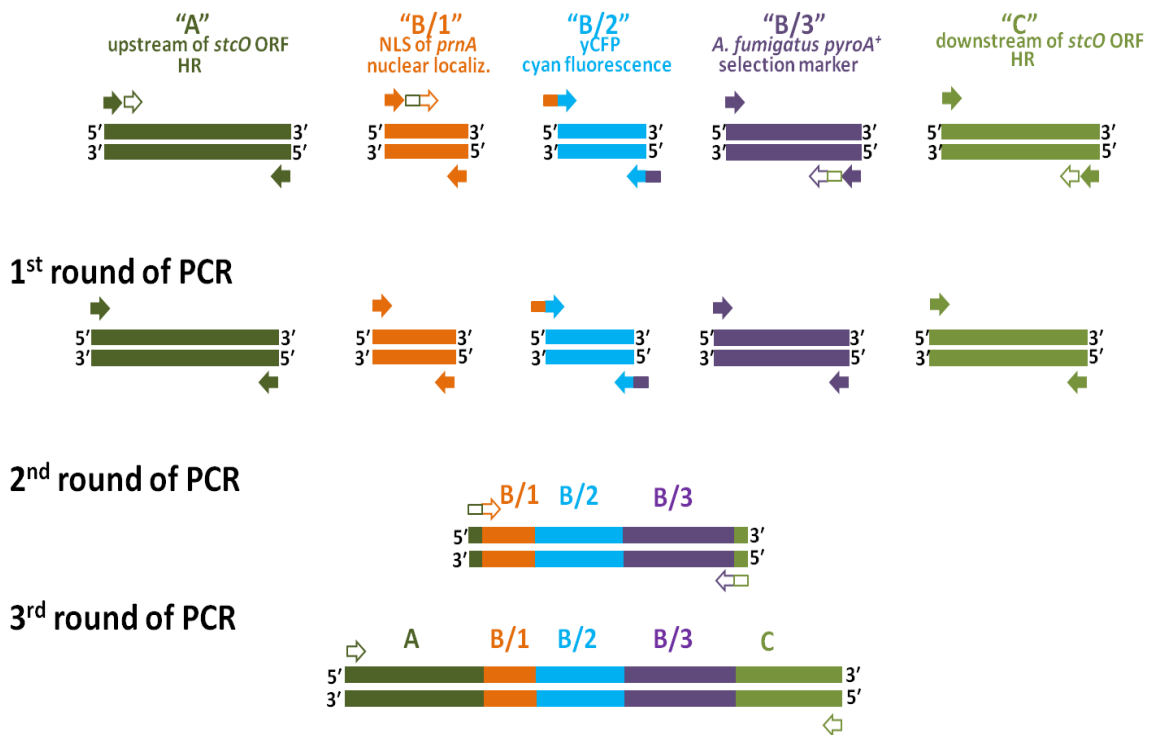


Fig. 31: Schematic presentation of the construction of the five-partite cassette by double joint PCR method.

By using the double joint PCR, the basic components of five-partite cassette was fused into a single product. The primers were designed such as regular, chimeric, regular-nested and chimeric-nested for the consecutive PCR reactions. In the 1st round of PCR, the five basic components were amplified by using regular and chimeric primers. In the 2nd round of PCR, which served as the first assembling reaction, the B components (B/1, B/2 and B/3) were combined together by using nested-chimeric primers. In the 3rd round of PCR, the middle component (B/1, B/2 and B/3) was fused with the A and C components through a second assembling reaction by using nested-regular primers. In this schematic presentation, the arrows mark the used primers. The filled arrows with single colour indicate regular primers. The empty arrows mark the nested primers. The arrows with two colours indicate the chimeric primers.

We replaced the open reading frame of the *stcO* gene with the gene of the yeast codon optimized cyan fluorescent protein (*ycfp*). We constructed a five-partite cassette, where the A and C components were the genomic regions upstream and downstream to the *stcO* open reading frame, respectively (Fig. 31). The 3' end of the upstream region (component A) contained the *stcO* promoter. These A and C regions served the targeted integration site of the cassette by providing DNA sequences for homologous recombination (Fig. 31).

The B1 region carried the start codon of the reporter followed by the nuclear localization signal of the PrnA transcription factor in order to target the fluorescent protein into the nucleus (Fig. 31). The B2 component was the coding sequence of the cyan fluorescent protein without its start codon (Fig. 31). The B3 component was the wild type *pyroA* allele of *Aspergillus fumigatus*, which served as a heterolog selection marker gene (Fig. 31). We designed regular, chimeric, regular-nested and chimeric-nested primers for the two consecutive PCR reactions (see 3.7.1 Section) (Fig. 31). First we amplified the five basic components using regular and chimeric primers (indicated on Fig. 31). This PCR was followed by the first assembling, in which we combined the B1, B2 and B3 components together using nested-chimeric primers. The joined middle components were fused with the A and C components in a second assembling reaction using nested-regular primers (Fig. 31). The assembled five-partite cassette was then transformed into red fluorescent H1 histone labelled pyridoxine auxotroph recipient strain (HZS. 576) and out of hundreds of pyridoxine prototrophic transformants, nine were selected for microscopic monitoring, southern blot analysis and PCR analysis for the verification of locus integration. The Southern analysis was carried out on BamHI digested total DNA of parental control (HZS. 576) and the selected transformants by using DIG-DNA labelled nested C component (2421bp nested *stcO* downstream region) (Fig. 31). All the nine transformants were proved to carry single copy integration in the targeted locus, according to the southern blot result (Fig. 32 Panel C). We expected such success, because the recipient strain was *nkuAA*, therefore ectopic integrations were not probable (for more detailed explanation see section in materials and method). Additionally, we monitored the target locus integration by carrying out PCR analysis on the transformants with using primer pairs „stcO upst frw”- „NLS CFP chim rev” and „Afu pyroA CFP chim”- „stcO down rev”. The generated 3582 nt and 5444 nt long PCR products proved targeted integration by homologous recombination. One of the transformants (*trf1*, named as HZS.606) was selected for further studies.

HZS.606 was crossed with HZS.260 and co-segregation of *pyroA*⁺ was observed with the STC non-producing phenotype (50 *pyroA*⁺ progeny grown on nitrate-lactose medium for 6 days were screened for STC production by thin layer chromatography (TLC)).

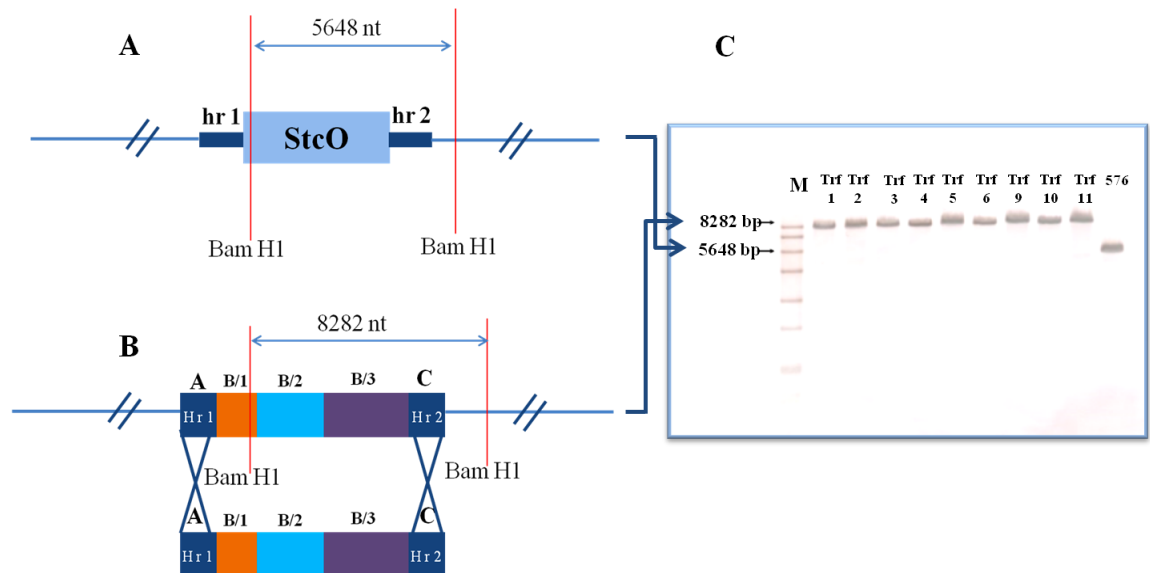


Fig. 32: Southern strategy for the verification of the locus integration of the reporter substitution cassette by homologous recombination.

A: Scheme of the *stcO* genomic region in the wild type control.

B: At the bottom the scheme of the five-partite reporter substitution cassette is shown. At the top the substituted genomic region is shown where the nuclearly targeted (orange box marks NLS) *ycfp* gene (blue box) coupled with the *AfupyroA*⁺ selection marker gene (purple box) replaces the *stcO* by double crossing over formed in Hr1 and Hr2 regions. Red vertical lines mark the cleavage sites of BamHI restriction endonuclease. The horizontal double arrows mark the cleaved BamHI fragments, which provide the hybridization signal. The size of the cleaved product is indicated in nucleotide length (nt). The DNA probe was made from the nested C-component (blue box Hr2) by using DIG-DNA labeling. Crossed lines indicate homolog recombination events.

C: Southern membrane developed with the labeled C-component as DNA probe. (M: DIG-labeled DNA molecular weight sizes (Fermentas); lanes Trf1-6 and Trf9-11: hybridization signals of the transformants Trf1-6 and Trf9-11; 576: hybridization signal of the control strain HZS.576.

4.9. Investigation of the role of StcO in the STC biosynthesis

The homolog recombination of the reporter construction resulted in a nucleus targeted cyan fluorescent cassette in the *stcO* locus driven by the native *stcO* promoter. Since the *stcO* open reading frame was replaced with the gene of cyan fluorescent protein, the obtained single copy integration carrying transformants were *stcO* deletion mutants. First we characterized the *stcO* deletion by studying the growth ability and the STC production of the selected mutant HZS.606. The deletion mutant strain showed no alteration in growth ability from that of wild type and parental M control strains (Fig. 33,

panel A) and was sexually competent as wild-type controls (Fig. 33, panel C). The remarkable inefficient utilization of nicotinate as sole nitrogen source resulted in a weak biomass production (Fig. 33, panel A). On nicotinate medium, the hyphae of the colonies run separately in a monolayer even after 4 days of incubation, which makes the nicotinate medium appropriate for cultivation of *A. nidulans* for microscopic analysis.

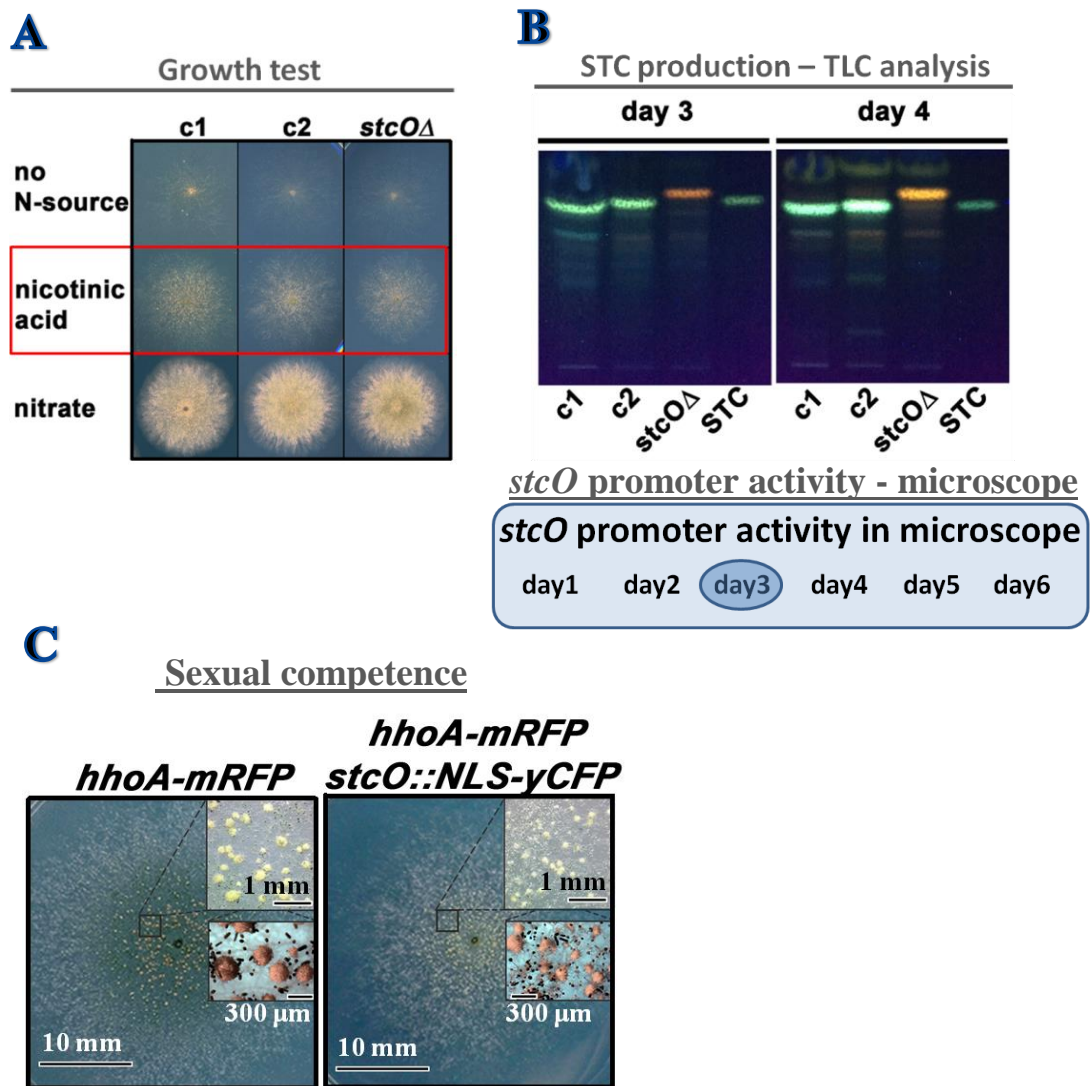


Fig. 33: Characterization of *stcO* deletion mutant by growth test (A), thin layer chromatography (B) and investigation of sexual competence (C).

Growth test and STC production of *stcO* reporter strain. (A) Growth test of the *stcO* reporter and control strains on nitrogen source-free minimal medium (no N-source), nicotinic acid-glucose medium (nicotinic acid) and nitrate-lactose (nitrate) medium. Plates were incubated for 3 days at 37 °C in dark with at least one second daylight exposure/day. (B) TLC analysis showing the STC production of the *stcO* reporter and control strains after 3 and 4 days of incubation in dark at 37 °C. c1: wild type control (H.ZS.450); c2: parental control (H.ZS.576); *stcOΔ*: *stcO* reporter strain (H.ZS.606); STC: sterigmatocystin standard. (C) Selfing resulted in the formation of control-like (*hhoA-mRFP*) cleistothecia in the *stcOΔ* reporter strain (*hhoA-mRFP stcO-NLS-yCFP*). (Scale bars are shown).

We also monitored the *stcO* promoter activity by microscope and the STC content by TLC in both the controls and the deletion strains from the first day of incubation until the sixth day (data not shown). The first samples, in which we detected STC came from the third day of incubation (Fig. 33, panel B). In Fig. 33, panel B we show the STC content of the controls and *stcOΔ* strain after 3 and 4 days of incubation. Only the control strains produced STC, the deletion strain did not contain STC. The fourth day of incubation the STC production increased in the control strains, which was seemingly in contradiction with the observed *stcO* promoter activities in the reporter strain. The contradiction comes from the microscopic observation, that the first time we could detect *stcO* promoter activity was the third day of incubation. This coincides with the timing of the beginning of STC production. However, the *stcO* promoter activity ceased to zero according to the microscopic observation by the fourth day of incubation and was absent from the later time points too. As the TLC analysis proved, the STC production is still maintained at later than 3 days incubation times, which can be explained by the stability and long life span of the StcO enzyme. The lack of STC in the *stcO* deletion strain experimentally proved that StcO plays an essential role in STC biosynthesis.

4.10. Investigation of the *stcO*-active vegetative hyphae that surround the center of sexual differentiation

In our experimental setup, the reporter strain was grown on nicotinate media covered with cellophane for 3 days. The cellophane with the colony was cut as it is shown in Fig. 34, peeled off from the media and placed on a slide. Two fields were documented from the sample. Field 1 was free from Hülle cells and field 2 contained Hülle cells.

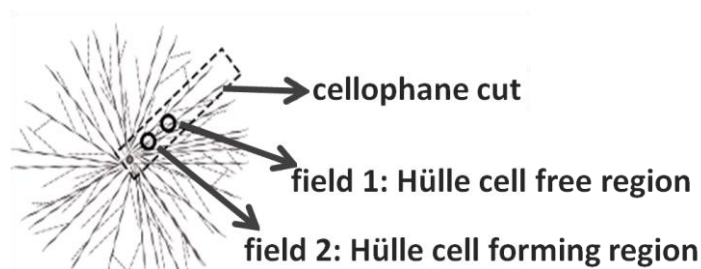


Fig. 34: Schematic presentation of the preparation of microscopic samples.

From field 1, we could detect only the red fluorescent protein labeled H1 histones in the nuclei. There was no sign of cyan fluorescent nuclei, which would have indicated *stcO* promoter activity (Fig. 35).

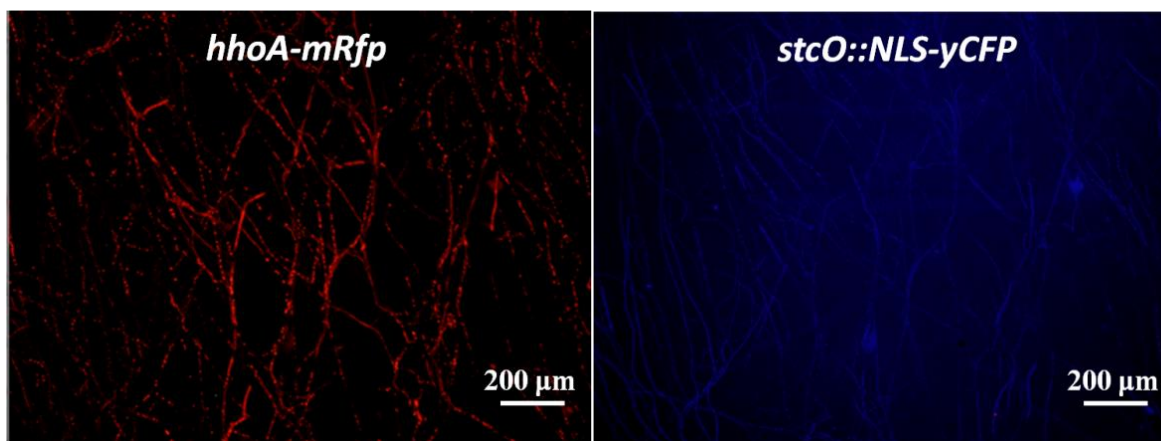


Fig. 35: Field 1 Hülle cell free region of *stcO* reporter strain.

hhoA-mRfp: red fluorescence showing image. Red fluorescence is generated by the H1 histone fused red fluorescent protein; *stcO::NLS-yCFP*: blue fluorescence (originated from nuclear targeted localization of yeast optimized cyan fluorescent protein driven by the native *stcO* promoter) signal detecting image. Blue fluorescence signal was not detected, indicating that the *stcO* promoter is inactive in the field. Scale bars are shown at the bottom right of the images. Images were taken by using Olympus BX51 fluorescent microscope U-MNU2 Olympus cube (BP 360-370 excitation filter, DM 400 dichromatic mirror, LP 420 emission filter) and U-M41035 RFP Olympus cube (U-HQ546/12, U-Q560LP, U-HQ6058/75m)

The hyphae from Hülle cell free region of the colony of *stcO* reporter strain (H.ZS.606) do not show *stcO* promoter activity (cyan fluorescence at the right panel of Fig. 35), while the mRFP labeled H1 histones are clearly detected (red fluorescence at the left panel of Fig. 35). From field 2, which carried groups of Hülle cells, beside the red fluorescent protein labelled H1 histones, we could detect nuclearly localized cyan fluorescence signals too, which indicate that the *stcO* promoters are active (Fig. 36). Remarkably, the cyan fluorescent nuclei were seen only in those vegetative hyphae, which were localized in the proximity of the groups of Hülle cells as it can be seen in this picture. As the distance from Hülle cells grows, the *stcO* promoter activity ceased to zero.

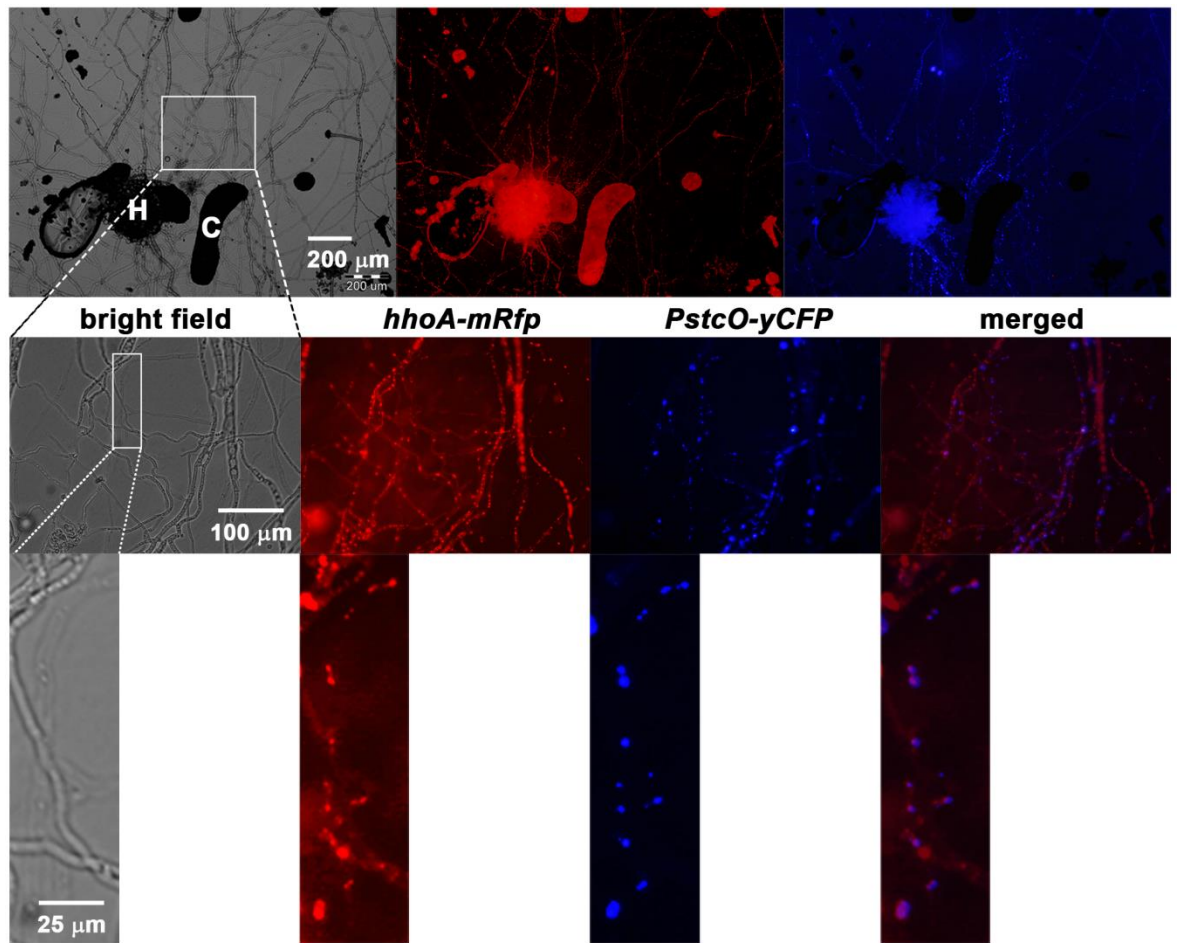


Fig. 36: Field 2 Hülle cell forming region of *stcO* reporter strain

hhoA-mRfp: red fluorescence showing image. Red fluorescence is generated by the H1 histone fused red fluorescent protein; *stcO::NLS-yCFP*: blue fluorescence (originated from nuclear targeted localization of yeast optimized cyan fluorescent protein driven by the native *stcO* promoter) signal detecting image. H marks Hülle cells and C marks conidiospores. Scale bars are shown at the bottom right of the images. Magnification of certain areas is marked with white rectangles and dotted lines. Images were taken by using Olympus BX51 fluorescent microscope U-MNU2 Olympus cube (BP 360-370 excitation filter, DM 400 dichromatic mirror, LP 420 emission filter) and U-M41035 RFP Olympus cube (U-HQ546/12, U-Q560LP, U-HQ6058/75m)

We also monitored the autofluorescence of samples. We found that intracellular compounds show a wide range of autofluorescence after the 3-4 days of incubation. This might interfere with microscopic studies performed on fluorescent microscopes equipped with multifunctional filters with a relatively large bandpass. Such filters can detect a much wider emission wavelength range than that is required for the detection of RFP or CFP fluorescent signals (such as the U-MNU2 and U-M41035 Olympus cubes used in this study) (Fig. 37).

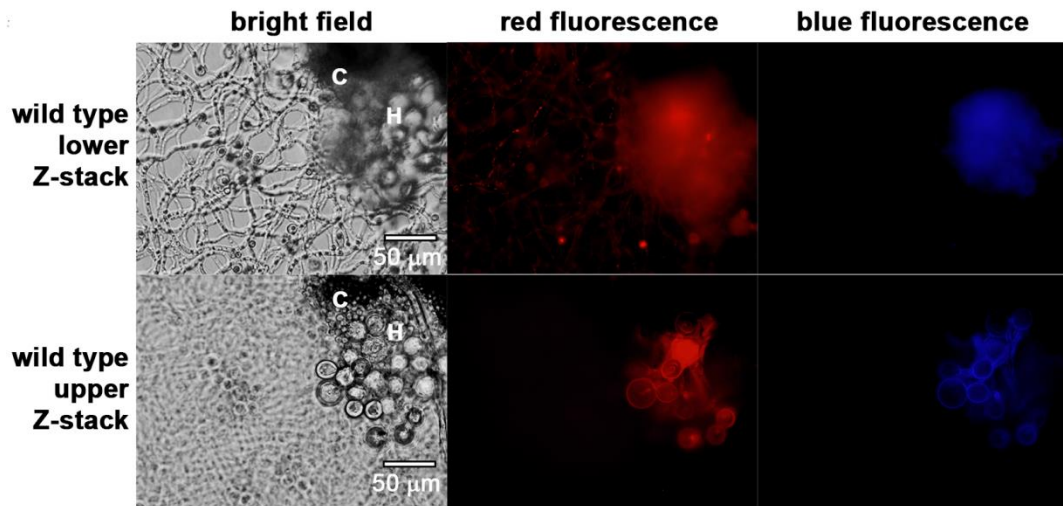


Fig. 37: Autofluorescence of wild type strain.

Top: lower Z-stack showing hyphae; Bottom: upper Z-stack showing Hülle cells. Used strain was: wild type HZS.450. The wild type strain was grown on nicotinate-glucose cellophane plates in dark at 37 °C for 72 hours. H indicates hülle cells, C indicates conidiospores. Scale bars are shown.

In our experimental setup, the unlabeled control strain (HZS.450) grown on nicotinic acid-glucose cellophane plate for 3 days showed red and cyan autofluorescence in the Hülle cells (Fig. 37, bottom) and red autofluorescence in the vacuoles or vesicles of the hyphae (Fig. 37, top), while the conidia did not show any fluorescence (Fig. 37). We monitored three time points (48, 72 and 96 hours) and found that the *stcO* promoter became active only on the third day of incubation (Fig. 37, Fig. 33 panel B). In the fourth day of incubation the *stcO* promoter activity ceased and was rarely detected (data not shown). As it is shown in Fig. 36, the *stcO* promoter is active only in those hyphae, which surround the Hülle cells (Panel A), and its activity diminishes with the distance of the hyphae to the Hülle cells. Monitoring of the *stcO* promoter activity in the Hülle cells was not possible in our experimental setup due to their strong autofluorescence. According to our observations, we propose that STC production is initiated at the core of sexual development.

4.11. Discussion of the intracolony localization of STC production

The role of STC as protective agent against arthropod fungivores has been well established and the heterogeneous distribution of STC in the colony in association with the sexual structures was proposed previously (Staadén *et al.*, 2011; Doll *et al.*, 2013). In

addition, studies on sexual development and STC biosynthesis revealed that these processes share common master regulators (Kato *et al.*, 2003; Bayram *et al.*, 2009; Hicks *et al.*, 2001, Atoui *et al.*, 2008; Wieser *et al.*, 1997) and thereby they are coupled in environmental conditions that allow their manifestation (reviewed in Bayram and Braus, 2012). Here we show that *StcO* plays an essential role in STC biosynthesis (Fig. 33, panel B) and the activation of the *stcO* gene is an indicator of STC production at the third day of incubation. At the fourth day of incubation, we did not detect any *stcO* promoter activity (data not shown), however the amount of STC further increased in comparison to the amount of STC detected at the third day (Fig. 33, panel B). The *stcO* activated hyphae could be seen only in the proximity of groups of hülle cells (forming primordia) and the promoter activity diminished with the distance from the Hülle cells. Mutants (e.g., *sfaDΔ*) with abolished cleistothecia formation and normal Hülle cells show no sign of STC production (Seo *et al.*, 2006), indicating that the presence of Hülle cells is not deterministic for STC production. Notably, STC is normally produced in liquid cultures where sexual structures (including Hülle cells) are not formed. Uncoupling of these two processes might be governed by a variety of signal transduction pathways, which transduce and transmit environmental signals that determine sexual development and STC production. Sexual development depends on the MAP kinase pathways, while STC production relies on both MAP kinase- and PKA pathways, the latter being repressive on STC production (reviewed in Bayram and Braus, 2012). Therefore it is possible that while MAP kinase pathway does not support sexual development, repression of PKA pathway might be relieved and allow AflR activation and subsequent STC production. According to the abovementioned phenomena together with our results, we propose that on solid medium STC production is defined by (an) early sexual developmental factor(s) that locally initiates sexual development. Moreover, according to the observed pattern of the *stcO* promoter activity, the promoting factors(s)/signal(s) of STC production can be subsequently transmitted to the vegetative hyphae located close to the core of sexual development. The lack of activity in distant hyphae indicates that the vegetative mycelium might consist of morphologically uniform, but functionally different hypha cells. Future works should elucidate the underlying mechanism of signal transmission for STC production from the origin to the nearby vegetative hyphal compartments.

5. SUMMARY

Beside the linker histones (H1 and H5), the B-type high mobility group box domain proteins (HMGB), as architectural components of the chromatin, participate in various functions of chromatin, such as recombination, repair, inducing or repressing gene expressions. They are able to interact with both DNA and protein components of the chromatin through their high mobility group box (HMG-box) domains. Amongst the fungal HMGB proteins, role of the yeast HMGB proteins was studied in detail, providing vast knowledge on the mode-of-action, molecular- and physiological role of HMGB proteins. However, very few data is known about the role of HMGB proteins of filamentous fungi. Detailed study on the function of mitochondrial HMGB protein of *P. anserina* (mtHMG1) and *A. nidulans* (HmbB) revealed their role in the maintenance of mitochondrial genome and additionally, nuclear roles were also proposed. Besides the mitochondrial HMGB proteins, four nuclear HMGB proteins were identified in *P. anserina* and two in *A. nidulans* (HmbA and HmbC). A recent study on the HMGB proteins of *P. anserina* revealed that they are involved in the sexual development and fruiting body formation of the fungus. Two of them, PaHMG6 and mtHMG1, also play role in the positive and negative regulation of the expression of the mating-type transcription factors, respectively. In this work we aimed to study the role of *A. nidulans* HMGB proteins in the sexual development and found that some of their functions are specific.

Through the study of sexual development of control and *hmbA*, *hmbB* and *hmbC* deletion mutants both in *veA*⁺ and *veA1* genetic background we revealed that HmbA, HmbB and HmbC architectural chromatin components of *A. nidulans* are required for normal sexual development, especially for the formation and viability of ascospores and the spatial distribution of cleistothecia. Furthermore, we proposed that HmbC functionally interacts with VeA, the key regulator of development and secondary production. We suggested that HmbA and HmbB might be involved in sensing of and responding to the changes of environmental oxygen levels. All HMGB proteins, HmbA, HmbB and HmbC were found to be critical for the normal expression of the mating-type transcription factor genes. We excluded the possibility that all three HMGB linker proteins are required for the direct activation of MAT gene expression. Instead, we propose an alternative explanation for the observed changes: HmbA, HmbB and HmbC might operate on upstream regulator(s) of MAT genes that is (are) most probably involved in the sensing of

environmental and/or intracellular factors and/or the transduction of related signals that affect the activation of the MAT genes. Future research should elucidate the potential role of HMGB proteins in the upstream regulation of MAT genes. On the other hand, despite the uniform downregulation of the mating type transcription genes in the *hmbA*, *hmbB* and *hmbC* deletion mutants, we found that only the *hmbA* deletion phenocopied the mating type gene deletion phenotypes, *hmbB* and *hmbC* deletions resulted in various levels of defects in ascospore production and ascospore viability. As an explanation for the various levels of defects observed in *hmbB* and *hmbC* deletion mutants we proposed that HmbA, HmbB and HmbC might directly influence the gene expression of various MAT-regulated genes. Additionally, we suppose that *hmbA*, *hmbB* and *hmbC* can provide the functional backups for each other's loss.

Considering all of the phenotypes of the *hmbA* Δ , *hmbB* Δ and *hmbC* Δ strains, and the transcriptional changes observed in case of the expression of sexual development involved regulators we supposed that besides the pronounced down-regulation of MAT genes, a qualitatively different perturbation in the expression of other genes might further contribute to the *hmbA* Δ -, *hmbB* Δ - and *hmbC* Δ -specific phenotypes.

Some of the physiological functions of HMGB proteins we revealed are specific for *A. nidulans* compared to yeast and *P. anserina*. This includes that HmbA and HmbB play a role in sensing of and/or response to environmental signals. By revealing the functional connections of HmbA and HmbB with signal transduction pathways, one would gain a deeper understanding of the regulatory machinery that governs physiological responses to environmental changes. On the other hand, we found that HmbC functionally interacts with VeA, a key regulator of the coordination of asexual and sexual development, as well as of secondary metabolism. By revealing the functional interactions of HmbC, one would gain a deeper insight into the regulation of these biological processes. Finally, HmbA, HmbB and HmbC are equally important in the positive regulation of mating-type genes, and thereby have a great impact on ascospore production in *A. nidulans*. The knowledge on the regulation of fungal mating-type genes is scarce, thereby clarifying, whether these HMGB proteins influence the mating-type gene expression directly or indirectly (e.g. via the modulation of upstream regulatory factors) would be of great interest. Additionally, future works should elucidate the gene-expression modulatory role of the HMGB proteins on a

genome-scale that might lead to a more detailed characterization of the physiological roles of HmbA, HmbB and HmbC.

Sexual development is coupled with the production of the toxic secondary metabolite, STC at regulatory level. Studies focusing on the sexual development revealed that many regulatory loss-of-function mutants fail to produce STC, which ultimately connects these two biological processes through sharing common regulators such as the master regulator LaeA and VeA. Additionally, studies on grazing behaviour of fungivore arthropodes revealed that they sense STC and avoid its consumption. Since the fungivore arthropodes do not graze on sexual structures, it was thought that STC production is linked with sexual structures. In order to provide experimental evidence for this latter hypothesis, we visualized the intra-colonial localization of STC producing hyphae by the development and application of a reporter system using the promoter of one of the putative biosynthetic gene, *stcO*, fused with the gene of the cyan fluorescent protein (*ycfp*). Choosing the *stcO* gene for the reporter system endowed us to unravel the role of StcO in the STC biosynthesis. Since the *stcO* ORF was replaced by the *ycfp* gene, the reporter strain could be regarded as a deletion mutant. Measuring the STC content of the reporter strain we proved that StcO plays an essential role in STC biosynthesis. The growth properties and sexual competence of the *stcO* deletion strain does not differ from those of wild type controls. Microscopy of the *stcO* reporter strain revealed that the *stcO* promoter activity begins at the third day of incubation and ceases to zero for the fourth day of incubation. Start of the STC production and start of the *stcO* promoter activity coincide. Additionally we revealed that although the promoter activity diminishes for the fourth day of incubation, the STC production keeps on going. This might be due to the long life-span and stability of the StcO protein. We showed that STC is produced only on those vegetative hyphal compartments, which are in the close proximity of groups of Hülle cells. Most probably the *stcO* promoter activation was originated from the center of sexual differentiation. We propose that on solid medium STC production is defined by (an) early sexual developmental factor(s) that locally initiates sexual development. Moreover, according to the observed pattern of the *stcO* promoter activity, the promoting factor(s)/signal(s) of STC production can be subsequently transmitted to the vegetative hyphae located close to the core of sexual development. The lack of activity in distant hyphae indicates that the

vegetative mycelium might consist of morphologically uniform, but functionally different hypha cells. Future works should elucidate the underlying mechanism of signal transmission for STC production from the origin to the nearby vegetative hyphal compartments.

6. ÖSSZEFOGLALÁS

A B-típusú High Mobility Group box domén proteinek (HMGB) a kromatin fontos, nem hiszton típusú komponensei, melyek képesek nem-specifikus kölcsönhatások révén a DNS-hez kötődni, illetve a kromatin más fehérje alkotórészeivel interakcióba lépni. Hatással vannak a génextpresszióra, szerepet játszanak a károsodott DNS javításában és a rekombinációban. Kutatócsoportunk az *A. nidulans* fonalas gomba vizsgálata során 3 HMGB fehérjét azonosított, a HmbA-t, HmbB-t és a HmbC-t. A HmbB fehérje funkciójáról már számos adatot nyertünk, de a HmbA és HmbC funkciójáról, valamint a HmbB szexuális életsiklusban betöltött szerepéről még nincs információnk. Jelen munka során egyik célkitűzésünk a HmbA, HmbB és HmbC fehérjék szexuális életsiklusban betöltött szerepének feltárása *hmbA*, *hmbB* és *hmbC* delécós törzsek vizsgálatán keresztül, valamint annak megválaszolása, hogy a szexuális fejlődés egyik kulcs-szabályozó fehérjéje, a VeA, és a HMGB proteinek között van-e funkcionális interakció.

Jelen értekezésben a *veA*⁺ és *veA1* genetikai háttérrel rendelkező *hmbA*, *hmbB* és *hmbC* delécós törzsek szexuális struktúráinak vizsgálatával kimutattuk, hogy a HmbA, HmbB és HmbC fehérjék az aszkosórák kialakításának és életképességének fontos faktorai. Rámutattunk, hogy a HmbC funkcionális kölcsönhatásban áll a VeA regulátor fehérjével, amely fény által szabályozott módon koordinálja az aszexuális- és szexuális reprodukciót, valamint a toxikus másodlagos metabolitnak, az STC-nek a termelését. Eredményeink alapján a HmbA és a HmbB részt vesz a környezeti stimulusok érzékelésében is és azok jelátviteli folyamataiban és/vagy a válaszreakciók kialakításában. A szexuális életsiklust irányító transzkripciós faktorok mRNS analízise során fényt derítettünk arra, hogy a három HMGB protein a vizsgált szexuális folyamatban érintett gének közül 3 kifejeződését gátolja, 13 gén kifejeződését pedig serkenti. Ez utóbbiak között a legjelentősebb a párosodási-típus (MAT) gének regulációja volt. Érdekes módon mindhárom HMGB protein egyformán szükségesnek bizonyult a *matA* és a *matB* gének normális szintű kifejeződéséhez. Mivel kicsi a valószínűsége annak, hogy mindhárom HMGB fehérje közvetlenül szabályozza a MAT gének kifejeződését, lehetségesnek tartjuk, hogy a HmbA és/vagy HmbB és/vagy HmbC a MAT gének “upstream” regulátorai, és akár a környezeti- és intracelluláris faktorok jelátvitelében is szerepet játszhatnak, ezáltal szabályozva a MAT gének aktivációját. Mivel a MAT deléciós fenotípus csak a *hmbA* deléciós törzsben teljesebben ki, valószínűnek tartjuk, hogy a HmbB és HmbC fehérjék

kikerülve a MAT géneket, közvetlenül is befolyásolhatnak MAT gének szabályozása alatt álló géneket. A MAT “upstream” és a MAT elkerülő “downstream” regulátor szerep igazolása további kutatást igényel, amely a jövőben fog megvalósulni.

A szexuális fejlődés és a karcinogén hatású másodlagos metabolit, az STC termelése a VeA kulcs-szabályozó fehérje révén kapcsolatos. Számos, gombaevő rovarral végzett kísérlet eredménye alapján úgy gondolják, hogy a gombák által termelt STC a szexuális képletekben akkumulálódik, azonban ezt eddig még senki nem igazolta. Jelen dolgozat második célkitűzése az STC termelés *in vivo* intracelluláris lokalizációjának vizsgálata volt. A megvalósításhoz egy yCFP riporter rendszert hoztunk létre, ahol az STC bioszintézis génklaszter egy kiválasztott tagjának, az *stcO* génnek a kifejeződését tudjuk tanulmányozni fluoreszcens mikroszkópban. Mivel egyértelműen szeretnénk volna a yCFP jelet detektálni, ezért az *stcO* promóter által vezérelt yCFP-ről keletkezett fehérjét a sejtmagba irányítottuk.

Az *stcO* riporter törzs (egyben *stcO* deléciós törzs) vizsgálatával igazoltuk, hogy az StcO esszenciális szerepet játszik az STC bioszintézisében és az *stcO* gén az inkubáció 3. napján történő aktiválódása együtt jár az STC termelésével. Az inkubáció 4. napján nem detektáltunk promóter aktivitást, azonban az STC mennyisége tovább nőtt a 3. napon észlelt STC mennyiséghez képest, amely az StcO fehérje stabilitását fémjelzi és az STC termelés fenntartását. Kimutattuk, hogy az *stcO* csak azokban a hifákban aktív, amelyek a Hülle sejtek csoportjainak a közelében vannak, valamint azt, hogy a promóter aktivitása fokozatos csökkenést és megszűnést mutat a Hülle sejtektől való távolság növekedésével. Feltételezzük, hogy a szilárd médiumon való STC termelődést egy korai szexuális fejlődési faktor határozza meg, amely helyspecifikusan iniciálja a szexuális fejlődést. Az *stcO* promóter aktivitás mintázata alapján úgy gondoljuk, hogy az STC termelést támogató faktor(ok)/szignál(ok) egyik vegetatív kompartmentről a másik kompartmentre terjednek egy adott távolságig. Itt megjegyzendő, hogy az *stcO* promóteraktivitás megszűnik az inkubáció 4. napjára, tehát a 3. napon promóteraktivitást mutató legtávolabbi vegetatív kompartmentek az STC termelés térbeli kiterjedésének a határát jelentik. A távoli hifákban az *stcO* promóteraktivitás hiánya azt jelzi, hogy a vegetatív micélium morfológiailag egységes, de funkcionálisan különböző hifa sejtekből áll, azaz a *distalis* vegetatív kompartmentekben nincs STC termelés. Csak további vizsgálatok deríthetnek fényt arra, hogy milyen molekuláris mechanizmus rejlik az STC termelés iniciálás terjedése mögött.

7. ACKNOWLEDGEMENT

First and foremost, I wish to praise and thank the “Almighty” who provided me vision and strength and through my life.

*I would like to express my gratitude to **the University of Szeged** for the opportunity provided for my study in Hungary.*

*I would like to express my profound gratitude towards our Head of the Department and head of the Doctoral school of Biology **Prof. Csaba Vágvölgyi** for giving me the opportunity to study my PhD in the department of Microbiology, Faculty of Science and Informatics, University of Szeged.*

*I am profoundly grateful to my supervisor **Dr. Zsuzsanna Hamari** for her valuable guidance, help and blessing rendered throughout my PhD study periods, especially for her constant support during my PhD thesis.*

My special thanks to all the faculty members of the Department of Microbiology.

I also would like to extend my thanks to Judit Ámon and Eszter Bokor for their tremendous help during my experimental work in the laboratory. A special thanks to my friends for joining their hands during my work and encouraged me mentally during my difficult time.

I sincerely thank to Dr. Erika Kerekes and Dr. Németh Tibor for reviewing my PhD thesis.

I convey my gratitude to my family members for their moral support filled with affection, tolerance, concern, cordial, and encouragement throughout my life.

Last but not least I wish to acknowledge one and all, who are directly and indirectly involved in “Stipendium Hungaricum Scholarship” program for providing me the greatest opportunity to study in Hungary.

This work was supported by the Hungarian Government and the European Union within the frames of the Széchenyi 2020 Programme through grant GINOP-2.3.2-15-2016-00006.

Keisham Kabichandra Singh

8. REFERENCES

- Adams, T H., Wieser, J K., & Yu, J H. (1998). Asexual sporulation in *Aspergillus nidulans*. *Microbiology and Molecular Biology Reviews : MMBR*, 62(1), 35–54.
- Ahmed, Y L., Gerke, J., Park, H S., Bayram, O., Neumann, P., Ni, M., Ficner, R. (2013). The velvet family of fungal regulators contains a DNA-binding domain structurally similar to NF-kappaB. *PLoS Biology*, 11(12), e1001750.
- Ait Benkhali, J., Coppin, E., Brun, S., Peraza-Reyes, L., Martin, T., Dixelius, C., Debuchy, R. (2013). A network of HMG-box transcription factors regulates sexual cycle in the fungus *Podospora anserina*. *PLoS Genetics*, 9(7), e1003642.
- Amon, J., Keisham, K., Bokor, E., Kelemen, E., Vagvolgyi, C., & Hamari, Z. (2018). Sterigmatocystin production is restricted to hyphae located in the proximity of hulle cells. *Journal of Basic Microbiology*, 58(7), 590–596.
- Bokor, E., Ámon, J., Keisham, K., Karácsony, Z., Vágvolgyi, C., & Hamari, Z. (2019). HMGB proteins are required for sexual development in *Aspergillus nidulans*. *PLoS One*, 14(4):e0216094.
- Albert, B., Colleran, C., Leger-Silvestre, I., Berger, A B., Dez, C., Normand, C., Gadai, O. (2013). Structure-function analysis of Hmo1 unveils an ancestral organization of HMG-Box factors involved in ribosomal DNA transcription from yeast to human. *Nucleic Acids Research*, 41(22), 10135–10149.
- Aramayo, R., Adams, T H., & Timberlake, W E. (1989). A large cluster of highly expressed genes is dispensable for growth and development in *Aspergillus nidulans*. *Genetics*, 122(1), 65–71.
- Atoui, A., Bao, D., Kaur, N., Grayburn, W S., & Calvo, A M. (2008). *Aspergillus nidulans* natural product biosynthesis is regulated by mpkB, a putative pheromone response mitogen-activated protein kinase. *Applied and Environmental Microbiology*, 74(11), 3596–3600.
- Bagagli E, Valadares M C C, Azevedo J L (1991). Parameiosis in the entomopathogenic fungus *Metarhizium anisopliae* (Metsh.) Sorokin. *Braz J Gen* 14: 261-271.
- Balazs A, Pocsí I, Hamari Z, Leiter E, Emri T, *et al.* (2010). AtfA bZIP-type transcription factor regulates oxidative and osmotic stress responses in *Aspergillus nidulans*. *Mol Genet Genomics*. 283:289-303.
- Bayram, O., & Braus, G. H. (2012). Coordination of secondary metabolism and development in fungi: the velvet family of regulatory proteins. *FEMS Microbiology Reviews*, 36(1), 1–24.
- Bayram, O., Braus, G H., Fischer, R., & Rodriguez-Romero, J. (2010). Spotlight on *Aspergillus nidulans* photosensory systems. *Fungal Genetics and Biology: FG & B*, 47(11), 900–908.
- Bayram, O., Sari, F., Braus, G H., & Irniger, S. (2009). The protein kinase ImeB is required for light-mediated inhibition of sexual development and for mycotoxin production in *Aspergillus nidulans*. *Molecular Microbiology*, 71(5), 1278–1295.
- Bayram O, Biesemann C, Krappmann S, Galland P & Braus GH (2008). More than a repair enzyme: *Aspergillus nidulans* photolyase-like CryA is a regulator of sexual development. *Mol Biol Cell* 19: 3254–3262.
- Bayram O, Krappmann S, Ni M *et al.* (2008). VelB/VeA/LaeA complex coordinates light signal with fungal development and secondary metabolism. *Science* 320: 1504–1506.

- Bianchi, M E, Agresti A (2005). HMG proteins: dynamic players in gene regulation and differentiation. *Curr Opin Genet Dev.* 15(5):496–506.
- Biswas D, Imbalzano AN, Eriksson P, Yu Y, Stillman DJ (2004). Role for Nhp6, Gcn5, and the Swi/Snf complex in stimulating formation of the TATA-binding protein-TFIIA-DNA complex. *Mol Cell Biol.* 24:8312-8321.
- Bennett, J W., and K E. Papa. (1988). The aflatoxigenic *Aspergillus*, p. 264–280.
- Blumenstein A, Vienken K, Tasler R, Purschwitz J, Veith D, Frankenberg- Dinkel N & Fischer R (2005). The *Aspergillus nidulans* phytochrome FphA represses sexual development in red light. *Curr Biol*15: 1833–1838.
- Brown, D W., Yu, J H., Kelkar, H S., Fernandes, M., Nesbitt, T C., Keller, N P., Leonard, T J (1996). Twenty-five coregulated transcripts define a sterigmatocystin gene cluster in *Aspergillus nidulans*. *Proceedings of the National Academy of Sciences of the United States of America*, 93(4), 1418–1422.
- Bok J W, Keller N P (2004). LaeA, a regulator of secondary metabolism in *Aspergillus spp.* *Eukaryot. Cell.* 3:527–535.
- Bonaldi T, Langst G, Strohner R, Becker P B, Bianchi M E (2002). The DNA chaperone HMGB1 facilitates ACF/CHRAC-dependent nucleosome sliding. *Embo J.* 21(24):6865–6873.
- Bonatelli J R R, Azevedo J L, Valent G U (1983). Parasexuality in a citric acid producing strain of *Aspergillus niger*. *Braz J Gen* 3: 399-405.
- Braus G H, Krappmann S, Eckert S E (2002). Sexual development in ascomycetes: fruit body formation of *Aspergillus nidulans*. In: Osiewacz HD, editor. *Molecular biology of fungal development*. Boca Raton, FL: CRC Press. pp. 215–244.
- Brewer, L R., Friddle, R., Noy, A., Baldwin, E., Martin, S S., Corzett, M., Baskin, R J. (2003). Packaging of single DNA molecules by the yeast mitochondrial protein Abf2p. *Biophysical Journal*, 85(4), 2519–2524.
- Busby T M, Miller K Y, Miller B L (1996). Suppression and enhancement of the *Aspergillus nidulans* medusa mutation by altered dosage of the bristle and stunted genes. *Genetics* 143:155-63.
- Bustin M (2001). Revised nomenclature for high mobility group (HMG) chromosomal proteins. *Trends Biochem Sci.* 26 (3):152–153.
- Bustin, S. A., et al., (2009). The MIQE guidelines: minimum information for publication of quantitative real-time PCR experiments. *Clin Chem.* 55, 611-22.
- Bustin, M. (2010). High mobility group proteins. *Biochimica et Biophysica Acta*. Netherlands. <https://doi.org/10.1016/j.bbagr.2010.01.006>.
- Casselton, L., & Zolan, M. (2002). The art and design of genetic screens: filamentous fungi. *Nature Reviews. Genetics*, 3(9), 683–697.
- Champe, S P., Nagle, D L., & Yager, L N. (1994). Sexual sporulation. *Progress in Industrial Microbiology*, 29, 429–454.
- Chen, X J., & Butow, R A. (2005). The organization and inheritance of the mitochondrial genome. *Nature Reviews. Genetics*, 6(11), 815–825.
- Clutterbuck, A J. (1969). A mutational analysis of conidial development in *Aspergillus nidulans*. *Genetics*, 63(2), 317–327.
- Coppin, E., Debuchy, R., Arnaise, S., & Picard, M. (1997). Mating types and sexual development in filamentous ascomycetes. *Microbiology and Molecular Biology Reviews* : *MMBR*, 61(4), 411–428.

- David, H., Ozcelik, I S., Hofmann, G., & Nielsen, J. (2008). Analysis of *Aspergillus nidulans* metabolism at the genome-scale. *BMC Genomics*, 9, 163. <https://doi.org/10.1186/1471-2164-9-163>.
- Dequard-Chablat, M., & Allandt, C. (2002). Two copies of mthmg1; encoding a novel mitochondrial HMG-like protein, delay accumulation of mitochondrial DNA deletions in *Podospora anserina*. *Eukaryotic Cell*, 1(4), 503–513.
- Diffley, J F., & Stillman, B. (1991). A close relative of the nuclear, chromosomal high-mobility group protein HMG1 in yeast mitochondria. *Proceedings of the National Academy of Sciences of the United States of America*, 88(17), 7864–7868.
- Doll K, Chatterjee S, Scheu S, Karlovsky P, Rohlf M (2013). Fungal metabolic plasticity and sexual development mediate induced resistance to arthropod fungivory. *Proc R Soc B* 280: 20131219. <http://dx.doi.org/10.1098/rspb.2013.1219>
- Dutton, J R., S. Johns and B L. Miller (1997). StuAp is a sequence-specific transcription factor that regulates developmental complexity in *Aspergillus nidulans*. *EMBO J*. 16: 5710–5721.
- Dyer P S, Ingram D S & Johnstone K (1992). The control of sexual morphogenesis in the Ascomycotina. *Biol Rev* 67: 421–458.
- Dyer, P S., & O Gorman, C M. (2012). Sexual development and cryptic sexuality in fungi: insights from *Aspergillus* species. *FEMS Microbiology Reviews*, 36(1), 165–192.
- Ehrlich K C, Montalbano B G, Cary J W (1999). Binding of the C6-zinc cluster protein, AFLR, to the promoters of aflatoxin pathway biosynthesis genes in *Aspergillus parasiticus*. *Gene*. 230:249–257.
- Falciola L, Spada F, Calogero S, Langst G, Voit R, Grummt I, Bianchi M E (1997). High mobility group 1 protein is not stably associated with the chromosomes of somatic cells. *J Cell Biol*. 137(1):19–26.
- Fan Y, Sirotkin A, Russell RG, Ayala J, Skoultchi AI (2001). Individual somatic H1 subtypes are dispensable for mouse development even in mice lacking the H1(0) replacement subtype. *Mol Cell Biol*. 21:7933-7943.
- Fernandes M, Keller N P, Adams T H (1998). Sequence-specific binding by *Aspergillus nidulans* AfIR, a C6 zinc cluster protein regulating mycotoxin biosynthesis. *Mol Microbiol*. 28:1355–1365.
- Friddle, R W., Klare, J E., Martin, S S., Corzett, M., Balhorn, R., Baldwin, E P., Noy, A. (2004). Mechanism of DNA compaction by yeast mitochondrial protein Abf2p. *Biophysical Journal*, 86(3), 1632–1639.
- Fox, E M., & Howlett, B J. (2008). Secondary metabolism: regulation and role in fungal biology. *Current Opinion in Microbiology*, 11(6), 481–487.
- Galagan, J E., Calvo, S E., Cuomo, C., Ma, L J., Wortman, J R., Batzoglou, S., Birren, B W. (2005). Sequencing of *Aspergillus nidulans* and comparative analysis with *A. fumigatus* and *A. oryzae*. *Nature*, 438(7071), 1105–1115.
- Giavara S, Kosmidou E, Hande M P, Bianchi M E, Morgan A, d'Adda di Fagagna F, Jackson S P (2005). Yeast Nhp6A/B and mammalian Hmg1 facilitate the maintenance of genome stability. *Curr Biol*. 15(1):68–72.
- Guzman-de-Peña, D J. Aguirre, and J. Ruiz-Herrera (1998). Correlation between the regulation of sterigmatocystin biosynthesis and asexual and sexual sporulation in *Emericella nidulans*. *Antonie Leeuwenhoek* 73:199– 205

- Han K H, Han K Y, Yu J H, Chae K S, Jahng K Y & Han D M (2001). The *nsdD* gene encodes a putative GATA- type transcription factor necessary for sexual development of *Aspergillus nidulans*. *Mol Microbiol* 41: 299–309.
- Han K H, Lee D B, Kim J H, Kim M S, Han K Y, Kim W S, Park Y S, Kim H B & Han D M (2003). Environmental factors affecting development of *Aspergillus nidulans*. *J Microbiol* 41: 34–40.
- Han KH, Prade RA (2002). Osmotic stress-coupled maintenance of polar growth in *Aspergillus nidulans*. *Mol Microbiol* 43:1065-78.
- Hicks, J K., Yu, J H., Keller, N P., & Adams, T H. (1997). *Aspergillus* sporulation and mycotoxin production both require inactivation of the FadA G alpha protein-dependent signaling pathway. *The EMBO Journal*, 16(16), 4916–4923.
- Johns EB (1982). The HMG chromosomal proteins. *Boston: Academic Press*. ISBN 0-12-386050-4.
- Hoffmann B, Wanke C, Lapaglia SK, Braus GH (2000). c-Jun and RACK1 homologues regulate a control point for sexual development in *Aspergillus nidulans*. *Mol Microbiol*; 37:28-41.
- Kanki, T., Ohgaki, K., Gaspari, M., Gustafsson, C M., Fukuoh, A., Sasaki, N., Kang, D. (2004). Architectural role of mitochondrial transcription factor A in maintenance of human mitochondrial DNA. *Molecular and Cellular Biology*, 24(22), 9823–9834.
- Karacsony, Z., Gacser, A., Vagvolgyi, C., Scazzocchio, C., & Hamari, Z. (2014). A dually located multi-HMG-box protein of *Aspergillus nidulans* has a crucial role in conidial and ascospore germination. *Molecular Microbiology*, 94(2), 383–402.
- Kasahara K, Ki S, Aoyama K, Takahashi H, Kokubo T (2008). *Saccharomyces cerevisiae* HMO1 interacts with TFIID and participates in start site selection by RNA polymerase II. *Nucleic Acids Res*. 36:1343-1357.
- Kato N, Brooks W, Calvo A M (2003). The expression of sterigmatocystin and penicillin genes in *Aspergillus nidulans* is controlled by *veA*, a gene required for sexual development. *Eukaryot Cell*. 2:1178–1186.
- Kaufman, B A., Durisic, N., Mativetsky, J M., Costantino, S., Hancock, M A., Grutter, P., & Shoubridge, E. A. (2007). The mitochondrial transcription factor TFAM coordinates the assembly of multiple DNA molecules into nucleoid-like structures. *Molecular Biology of the Cell*, 18(9), 3225–3236.
- Kelkar H S, Keller N P, Adams T H. (1996). *Aspergillus nidulans* *stcP* encodes an O-methyltransferase that is required for sterigmatocystin biosynthesis. *Appl Environ Microbiol*. 62:4296–4298.
- Keller N P, Turner G, Bennett J W (2005). Fungal secondary metabolism – from biochemistry to genomics. *Nat. Rev. Microbiol*. 3: 937–947.
- Keller N P, Nesbitt C, Sarr B, Phillips T D, Burow G B (1997). pH Regulation of sterigmatocystin and aflatoxin biosynthesis in *Aspergillus spp.* *Phytopathology*. 87:643–648.
- Kim H S, Han K Y, Kim K J, Han D M, Jahng K Y & Chae K S (2002). The *veA* gene activates sexual development in *Aspergillus nidulans*. *Fungal Genet Biol* 37: 72–80.
- Kim H R, Chae K S, Han K H, Han D M. (2009). The *nsdC* gene encoding a putative C2H2-type transcription factor is a key activator of sexual development in *Aspergillus nidulans*. *Genetics*; 182:771-83.

- Kolodrubetz, D., & Burgum, A. (1990). Duplicated NHP6 genes of *Saccharomyces cerevisiae* encode proteins homologous to bovine high mobility group protein 1. *The Journal of Biological Chemistry*, 265(6), 3234–3239.
- Krappmann S, Jung N, Medic B, Busch S (2006). The *Aspergillus nidulans* F-box protein GrrA links SCF activity to meiosis. *Mol Microbiol*; 61:76-88.
- Kruger M, Fischer R. (1998). Integrity of a Zn finger-like domain in SamB is crucial for morphogenesis in ascomycetous fungi. *EMBO J* 17:204-14.
- Kruger M, Fischer R. Isolation of two *apsA* suppressor strains in *Aspergillus nidulans*. *Genetics* 1996; 144:533-40.
- Kucej, M., Kucejova, B., Subramanian, R., Chen, X J., & Butow, R. A. (2008). Mitochondrial nucleoids undergo remodeling in response to metabolic cues. *Journal of Cell Science*, 121(11), 1861–1868.
- Kumar, P., Mahato, D K., Kamle, M., Mohanta, T K., & Kang, S. G. (2016). Aflatoxins: A Global Concern for Food Safety, Human Health and Their Management. *Frontiers in Microbiology*, 7, 2170.
- Kuroiwa, T. (1982). Mitochondria nuclei. *International Review of Cytology*, 75, 1–59.
- Kucej, M., & Butow, R A. (2007). Evolutionary tinkering with mitochondrial nucleoids. *Trends in Cell Biology*, 17(12), 586–592.
- Kwon NJ, Shin KS, Yu JH. (2010). Characterization of the developmental regulator FlbE in *Aspergillus fumigatus* and *Aspergillus nidulans*. *Fungal Genet Biol* 47:981-93.
- Lara-Ortiz, T H. Riveros-Rosas and J. Aguirre (2003). Reactive oxygen species generated by microbial NADPH oxidase *NoxA* regulate sexual development in *Aspergillus nidulans*. *Mol. Microbiol.* 50: 1241–1255.
- Lara-Rojas F, Sanchez O, Kawasaki L, Aguirre J (2011). *Aspergillus nidulans* transcription factor AtfA interacts with the MAPK SakA to regulate general stress responses, development and spore functions. *Mol Microbiol* 80:436-54.
- Larionov A, Krause A, Miller W (2005). A standard curve based method for relative real time PCR data processing. *BMC Bioinformatics* 6:62.
- Laser H, Bongards C, Schuller J, Heck S, Johnsson N, et al. (2000). A new screen for protein interactions reveals that the *Saccharomyces cerevisiae* high mobility group proteins Nhp6A/B are involved in the regulation of the GAL1 promoter. *Proc Natl Acad Sci U S A.* 97:13732-13737.
- Lee B N & Adams T H (1994). The *Aspergillus nidulans fluG* gene is required for production of an extracellular developmental signal and is related to prokaryotic glutamine synthetase. *Genes Dev.* 8: 641–651.
- Lee BY, Han SY, Choi HG, Kim JH (2005). Screening of growth- or development-related genes by using genomic library with inducible promoter in *Aspergillus nidulans*. *J Microbiol* 43:523-28.
- Lennox RW, Cohen LH (1983). The histone H1 complements of dividing and nondividing cells of the mouse. *J Biol Chem.* 258:262-268.
- Lin Q, Sirotkin A, Skoultchi AI (2000). Normal spermatogenesis in mice lacking the testis-specific linker histone H1t. *Mol Cell Biol.* 20:2122-2128.
- Lopez S, Livingstone-Zatchej M, Jourdain S, Thoma F, Sentenac A, et al. (2001.) High-mobility-group proteins NHP6A and NHP6B participate in activation of the RNA polymerase III *SNR6* gene. *Mol Cell Biol.* 21:3096-3104.
- Lu, J., Kobayashi, R. & Brill, S J. (1996). Characterization of a high mobility group 1/2 homolog in yeast. *J. Biol. Chem.* 271, 33678–33685.

- MacAlpine, D M., Perlman, P S., & Butow, R A. (1998). The high mobility group protein Abf2p influences the level of yeast mitochondrial DNA recombination intermediates in vivo. *Proceedings of the National Academy of Sciences of the United States of America*, 95(12), 6739–6743.
- Martinelli, S D., and A J. Clutterbuck. (1971). A quantitative survey of conidiation mutants in *Aspergillus nidulans*. *J. Gen. Microbiol.* 69:261–268.
- Merz, K., Hondele, M., Goetze, H., Gmelch, K., Stoeckl, U. & Griesenbeck, J. (2008). Actively transcribed rRNA genes in *S. cerevisiae* are organized in a specialized chromatin associated with the high- mobility group protein Hmo1 and are largely devoid of histone molecules. *Genes Dev.* 22, 1190–1204.
- Miller, K Y., Toennis, T M., Adams, T H., & Miller, B L. (1991). Isolation and transcriptional characterization of a morphological modifier: the *Aspergillus nidulans* stunted (*stuA*) gene. *Molecular & General Genetics : MGG*, 227(2), 285–292.
- Miller, K Y., J. Wu and B L. Miller, (1992). *StuA* is required for cell pattern formation in *Aspergillus*. *Genes Dev.* 6: 1770–1782.
- Miller J D and Marasas WFO (2002). Ecology of Mycotoxins in Maize and Groundnuts. Supplement to LEISA (*Low External Input and Sustainable Agriculture*) Magazine, 23–24.
- Mims, C.W., Richardson, E.A. & Timberlake, W.E. *Protoplasma* (1988). 144: 132. <https://doi.org/10.1007/BF01637246>
- Miyakawa, I., Okamuro, A., Kinsky, S., Visacka, K., Tomaska, L., & Nosek, J. (2009). Mitochondrial nucleoids from the yeast *Candida parapsilosis*: expansion of the repertoire of proteins associated with mitochondrial DNA. *Microbiology (Reading, England)*, 155(Pt 5), 1558–1568.
- Miyakawa, I., Kanayama, M., Fujita, Y., & Sato, H. (2010). Morphology and protein composition of the mitochondrial nucleoids in yeast cells lacking Abf2p, a high mobility group protein. *The Journal of General and Applied Microbiology*, 56(6), 455–464.
- Mooney, J L., & Yager, L N. (1990). Light is required for conidiation in *Aspergillus nidulans*. *Genes & Development*, 4(9), 1473–1482.
- Moreira JM, Holmberg S (2000). Chromatin-mediated transcriptional regulation by the yeast architectural factors NHP6A and NHP6B. *EMBO J.* 19:6804-6813.
- Nayak, V., Zhao, K., Wyce, A., Schwartz, M F., Lo, W.-S., Berger, S L., & Marmorstein, R. (2006). Structure and dimerization of the kinase domain from yeast Snf1, a member of the Snf1/AMPK protein family. *Structure (London, England : 1993)*, 14(3), 477–485.
- Ngo, H B., Kaiser, J T., and Chan, D C. (2011). The mitochondrial transcription and packaging factor Tfam imposes a U-turn on mitochondrial DNA. *Nature Publishing Group* 18, 1290–1296.
- Ni M, Yu JH. (2007). A novel regulator couples sporogenesis and trehalose biogenesis in *Aspergillus nidulans*. *PLoS One*, 2:e970.
- Paoletti M, Seymour F A, Alcocer M J, Kaur N. (2007). Mating type and the genetic basis of self-fertility in the model fungus *Aspergillus nidulans*. *Curr Biol* 17:1384-9.
- Park, H S., Ni, M., Jeong, K C., Kim, Y H., & Yu, J H. (2012). The role, interaction and regulation of the velvet regulator *VelB* in *Aspergillus nidulans*. *PloS One*, 7(9), e45935.
- Pascon RC, Miller BL (2000). Morphogenesis in *Aspergillus nidulans* requires Dopey (DopA), a member of a novel family of leucine zipper-like proteins conserved from yeast to humans. *Mol Microbiol* 36:1250-64.
- Pontecorvo, G., Roper, J A., Hemmons, L M., Macdonald, K D., & Bufton, A. W J. (1953). The genetics of *Aspergillus nidulans*. *Advances in Genetics*, 5, 141–238.

- Purschwitz J, Müller S, Kastner C, Schöser M, Haas H, Espeso E A, Atoui A, Calvo A M & Fisher R (2008). Functional and physical interaction of the blue- and red- light sensors in *Aspergillus nidulans*. *Curr Biol* 18: 255–259.
- Pyrzak W, Miller K Y, Miller B L (2008). Mating type protein Mat1-2 from asexual *Aspergillus fumigatus* drives sexual reproduction in fertile *Aspergillus nidulans*. *Eukaryot Cell* 7:1029-40.
- Quackenbush J (2001). Computational analysis of microarray data. *Nat Rev Genet* 2:418-27.
- Rai J N, Tewari J P & Sinha A K (1967). Effect of environmental conditions on sclerotia and cleistothecia production in *Aspergillus*. *Mycopathol Mycol Appl* 31: 209–224.
- Ray, S., & Grove, A. (2009). The yeast high mobility group protein HMO2, a subunit of the chromatin-remodeling complex INO80, binds DNA ends. *Nucleic Acids Research*, 37(19), 6389–6399.
- Ramon A, Muro-Pastor MI, Scazzocchio C, Gonzalez R (2000). Deletion of the unique gene encoding a typical histone H1 has no apparent phenotype in *Aspergillus nidulans*. *Mol Microbiol* 35:223-33.
- Rhoades AR, Ruone S, Formosa T (2004). Structural features of nucleosomes reorganized by yeast FACT and its HMG box component, Nhp6. *Mol Cell Biol*. 24:3907-3917.
- Rubio-Cosials, A., Sidow, J F., Jimenez-Menendez, N., Fernandez-Millan, P., Montoya, J., Jacobs, H T., Sola, M. (2011). Human mitochondrial transcription factor A induces a U-turn structure in the light strand promoter. *Nature Structural & Molecular Biology*, 18(11), 1281–1289.
- Sarikaya Bayram, O., Bayram, O., Valerius, O., Park, H S., Irniger, S., Gerke, J., Braus, G H. (2010). *LaeA* control of velvet family regulatory proteins for light-dependent development and fungal cell-type specificity. *PLoS Genetics*, 6(12), e1001226.
- Sambrook, J., Fritsch, E F., and Maniatis, T. (1989). *Molecular Cloning: A Laboratory Manual*, 2nd Ed., Cold Spring Harbor Laboratory Press, Cold Spring Harbor, NY.
- Sharman A C, Hay-Schmidt A, Holland P W (1997). Cloning and analysis of an HMG gene from the lamprey *Lampetra fluviatilis*: gene duplication in vertebrate evolution. *Gene*. 184(1):99–105.
- Shen X, Ranallo R, Choi E, Wu C (2003). Involvement of actin-related proteins in ATP-dependent chromatin remodeling. *Mol Cell* 12:147-155.
- Shimizu, K., and N. P. Keller (2001). Genetic involvement of cAMP-dependent protein kinase in a G protein signaling pathway regulating morphological and chemical transitions in *Aspergillus nidulans*. *Genetics* 157:591–600.
- Sohn K T & Yoon K S (2002). Ultrastructural study on the cleistothecium development in *Aspergillus nidulans*. *Mycobiology* 30: 117–127.
- Stros M (2010). HMGB proteins: interactions with DNA and chromatin. *Biochim. Biophys. Acta*. 1799:101–113.
- Stott, K., Tang, G S F., Lee, K B., & Thomas, J O (2006). Structure of a complex of tandem HMG boxes and DNA. *Journal of Molecular Biology*, 360(1), 90–104.
- Tanaka M, Hennebold JD, Macfarlane J, Adashi EY (2001). A mammalian oocyte-specific linker histone gene H1oo: homology with the genes for the oocyte-specific cleavage stage histone (cs-H1) of sea urchin and the B4/H1M histone of the frog. *Development*. 128:655-664.

- Thakur M L (1973). Effect of osmotic concentration and pH on sclerotia and cleistothecia production in alkaline and fertile soil *Aspergilli*. *Microbios* 7: 215–220.
- Timberlake, W E., & Clutterbuck, A J. (1994). Genetic regulation of conidiation. *Progress in Industrial Microbiology*, 29, 383–427.
- Todd RB, Hynes MJ, Andrianopoulos A (2006). The *Aspergillus nidulans* *rcoA* gene is required for *veA*-dependent sexual development. *Genetics* 174:1685-88.
- Tuncher A, Reinke H, Martic G, Caruso M L (2004). A basic-region helix-loop-helix protein-encoding gene (*devR*) involved in the development of *Aspergillus nidulans*. *Mol Microbiol* 52:227-41.
- Vallim M A, Miller K Y & Miller B L (2000). *Aspergillus* SteA (sterile12- like) is a homeodomain- C₂/H₂- Zn⁺² finger transcription factor required for sexual reproduction. *Mol Microbiol* 36: 290–301.
- Vandesompele, J., et al., (2002). Accurate normalization of real-time quantitative RT-PCR data by geometric averaging of multiple internal control genes. *Genome Biol.* 3, RESEARCH0034.
- Vienken K, Scherer M & Fischer R (2005). The Zn (II)₂Cys₆ putative *Aspergillus nidulans* transcription factor repressor of sexual development inhibits sexual development under low- carbon conditions and in submerged culture. *Genetics* 169: 619–630.
- Vienken K & Fischer R (2006). The Zn(II)₂Cys₆ putative transcription factor NosA controls fruiting body formation in *Aspergillus nidulans*. *Mol Microbiol* 61: 544–554.
- Visacka, K., Gerhold, J M., Petrovicova, J., Kinsky, S., Joers, P., Nosek, J., Tomaska, L. (2009). Novel subfamily of mitochondrial HMG box-containing proteins: functional analysis of Gcf1p from *Candida albicans*. *Microbiology (Reading, England)*, 155(Pt 4), 1226–1240.
- Waring, R B., Davies, R W., Scazzocchio, C., & Brown, T A. (1982). Internal structure of a mitochondrial intron of *Aspergillus nidulans*. *Proceedings of the National Academy of Sciences of the United States of America*, 79(20), 6332–6336.
- Wieser, J., B N. Lee, J W. Fondon, and T H. Adams (1994). Genetic requirements for initiating asexual development in *Aspergillus nidulans*. *Curr. Genet.* 27:62–69.
- Woloshuk C P, Foutz K R, Brewer J F, Bhatnagar D, Cleveland T E, Payne G A (1994). Molecular characterization of *aflR*, a regulatory locus for aflatoxin biosynthesis. *Appl Environ Microbiol.* Jul; 60(7):2408–2414.
- Wu J & Miller B L (1997). *Aspergillus* asexual reproduction and sexual reproduction are differentially affected by transcriptional and translational mechanisms regulated stunted gene expression. *Mol Cell Biol* 17: 6191–6201.
- Wu Q, Zhang W, Pwee K H, Kumar P P (2003). Cloning and characterization of rice HMGB1 gene. *Gene.* 312:103–109.
- Xiao L, Kamau E, Donze D, Grove A (2011). Expression of yeast high mobility group protein HMO1 is regulated by TOR signaling. *Gene.* 489: 55-62.
- Yager, L N. (1992). Early developmental events during asexual and sexual sporulation in *Aspergillus nidulans*. *Biotechnology (Reading, Mass.)*, 23, 19–41.
- Yu Y, Eriksson P, Bhoite LT, Stillman DJ (2003). Regulation of TATA-binding protein binding by the SAGA complex and the Nhp6 high-mobility group protein. *Mol Cell Biol.* 23:1910-1921.
- Yu J H, Butchko R A, Fernandes M, Keller N P, Leonard T J, Adams T H (1996). Conservation of structure and function of the aflatoxin regulatory gene *aflR* from *Aspergillus nidulans* and *A. flavus*. *Curr Genet.* May; 29(6):549–555.

- Yu J-H, Keller N (2005). Regulation of secondary metabolism in filamentous fungi. *Annu Rev Phytopathol.* 43: 437–458.
- Yu J, Chang P-K, Ehrlich K C, Cary J W, Bhatnagar D, Cleveland T E, Payne G A, Linz J E, Woloshuk C P, Bennett J W (2004). Clustered pathway genes in aflatoxin biosynthesis. *Appl Environ Microbiol.* 70:1253–1262.
- Yu, J H., Hamari, Z., Han, K H., Seo, J A., Reyes-Dominguez, Y., & Scazzocchio, C. (2004). Double-joint PCR: a PCR-based molecular tool for gene manipulations in filamentous fungi. *Fungal Genetics and Biology : FG & B*, 41(11), 973–981.
- Zelenaya-Troitskaya, O., Newman, S M., Okamoto, K., Perlman, P S., & Butow, R A. (1998). Functions of the high mobility group protein, Abf2p, in mitochondrial DNA segregation, recombination and copy number in *Saccharomyces cerevisiae*. *Genetics*, 148(4), 1763–1776.
- Zonneveld BJM (1988). Effect of carbon dioxide on fruiting in *Aspergillus nidulans*. *Trans Br Mycol Soc* 91: 625–629.